The Welfare Consequences of Urban Traffic Regulations

Isis Durrmeyer* Nicolás Martínez†

August 26, 2024

Abstract

We develop a structural model to represent individual transportation decisions, the equilibrium road traffic levels, and speeds inside a city. The micro-founded model incorporates a high level of heterogeneity: individuals differ in access to transportation modes, values of travel time, and schedule constraints; road congestion technologies vary within the city. We apply our model to the Paris metropolitan area and estimate the model parameters from publicly available data. We compare the road traffic equilibria under the welfare-maximizing policy and simple instruments (driving restrictions and uniform or per-kilometer road tolls) and measure the policies' consequences on the different welfare components: consumer surplus, tax revenues, and values of emissions avoided.

JEL Classification: L9, R41, Q52

Keywords: structural model, policy evaluation, transportation, congestion, distributional effects, air pollution

*Toulouse School of Economics, Université Toulouse 1 Capitole. E-mail: isis.durrmeyer@tse-fr.eu

†Toulouse School of Economics, Université Toulouse 1 Capitole. E-mail: nicolas.martinez@tse-fr.eu

We would like to thank Nano Barahona, Juan Camilo Castillo, Judy Chevalier, Philippe Gagnepain, Gaston Illanes, Luz Yadira Gómez-Hernández, Myrto Kalouptsidi, Nicolas Koch, Lorenzo Magnolfi, Andrea Pozzi, Stef Proost, Valentina Reig, Mathias Reynaert, Marcelo Sant'Anna, Chenyu Yang, and Xin Zhang for their helpful comments and suggestions. We would also like to thank the participants of various seminars and conferences. We acknowledge financial support from the European Research Council under grant ERC-2019-STG-852815 "PRIDISP" and Agence Nationale de Recherche under grant ANR-17-EUR-0010 (Investissements d'Avenir program).

1 Introduction

Road traffic reduction has been a key objective in large metropolitan areas because of the multiple negative externalities cars generate. For instance, INRIX estimates an annual aggregate cost of congestion of 87 billion dollars for the U.S.[1] Pollution levels and air quality are also tightly related to the number of cars on the road. Yet, policy effects are difficult to predict because the road traffic level is the consequence of an equilibrium in which individuals make their transportation decisions independently. However, these individual decisions affect everyone since car speeds, and individual trip durations ultimately depend on the traffic level. Predicting individual reactions to a change in their transportation environment is challenging since it requires knowing how road traffic equilibrium is modified after individuals make their transportation decisions. We define transportation environment as all the factors that affect individual transportation decisions and are exogenous to individuals, including the presence of urban traffic regulations. Observational studies that measure the direct impact of a change in the transportation environment are limited by only being able to compare two equilibria, failing to separately identify the individual reactions from the equilibrium adjustments.

We develop a novel framework to analyze individual responses to changes in their transportation environments in equilibrium. It is a structural model representing equilibrium traffic conditions in a metropolitan area, with essential dimensions of heterogeneity at the individual and geographical levels. The first part of the model represents the choice of a transportation mode and a departure time by individuals with heterogeneous but fixed travel patterns (origin, destination, and itinerary). Since individuals have distinct travel patterns, different available transportation modes, and schedule flexibility, they are likely to react differently to a change in the transportation environment. The first key feature of our model is that different transportation modes are imperfect substitutes. The second key feature is individual schedule constraints that limit their ability to substitute across departure time. More precisely, we rely on a discrete choice nested logit model, containing heterogeneity in choice sets, sensitivities to trip duration and costs. We expand the model by considering stochastic departure time constraints, affecting the availability of departure time substitution across individuals.

The second part of the model represents the road congestion technologies, which describes how driving speeds react to changes in the number of individuals using cars and how many kilometers they drive. Our model takes into account spatial heterogeneity by allowing the congestion technology to be different across areas of the city.

[1] Source: https://www.cnbc.com/2019/02/11/americas-87-billion-traffic-jam-ranks-boston-and-dc-as-worst-in-us.html.

The model has the advantage of being transparent, tractable, and estimable with combinations of data that are typically publicly available for many metropolitan areas. We also provide a methodology to verify whether the model parameters are such that the equilibrium is unique. This model differs from existing ones in three key aspects. First, the model represents equilibrium transportation decisions for the entire metropolitan area rather than focusing on a specific road. Second, it accounts for different types of roads with possibly different congestion technologies instead of considering one city-wide congestion technology. Third, all the model parameters are estimated and represent the joint distribution of preferences, schedule constraints, trip distances and itineraries, individual characteristics, and transportation mode choice set. This joint distribution is key to analyze the effects of changes in the transportation environment at the individual level. To be able to have a model with such individual heterogeneity, we must do some simplifications and consider some factors are exogenous. In particular, we hold fixed residential locations and trip destinations, and we do not allow individuals to change where they live or work in response to a change in the transportation environment.[2] We also assume that the transportation modes available to an individual are fixed. While the choice of holding a car and the car characteristics (e.g., fuel efficiency) may be affected by traffic regulations in the medium run, we keep them constant in our analysis. We focus on unavoidable trips (work or study trips) and thus consider individuals who have to take their trips and do not model the number of trips. Finally, we consider only two departure times: peak and off-peak hours.

We apply our model of transportation decisions and congestion to the Paris metropolitan area (Île-de-France region) and combine data from different sources to estimate the model parameters. We rely on transportation surveys conducted in 2010 and 2020, where respondents provided detailed information about all the trips taken the day before the interview. We construct a final sample of 15,480 individuals to estimate the transportation mode choice model. The surveys do not provide trip durations using the non-chosen alternative transportation modes or car trip durations for alternative departure times. We supplement the survey with data on expected travel times using Google Directions for public transport and TomTom application programming interfaces (API, hereafter) for private vehicles during peak and off-peak hours to overcome this issue. The survey does not contain any information about individual schedule constraints. We thus make the assumption that the ability to substitute between departure times depend on the professional activity and rely on workforce survey data to estimate a probability to be flexible and choose a departure time.

[2]In our data, the first reason for choosing a residence is the price or size of the house (with 42.5% of respondents), while proximity to work and public transport come after (with 16.5% and 1.9% of respondents, respectively).

We estimate the congestion technologies using high-frequency data on traffic density and speed from road sensors at hourly level for two years and 1,359 sensors covering the highways, the ring roads, and the city center. Finally, we leverage subway and suburb train ridership data to approximate overcrowding levels in the different metro and train lines at peak and off-peak hours.

We use our structural model and estimated parameters to predict the effects of policy instruments that reduce road traffic. We analyze the effects of simple instruments: road tolls and simple driving restrictions. The advantage of driving restrictions is the simplicity of implementation, only requiring compliance controls and are often used as emergency schemes, temporary measures put in place under pollution peaks episodes.[3] Driving restrictions constitute a command and control policy instrument. An alternative consists of sending price signals through road tolls. Indeed, road tolls have been introduced in many European cities. For instance, Stockholm and London use systems of congestion charges, restricting access to the city center during peak hours of weekdays to those who pay a fee. Price mechanisms have the advantage of sorting individuals according to the benefits they get from driving: those who stop driving at peak hours have good transportation alternatives to driving or fewer schedule constraints, limiting the welfare costs of traffic regulations. Driving restrictions affect all individuals identically, which seems inefficient. But they have the advantage of forcing all individuals to contribute to traffic reduction, even those who are very cost inelastic or have very slow alternatives to driving. In addition, road tolls generate tax revenue that can be redistributed to individuals, mitigating the surplus losses.

In the main analysis, we compare the effects of three simple policies: driving restrictions, fixed tolls, and variable tolls. The policies are restricted to peak hours, so we consider individuals free to drive during off-peak hours. First, we analyze the aggregate effects of different policy stringency levels. We find that all the regulations are costly for individuals, as speed gains cannot compensate for the losses from the constraints imposed by the policies. Under moderate stringency levels, both tolls improve aggregate welfare if their revenues are redistributed. From the aggregate consumer surplus perspective only, driving restrictions hurt individuals less than the uniform toll. Driving restrictions force everyone to contribute to the traffic reduction while tolls must be high to induce the same traffic reduction. Across tolls, the variable toll is more efficient than the uniform toll since it targets long-distance commuters, who exert the largest congestion externalities. However, the uniform toll is best

[3]Paris and the surrounding region have used alternate traffic restrictions based on license plate digits six times between 1997 and 2016. The longest alternate-day travel scheme lasted four days from December 6^{th} to 9^{th} 2016. Since 2017, emergency plans triggered due to pollution peaks have relied on targeted driving restrictions based on car vintage and fuel type combination.

at maximizing the tax revenue. These results indicate that the policymaker must arbitrage between different objectives.

Next, we fix a stringency level and measure the policy costs and benefits. We find consumer surplus losses between €0.7 million and €1.5 million for morning trips. We also measure the impacts of the policies on global pollutant emissions (carbon emissions, CO_2 hereafter) and local pollutant emissions: nitrogen oxide (NO_X), particulate matter (PM), and hydrocarbon (HC) emissions. The benefits from reducing emissions, computed using standard social values, compensate only between 2.4% and 4.5% of the surplus losses. We also go beyond the aggregate impacts of tolls and driving restrictions and analyze their distributional effects. The variable tolls generate the largest inequalities across individuals. Individuals with long-distance trips that do not have suitable public transport alternatives are most negatively impacted.

Lastly, we investigate whether we can reduce surplus losses by using more sophisticated policy instruments or by combining policies with other interventions. We study a first-best benchmark where the policy maker sets personalized tolls to maximize welfare. Welfare gains are 63% larger and emissions reductions 27% larger than under the variable toll. However, the aggregate consumer surplus always decreases, and welfare improves because of the high tax revenues. We also study more realistic policies like car vintage or fuel-based driving restrictions, area-specific or combined variable and fixed tolls, and driving licenses allocated through an auction. These instruments do not perform significantly better than the simple ones for consumer surplus losses and emission reductions. We also measure the potential gains from differentiated tolls according to the area and nonlinear variable tolls. Finally, we evaluate the role of access to public transport, public transport efficiency, and cost for surplus. We find that connecting the 28.5% of the population which currently does not have access to public transportation and improving public transport speed are the best ancillary instruments to reduce policy surplus losses.

We contribute to the recent literature on modeling jointly transportation decisions and traffic equilibrium in a city. Almagro et al. (2024) consider a model closely related to ours and analyze the optimal combination of public transport policy and congestion charge that a budget constrained planner can implement. Barwick et al. (2024) analyze the joint role of commuting and housing choices in the equilibrium congestion levels and residential sorting in Beijing. They find an heterogeneous impact on congestion levels from residential choices in response to transportation policies. However, they do not considering departure time choices and have a more restrictive representation of congestion by using constant speed elasticities. Kreindler (2023) estimates a structural model of transportation decisions to analyze the

welfare effects of congestion pricing in India. He leverages data from a field experiment to estimate departure time substitution patterns and price sensitivity. His model differs from ours in several aspects: it includes separate costs for being early, late, or spending time in traffic and allows for substitution across routes rather than transportation modes.

Tarduno (2022) models route and departure time choices for a bridge crossing in the San Francisco metropolitan area. His results highlight the importance of accounting route substitution and characterizes second-best tolls that account for it. His model is different from ours since he abstracts from mode substitution, does not model the congestion technology, and ignores the effects of individual decisions on equilibrium speeds. Cook and Li (2023) evaluate the welfare effect of dynamic pricing in highway toll lanes. They model departure and route choice for drivers, as well as the congestion technology. While we do not consider dynamic pricing or route choice, we model mode choices and equilibrium speeds while accounting for the infrastructure and usage heterogeneity across different regions within a metropolitan area.

We relate and extend the transportation literature linking individuals' decisions and congestion. For instance, Basso and Silva (2014) model the choice between driving and taking the bus and the substitution between peak and off-peak hours over a single road to compare the effectiveness of public transport improvements and road tolls. Like in our model, both periods are associated with different congestion levels that depend on car and bus usage. However, the approach is different since they calibrate the model and ignore other transportation modes. Batarce and Ivaldi (2014) estimate a mode choice model with endogenous congestion based on the number of individual trips. Driving at any point in time generates congestion for the whole day.

Other empirical models that represent transportation decisions and congestion are based on the bottleneck model of Arnott et al. (1990) and Arnott et al. (1993). These models have the advantage of carefully describing congestion dynamics for a single road but ignore the substitution between driving and other transportation modes. Indeed, Anderson (2014) shows that the substitution between cars and public transport significantly affects congestion levels. Van Den Berg and Verhoef (2011) and Hall (2021) use bottleneck models to measure the distributional effects of road tolls. Both studies show that congestion pricing can improve consumer surplus without toll revenue redistribution due to sorting individuals according to their value of travel time. We find that road tolls do not increase aggregate consumer surplus without redistributing the toll revenue like Barwick et al. (2024) and Kreindler (2023), who make similar assumptions to ours. One reason for finding adverse effects of road tolls on consumer surplus is that we model traffic level at the period level instead of using a continuous time measure, ignoring the sorting of individuals within the period. Furthermore,

we consider all roads tolled while Hall (2018) and Hall (2021) consider policies that price a fraction of the roads.

The methodology of our paper relies on standard methods to estimate substitution patterns between transportation modes and departure times. We extend the standard models to allow and estimate unobserved stochastic flexibility constraints. Discrete choice models have indeed a long tradition of being used to model transportation mode choices (McFadden, 1974, Small, 2012) and estimate the value of travel time (VOT). Recent literature has relied on new data to estimate the VOT. For instance, Small et al. (2005) estimates individuals' VOT and valuations of travel time reliability using a mix of revealed and stated preferences data. Bento et al. (2020) use data from drivers entering an expressway subject to a toll in Los Angeles to disentangle the value of urgency from the VOT of individuals, highlighting the role of schedule constraints on individuals' willingness to pay for road tolls. Buchholz et al. (2024) exploits data from a ride-sharing platform to retrieve individuals' VOT. They exploit variations in prices and waiting times to recover the distribution of VOT in the population. Recent work have implemented field experiments to elicit directly travel time valuations (Kreindler, 2023, Goldszmidt et al., 2020, Hintermann et al., 2021). Our estimates of the VOT are more reliant on the model structure since we use standard cross-sectional survey data. Nevertheless, our results are consistent with the estimates from this literature.

Our reduced-form model for the congestion technology extends the work from the literature in two ways. First, we do not impose a linear or log-linear relationship between speed and traffic density as in Russo et al. (2021), Yang et al. (2020), Couture et al. (2018), Akbar and Duranton (2017). We estimate the relationships between speed and traffic density flexibly and find that the marginal impact of traffic on speed is not constant. Second, we do not assume a single congestion level for the whole city. Instead, we estimate five area-specific congestion technologies and model the equilibrium traffic level in each area and each period. Both differences from the standard literature have an important consequence: the marginal cost of congestion varies with the traffic level and the city area.

This paper relates to the literature measuring the impacts of existing traffic regulations using direct policy evaluation methods. The initial literature focused on developing countries with long traditions of urban traffic policies. Davis (2008), and Gallego et al. (2013) show that driving restrictions reduce pollution in the short run but are harmful in the long run because individuals bypass the restriction by purchasing a second car. Recent studies evaluate European policies such as low emissions zones, congestion charges, and road closures (Galdon-Sanchez et al., 2021, Tassinari, 2022, Herzog, 2022, Bou Sleiman, 2021). Our analysis is different in terms of method and focus. First, we evaluate hypothetical policies. Second,

we analyze the heterogeneity of the policy effects across individuals and their distributional consequences. We can also provide estimates for unobserved outcomes that can be expressed as a function of the model parameters, like consumer surplus. Previous literature on urban traffic policies in Paris (De Palma and Lindsey, 2006, Kilani et al., 2014) models the equilibrium traffic level with a less detailed characterization of individual preferences and limited mode substitution. The Metropolis model (De Palma et al., 1997) incorporates a version of the bottleneck model into a calibrated citywide traffic simulator for the Paris metropolitan area. However, this model relies on external parameters. One advantage of our framework is that all parameters are estimated, and the model equations are transparent. De Palma et al. (2017) and Haywood and Koning (2015) study the role of public transport quality in Paris for driving decisions. These studies focus on specific subway lines and ignore alternative transportation modes.

Our analysis is related to spatial equilibrium models representing the locations of individuals and activities and investigating the role of transportation policies. For instance, some recent papers has focused on infrastructure improvements and transportation policies (see Allen and Arkolakis, 2022, Tsivanidis, 2022, Herzog, 2022). Carstensen et al. (2022) model the residential and work location choices and how they are affected by a distance-based commuting cost in a dynamic framework. While our model is very different from these general spatial equilibrium models, some results from our paper could be useful for this literature to account for traffic condition adjustments.

2 A structural model of transportation decisions and traffic conditions

We develop an equilibrium model representing the individual choice of a transportation mode and departure time. The model considers that car trip durations are endogenous and depend on the congestion levels on the roads, which are directly related to the number of drivers and how long they drive. We approximate this by the number of kilometers individuals drive in each time period. To represent the relationship between speed and traffic density, we model road congestion technologies for different areas in the city. Finally, we describe how to solve for the equilibrium of the model and check whether the equilibrium is unique. Table 17 in Appendix A includes an index of the mathematical notation used in the paper.

2.1 Transportation mode choice model

First, we introduce the structural model representing individuals choosing which transportation mode to use and their departure time for their morning commute trip. We consider that

the origins and destinations of trips are given and exogenous. We also make the assumption that the itinerary from the origin to the destination is fixed. The city is split into A mutually exclusive areas. We do not allow for an outside option, as we model the choice of individuals facing unavoidable trips. We make the simplification that individuals choose between T discrete periods. There are J different transportation modes. Our model is a nested discrete choice model, and we follow the standard distributional assumptions from the literature (see Train, 2009). The nests are the different transportation modes. We assume individuals make a sequential decision: first, they choose a transportation mode, and then they decide when they leave home. The consequence of this modeling assumption is that we allow individuals to have correlated preference shocks for the same transportation mode across departure periods. The utility function of an individual n associated with transportation mode j, and departure time t is assumed to be a function of the mode and departure period characteristics X_{njt} (which includes the trip cost, trip duration, and mode and period specific intercepts):

$$u_{njt} = \beta_n' X_{njt} + \epsilon_{njt}. \tag{1}$$

β_n is a vector of coefficients of preferences for these variables for consumer n and ϵ_{njt} is a random idiosyncratic term. This assumption implies that the different modes and departure periods are imperfect substitutes. We allow for correlation between these idiosyncratic terms across different periods by decomposing the preference shocks into a mode-specific shock ζ_{nj} common to all departure periods and a mode and period-specific shock $\tilde{\epsilon}_{njt}$:

$$\epsilon_{njt} = \zeta_{nj} + \sigma\tilde{\epsilon}_{njt}. \tag{2}$$

σ represents the degree of independence between the preference shocks ϵ_{njt} across different periods for the same transportation mode and is a parameter to estimate. When $\sigma = 1$, the preference shocks are independent, while if $\sigma = 0$, the preference shocks are identical within a mode and the departure periods are perfect substitutes. We assume here a simple correlation structure where there is a common mode specific shock. This implies that different period preference shocks have the same correlation. Distant periods might be less substitutable than closer ones; our model captures this through the mode and period-specific constants that should be more similar. There is another assumption behind Equation (2): σ does not depend on the mode and thus the preference shocks ϵ_{njt} have the same correlation across all transportation modes.

Each individual has a choice set which comprises all transportation modes ($\mathcal{J}_n$) and periods ($\mathcal{T}_n$) she can access. Individuals may have schedule constraints that make them unable to

travel at certain periods. Each individual chooses the combination of mode j^* and departure time t^* that maximizes their utility:

$$\{j^*, t^*\} = \underset{j \in \mathcal{J}_n, t \in \mathcal{T}_n}{\arg\max}\, u_{njt}.$$

We assume that $\tilde{\epsilon}_{njt}$ are identically and independently distributed across individuals and follow a type one extreme value distribution. We assume that ζ_{nj} follows the only distribution such that ϵ_{njt} is also distributed according to an extreme value (see Cardell, 1997). The probability that individual n chooses the transportation mode j and departure time t is:

$$s_{njt|\mathcal{T}_n} = \frac{\exp\left(\frac{\beta_n' X_{njt}}{\sigma}\right)}{D_{nj}^{1-\sigma} \sum_{j' \in \mathcal{J}_n} D_{nj'}^{\sigma}}, \tag{3}$$

where $D_{nj'} = \sum_{t \in \mathcal{T}_n} \exp\left(\frac{\beta_n' X_{nj't}}{\sigma}\right)$.

We now consider that individuals' schedule constraints are stochastic, which means that they may vary daily. Another interpretation of stochastic constraints is that there are unobserved constraints, and the model approximates this unobserved level of individual heterogeneity (see Crawford et al., 2021 for a survey on unobserved choice set heterogeneity). There are L possible combinations of periods. We denote by π_{nl} the probability that individual n has access to the subset of periods $\mathcal{T}_l$. In this model, the expected probability of choosing the combination of mode and period j and t is:

$$s_{njt} = \sum_{l=1}^{L} \pi_{nl} s_{njt|\mathcal{T}_l} = \sum_{l=1}^{L} \pi_{nl} \frac{\exp\left(\frac{\beta_n' X_{njt}}{\sigma}\right)}{D_{njl}^{1-\sigma} \sum_{j' \in \mathcal{J}_n} D_{nj'l}^{\sigma}}, \tag{4}$$

where $D_{njl} = \sum_{t' \in \mathcal{T}_l} \exp\left(\frac{\beta_n' X_{njt'}}{\sigma}\right)$.

To ease notation, when referring to driving as a transportation mode, we use index $\mathbf{d}$. Therefore, individual n's probability of driving in period t is $s_{n\mathbf{d}t}$. The individual probabilities of choosing a mode depend on trip durations. The individual car trip duration is the sum of the duration driven in each area, which itself is the distance divided by the driving speed in that area:

$$\text{duration}_{nt} = \sum_{a=1}^{A} \frac{k_n^a}{v_t^a} \times \rho_{nt}. \tag{5}$$

k_n^a represents individual n's distance in area a and v_t^a is the speed in period t. Note that if the itinerary of an individual does not include an area, distance is set to 0. ρ_{nt} represents an

individual and period-specific multiplicative speed shock, which constitutes another structural parameter of the model. It captures individual-specific unobserved trip characteristics that make an individual average speed lower or higher than the average. We assume these shocks are exogenous to the traffic conditions and hold them constant when we simulate new traffic equilibria. We denote by $\mathbf{v}$ the vector of speeds for the different areas and periods and write the probability of driving at period t for individual n as $s_{n\mathbf{d}t}(\mathbf{v})$.

In our data, we observe a sample of N individuals, who represent the entire population in the metropolitan area using the individual weights $\omega_1, ..., \omega_N$. The total number of kilometers driven in period t within area a, K_t^a, is given by:

$$K_t^a = \sum_{n=1}^{N} \omega_n k_n^a s_{n\mathbf{d}t}(\mathbf{v}). \tag{6}$$

2.2 Road traffic conditions and congestion technology

We model congestion technology at the local level, with A mutually exclusive areas. The driving speed in an area depends on the congestion technology and the traffic level in that area only. Following the transportation literature, we base our congestion technology model on the fundamental traffic diagram (see Small et al., 2007). Geroliminis and Daganzo (2008) empirically show the existence of a fundamental traffic diagram at the city level, called a "macroscopic fundamental traffic diagram". Other applications include Yang et al. (2020), Couture et al. (2018), and Anderson and Davis (2020). We follow their approach but allow for heterogeneity within the city by considering area-specific congestion technologies.

Congestion levels can be different throughout the day, but we consider that congestion technology is fixed over time. Congestion technology represents all the elements that determine the speed at which individuals can drive at a given traffic level. It represents the type of road (highway or city road), the presence of traffic lights and intersections, and the number of entries or exits that may force drivers to slow down. In area a, the traffic level in period t is given by the total number of kilometers driven by the individuals in our sample, K_t^a, and from another unobserved source (trucks, buses, non-commuters) that we denote by K_{0t}^a. Thus the total traffic level is $K_t^a + K_{0t}^a$. K_t^a is given by Equation (6) and depends on speeds. In contrast, we assume that K_{0t}^a is fixed so that it does not depend on speeds. Formally, we define the speed in area a at time t, v_t^a to be a function of the total traffic level:

$$v_t^a = f^a(K_t^a + K_{0t}^a). \tag{7}$$

f^a represents the congestion technology that indicates how the speed decreases when the

number of kilometers driven increases.

2.3 Equilibrium of the model

This model's equilibrium consists of individual probabilities to drive in all periods and speeds for all areas and periods. We substitute the total number of kilometers driven, defined in Equation 6 as a function of the individual probabilities, in the speed function defined in Equation 7. We can thus express the equilibrium in terms of speeds only and get the following system of non-linear equations:

$$v_t^a = f^a\left(\sum_{n=1}^{N} \omega_n k_n^a s_{n\mathbf{d}t}(\mathbf{v}) + K_{0t}^a\right). \tag{8}$$

There is no general result that guarantees that the system of non-linear equations always has a unique solution. However, there are two special cases where the speed equilibrium is unique. The first case is when there is only one period and one area, so we have a single non-linear equation to solve. Because the speed function f^a is weakly decreasing, we are sure that if a speed equilibrium exists, it is unique. The second particular case is when we have one area and multiple periods. The proof of uniqueness relies on the fact that the Jacobian of the system of equations has positive terms on the diagonal and negative terms off-diagonal. The property of the Jacobian of the system of equations is the consequence of two key features of our model: the speed function is decreasing, and the different departure periods are substitutes. We provide the proofs of uniqueness under these two particular cases in Appendix B.

Even though there is no proof of the uniqueness of the equilibrium for the general model, we provide a method to check if the system of equations in speeds has a unique solution given our set of estimated parameters. The approach consists of defining the function:

$$g_t^a(\mathbf{v}, \kappa) = \kappa v_t^a + (1-\kappa) f^a(\mathbf{v})$$

and check whether there exists $\kappa \in [0, 1[$ such that $\mathbf{g}(.) = \left(g_1^1 \cdots g_T^1 \cdots g_1^A \cdots g_T^A\right)'$ is a contraction. By the Banach fixed-point theorem, if g is a contraction and there exists $\mathbf{v}^*$ such that $\mathbf{g}(\mathbf{v}^*, \kappa) = \mathbf{v}^*$, the solution $\mathbf{v}^*$ is unique. Note that this is a sufficient condition for equilibrium uniqueness. Recall that a function $\mathbf{g}(.)$ is a contraction if it is K-Lipschitz, with $K<1$, implying that $\forall \mathbf{v} \in [\underline{\mathbf{v}}, \overline{\mathbf{v}}]$ (the support of the speeds):

$$||\mathbf{g}(\mathbf{v}', \kappa) - \mathbf{g}(\mathbf{v}, \kappa)|| \leq K||\mathbf{v}' - \mathbf{v}||.$$

We use the supremum norm, so the Lipschitz coefficient K is given by:

$$\max_{a\in 1,\dots A}\max_{t\in 1,\dots,T}\max_{a'\in 1,\dots,A}\max_{t'\in 1,\dots,T}\max_{\mathbf{v}\in[\underline{\mathbf{v}},\overline{\mathbf{v}}]}\left|\frac{\partial g_t^a(\mathbf{v},\kappa)}{\partial v_{t'}^{a'}}\right|.$$

Suppose we can find $\kappa \in [0,1[$ such that $K<1$, the function $\mathbf{g}(.)$ is a contraction. Therefore, if the iteration process converges, it converges to a unique solution of the system of equations. If we find a set of κ such that the function $\mathbf{g}(.)$ is K-Lipschitz with $K<1$, we should select the value of κ that implies the lowest coefficient K to ensure the maximum speed of convergence. Therefore, we solve for:

$$\min_{\kappa\in[0,1[}\max_{a\in 1,\dots A}\max_{t\in 1,\dots,T}\max_{a'\in 1,\dots,A}\max_{t'\in 1,\dots,T}\max_{\mathbf{v}\in[\underline{\mathbf{v}},\overline{\mathbf{v}}]}\left|\frac{\partial g_t^a(\mathbf{v},\kappa)}{\partial v_{t'}^{a'}}\right|.$$

In practice, we do a grid search over some possible values of κ between 0 and 1. We do a non-linear optimization over speeds, and the objective function we maximize is the highest value of the absolute value of the elements of the Jacobian of $\mathbf{g}(.)$.

In this equilibrium model, only car trip durations are endogenous. In particular, we assume that the durations in public transport are fixed and unaffected by changes in traffic equilibrium. This assumption seems reasonable in our setting since, in the Paris metropolitan area, public transport itineraries very often rely on the railway system.[4] However, individuals may care about the comfort of public transport, which depends on the overcrowding level. In our application, we construct a proxy of the metro and train line-specific overcrowding levels to assess individuals' sensitivity to public transit comfort. However, we do not endogenize the overcrowding levels because our sample is not representative at the metro or train line level. We still explore, in robustness, how changes in overcrowding may change the results of our counterfactual analysis.

3 Specification and estimation of the transportation choice model

We estimate the transportation choice model parameters using a combination of two main datasets. First, we rely on data on individual commuting patterns in the Paris area from the 2010 and 2020 survey waves of "Enquête Globale Transport" (EGT hereafter). They are combined with a second self-constructed dataset on expected trip durations and itineraries for cars and public transport from TomTom and Google Maps APIs. We also leverage several

[4] In our sample, 75.5% of the trips by public transport involves the usage of a railway-based mode (subway, train, tramway).

ancillary datasets to complement the information on the different transportation modes and individual characteristics.

3.1 Overview of the data

The EGT data contains information about the departure time, precise origin and destination locations, transportation mode, and motive for every trip. In addition, the survey records household and individual socio-demographic characteristics such as age, professional activity, household size, income class, and housing characteristics. We model the choice of transportation mode and departure time for the morning commute. We consider two possible departure times: peak and off-peak hours, denoted t_1 (peak hours) and t_2 (off-peak hours). We consider 7-8.59 a.m. to be peak hours while 6-6.59 a.m. and 9-9.59 a.m. are off-peak hours. We assume individuals choose only one mode of transportation. If individuals take multiple modes, we keep the one reported as the primary mode.[5] To focus on unavoidable trips, we restrict the sample to trips related to work or study motives.[6]

We pick the individual as the observation unit rather than the household, assuming that individual decisions are independent within families. However, individuals from the same home still share access to the same transportation modes and household demographic characteristics. This assumption implies that two people can take the same car to make their respective trips without incurring any delay. In this case, we consider two vehicles are on the road.[7] While this simplification ignores potential cost savings and detours associated with carpooling, modeling such joint decisions would add too much complexity to the model.

We consider five transportation mode alternatives: biking, public transport, two-wheeled motor vehicles (motorcycles), walking, and driving.[8] If the household does not own a car or a motorcycle, the alternative is considered unavailable to the individual. If walking or biking takes more than 2.5 hours, we also define those alternatives as unavailable. If Google Maps cannot provide a public transport itinerary, we consider the option unavailable (this occurs for 13.4% of the final sample that combines 2010 and 2020).

We obtain a final sample of 15,470 individual trips, 12,353 from the 2010 survey and 3,117

[5]Only 7.7% (6.1%) of public transport trips in the 2010 (2020) survey also use a car. Around 1% of public transport trips also use a bicycle or motorcycle.

[6]Unavoidable trips cover a large share of transportation decisions, representing 72.3% of the total distance traveled during peak hours in the 2010 survey and 73.8% in the 2020 survey. For the off-peak hours, unavoidable trips represent 67.5% of the total distance traveled in 2010 and 55% in 2020.

[7]In our sample, only 7.2% (6.8%) of individuals report using a car as a passenger in 2010 (2020).

[8]Recent literature highlights the role of ridesharing and taxis on congestion levels (Rosaia, 2020 and Mangrum and Molnar, 2020). In the EGT data, only 0.12% (0.37%) of the trips in 2010 (2020) use a taxi or ridesharing. We thus ignore these transportation modes.

from the 2020 survey.[9] Using the weights provided by the surveys, we have transportation decisions representing 3.8 million individuals in both survey waves, corresponding to approximately one-third of the total population of the Paris metropolitan area (11.9 million inhabitants in 2011). We provide more information about the EGT data in Appendix C.1.

Since the EGT data only provides trip durations for chosen transportation modes, we must rely on additional data to compute travel times. For consistency across alternatives, we ignore self-reported trip durations. Instead, we consider predicted travel times for chosen and non-chosen transportation modes. We use Google Maps API to provide expected trip durations and itineraries by public transport and use TomTom API for expected driving times and itineraries.[10] We specify the trip query to a future date, so the predictions are not subject to the current traffic conditions and their idiosyncrasies. The predictions nevertheless rely on the expected traffic level to predict car trip durations. We thus use the predicted car trip durations at 8:30 a.m. for peak hours and 6:30 a.m. for off-peak hours. We provide more details about the queries in Appendix C.2.

The EGT surveys do not include information on individual schedule constraints. We complement our data with the "Enquête Emploi" workforce survey for 2019 and 2022 (workforce survey, hereafter).[11] These surveys explicitly ask workers if they can choose starting and ending working times. Since schedule constraints are likely specific to the occupation, we calculate the fraction of individuals with flexible work hours for 16 socio-professional categories (SPC hereafter). There are 16 SPCs. This dataset does not include information for students. We assume the students in high school or below have the lowest flexibility observed among workers. We assume that students in higher education have the largest observed flexibility. Appendix C.3 contains additional information about the workforce survey and how we aggregate a few SPCs.

3.2 Functional form assumptions, identification and estimation

We now explain how we estimate the parameters of the utility function presented in Equation 1. First, we parameterize the individual heterogeneity in preferences and assume that β_n are functions of finite number of observable demographic characteristics. σ, which represents the correlation of individual preference shocks across periods, is another parameter to estimate. We denote by $\boldsymbol{\theta}$ the vector that regroups these parameters.

[9] The Covid crisis stopped early the data collection of the 2020 survey and thus only contains interviews made in 2019.

[10] We did the queries in November 2023. These APIs can only provide trip durations now or for a future date, we cannot have expected trip durations that correspond exactly to the survey years.

[11] We do not exploit 2020 and 2021 data because the COVID crisis might have temporarily affected the working conditions.

In Section 2.1, we consider a model where individuals face stochastic constraints regarding their departure times. From an estimation perspective, the challenge arises because we lack information about whether individuals are constrained on the data collection day. We consider the constraints depend only on the SPC of individual n, denoted by $c(n)$. There are C SPCs. We make the SPC index explicit because we assume that the schedule constraints only vary by SPC. We denote $\phi_{c(n)}$ as the probability of being constrained, i.e., only one departure time is available, and $1-\phi_{c(n)}$ the probability of being unconstrained. Conditional on being constrained, the individual has a probability $\pi_{c(n)}$ that only the peak-hour option is available. The probability of having either peak or off-peak hours available is also a function of the SPC only. There are three possible combinations for the departure times available to individual n, $\mathcal{T}_n$: $\mathcal{T}_{12} = \{t_1, t_2\}$, $\mathcal{T}_1 = \{t_1\}$, or $\mathcal{T}_2 = \{t_2\}$ with probabilities that are respectively $1-\phi_{c(n)}$, $\phi_{c(n)}\pi_{c(n)}$, $\phi_{c(n)}(1-\pi_{c(n)})$.

In the workforce survey, we observe the probabilities to be constrained $(\phi_c)_{c=1,...,C}$, but we need to estimate the probabilities that only peak hour is available, $\boldsymbol{\pi} = (\pi_1, ..., \pi_C)$. We leverage the shares of individuals choosing peak hour conditional on the SPC by writing π_c as a function of the vector of parameters of preferences $\boldsymbol{\theta}$. We start by expressing the probability of choosing to travel at peak hours conditional on the SPC c that we denote μ_c and is observed:

$$\mu_c = \phi_c \pi_c + (1-\phi_c) \frac{\sum_{n\in\mathcal{C}} \omega_n \sum_{j\in\mathcal{J}_n} s_{njt_1|\mathcal{T}_{12}}(\boldsymbol{\theta})}{\sum_{n\in\mathcal{C}} \omega_n},$$

where $\mathcal{C}$ denotes the set of individuals with the SPC c. $s_{njt|\mathcal{T}_{12}}(\boldsymbol{\theta})$ corresponds to the mode shares conditional of having no schedule constraints, defined in Equation 3. We thus can write π_c as function of μ_c, ϕ_c and $\boldsymbol{\theta}$:

$$\pi_c(\boldsymbol{\theta}) = \frac{\mu_c}{\phi_c} - \frac{(1-\phi_c)}{\phi_c} \frac{\sum_{n\in\mathcal{C}} \omega_n \sum_{j\in\mathcal{J}_n} s_{njt_1|\mathcal{T}_{12}}(\boldsymbol{\theta})}{\sum_{n\in\mathcal{C}} \omega_n}$$

Since we need $\pi_c(\boldsymbol{\theta}) \in [0,1]$, we define:

$$\pi_c^*(\boldsymbol{\theta}) = \pi_c(\boldsymbol{\theta}) \mathbb{1}\{\pi_c(\boldsymbol{\theta}) \in [0,1]\} + \mathbb{1}\{\pi_c(\boldsymbol{\theta}) > 1\}. \tag{9}$$

This allows us to write the probability that individual n chooses the combination j and t as function of the parameters:

$$\begin{aligned} s_{njt}(\boldsymbol{\theta}) =& \phi_{c(n)} \pi^*_{c(n)}(\boldsymbol{\theta}) s_{njt|\mathcal{T}_1}(\boldsymbol{\theta}) + \phi_{c(n)}(1-\pi^*_{c(n)}(\boldsymbol{\theta})) s_{njt|\mathcal{T}_2}(\boldsymbol{\theta}) \\ &+ (1-\phi_{c(n)}) s_{njt|\mathcal{T}_{12}}(\boldsymbol{\theta}). \end{aligned}$$

Note that the equation above is the same as Equation 4, but it is adjusted to our setting

with two periods and partially observed schedule constraints. A last remark is that when individuals are constrained, they only choose a transportation mode, and the model becomes a logit, so the probabilities do not depend on σ. It implies that the identification of σ is only possible when the probability to be constrained is below one.

The identification of the unobserved schedule constraints represented by $\boldsymbol{\pi}^*$ comes from observing the departure time by SPC and the probability of having flexible hours (from the workforce survey). Controlling for the preference heterogeneity within SPCs, the observed departure time by SPC reveals the type of schedule constraints faced by individuals in the SPC. The key assumption for identification of $\boldsymbol{\pi}^*$ is that preferences do not systematically differ across socio-professional categories.

Finally, an individual n contribution to the likelihood is:

$$l_n = \Pi_{j \in \mathcal{J}_n} \Pi_{t=\{t_1,t_2\}} \left(s_{njt}(\boldsymbol{\theta})\right)^{y_{njt}},$$

where $y_{njt} = 1$ when the mode j and the period t are chosen and 0 otherwise.

We estimate $\boldsymbol{\theta}$ using the method of maximum likelihood; we want to find the values of the parameters that best rationalize the observed choices given the theoretical probabilities. We maximize the log-likelihood function:

$$LL(\boldsymbol{\theta}) = \sum_{n=1}^{N} \sum_{j \in \mathcal{J}_n} \sum_{t=\{t_1,t_2\}} \omega_n y_{njt} \log\left(s_{njt}(\boldsymbol{\theta})\right). \tag{10}$$

We recall that ω_n corresponds to the sample weight of the individual n. The identification of the parameters in $\boldsymbol{\theta}$ comes from observing a cross-section of individuals with different choice sets, trip characteristics, and demographic characteristics, making different choices.

The maximum likelihood method requires that the individual preference shocks are uncorrelated to the mode and period observed characteristics:

$$\mathbb{E}(\epsilon_{njt}|X_{njt}) = 0.$$

In particular, this means that individual shocks that affect the decision to drive should be uncorrelated with individual car trip duration. However, it contradicts the theoretical equilibrium model, where individual driving times are an equilibrium outcome. Unobserved factors may simultaneously affect individual preference for driving and speeds (e.g., rain) or all individuals' preferences simultaneously and thus speeds (e.g., an important event). Our data structure mitigates these concerns for two reasons. First, we do not rely on observed car trip durations but on the expected trip duration from TomTom on a future date. This

prediction is based on the expected traffic level and is not subject to real-time traffic or speed shocks (e.g., caused by rain). Second, individuals are surveyed on different days throughout the year (outside school holiday periods), so their unobserved preference shocks are less likely to be correlated.

In addition, our specification allows for a rich set of interactions between demographics, cost and travel time. Controlling for such individual-level heterogeneity is important to have independence of the unobserved preferences shocks and mode characteristics.

To further mitigate the risk of endogeneity of car trip durations, we use 93 zone fixed effects for the individual origins and destinations interacted with the car alternatives. These fixed effects capture unobserved driving conditions that might be correlated across individuals, such as better road infrastructures. Barwick et al. (2024) also use such fixed effects to mitigate endogeneity concerns.

Additionally, we use a control function approach to deal with the potential endogeneity of car trip durations. We construct a set of instruments and apply the control function approach suggested by Petrin and Train (2010). The control function method is a widespread approach to deal with endogeneity while relying on individual data and using the maximum likelihood estimation method (Agarwal, 2015, Dubois et al., 2018, Buchholz et al., 2024). Our instruments are inspired by Berry et al. (1995) instruments: they are characteristics of the choice sets of other individuals living in the origin or destination zone. We also use the free-flow duration as Almagro et al. (2024). In Appendix D.1, we provide details on the control function approach and the underlying assumptions.

3.3 Utility specification and variable constructions

We specify the utility as a linear function of the following variables: transportation mode-and-departure-time-specific intercepts, the trip's monetary cost, the trip duration and some public transport characteristics. Except for the mode and departure time dummies, none of these variables are readily available in the EGT data, and we explain how we construct them here. We consider a flexible functional form for the trip duration by interacting it with the trip distance using a local linear functional form. More specifically, we split the trip distance into five intervals and allow the parameters of the interaction between duration and distance to vary on each segment of the interval. The idea is that spending one additional minute might be different depending on the trip distance. We also allow the sensitivities to the trip duration and cost to vary with six age classes and nine income brackets.

We add some controls to represent the characteristics of public transport. We use the overcrowding level in the metro and suburb trains, a dummy if the public transport itinerary

relies on the railway system only (instead of using the bus or tramway), and the number of layovers. Following the literature on public transport congestion, such as De Palma et al. (2017) and Haywood and Koning (2015), we assume the utility is linear in the level of overcrowding in the public transit.

We rely on the self-constructed dataset on expected trip durations for driving and public transport. To estimate trip durations for walking and bicycle trips, we compute the average speed for individuals who chose to bike or walk using their declared trip durations and distances. We find a walking speed of 3.38 km/hr and 8.24 km/hr for biking.[12] These average speeds are combined with distance to compute trip durations for the two modes. Finally, we use the predicted car durations at off-peak hours for motorcycles, assuming they can bypass traffic.

The EGT data contains information on some characteristics of cars and motorcycles: vintage, fuel type, and horsepower. Using additional data, we estimate the fuel consumption and emissions per kilometer driven for the vehicles from these characteristics (see Appendix C.4). Fuel consumption is essential to estimate the cost of driving, while the emissions are used in counterfactual simulations to predict the environmental benefits of reducing traffic. For the cost of driving, we follow a similar approach as the American Automobile Association and construct a per-kilometer cost that includes fuel consumption, car depreciation, maintenance, and insurance. Car prices are not observed in the EGT data, so we predict them from the vintage, fuel type, and horsepower using additional proprietary data on car sales. The EGT contains household-level data on the annual maintenance and insurance costs and information on the number of kilometers driven annually. The precise methodology and related assumptions to estimate the driving costs are provided in Appendix C.5.1.

The survey also records whether individuals own a public transport pass and the type of subscription. Since public transit users are more likely to own a subscription and thus to pay a cheaper price, we control for the selection into public transport subscription by predicting the cost of the trip net of the rebate due to the subscription. We present our methodology in Appendix C.5.2.

Walking is always free, while biking is free only for households owning bicycles. If the individual has an annual bike-sharing subscription, we consider the per-trip cost of the subscription is the annual cost divided by twice the number of working days. In other cases, we consider biking to have the price of a single bike-sharing ticket, €1.7. Our final cost estimates are trip and individual-specific and account for the rebates from public

[12]Speeds are computed using the reported duration and trip distances. We check that the speeds are not sensitive to rounding errors in the reported trip durations by excluding observations reporting a multiple of 5 minutes.

transportation subscription, vehicle characteristics, and trip distances. Finally, we deflate the cost of the 2020 trips to 2010 euros.[13]

We construct a measure of overcrowding for all the subway and urban railway transit lines to capture the potential disutility of overcrowding in public railway transport. We use publicly available data from 2015 on passenger flows (the oldest year available) combined with historical data on hourly public transit schedules and train capacities. A train's capacity is the number of passengers in a train for a density of four persons per square meter. We approximate the overcrowding level by the hourly number of passengers divided by the line's capacity. A line's capacity is a function of two factors: train frequencies and train physical capacities. Since different lines operate different trains and have different frequencies, we obtain important heterogeneity in capacities across metro and train lines. We obtain individual overcrowding levels from the urban railway line-level overcrowding estimates by weighting the line-level overcrowding measures by the percentage of the trip duration spent on the line. We provide details on the data used and the construction of the overcrowding variable in Appendix C.6. Table 19 on the same Appendix C.6 provides the time-specific overcrowding measures for each line. On average, across metro and train lines, public railway transport is at 73% capacity at off-peak hours and reaches 180% at peak hours.

The EGT provides the household monthly income in ten brackets. We follow the approach of the French National Institute of Statistics and Economic Studies to calculate consumption units in a household. We count the first individual in a household as one consumption unit, other adults represent half a consumption unit, and children represent 0.3 consumption units. We divide the midpoint of each income bracket by the number of consumption units to obtain an estimate of income at the individual level. We then reclassify the individuals into the initial income categories. Taking into account the household size is important as only 19.4% of the sample remains in their initial income category. Finally, we aggregate the two highest income classes (between €4,500 and €5,500 and above €5,500) because there are few observations in the highest income bracket (0.5% of the sample).

Table 1 shows the distribution of trip characteristics and mode shares across the different demographic categories. We see that the youngest category (below 18 years old) have, on average, trip distances three to four times lower than the rest of the population. This can be explained by the proximity of schools to their residences. Car usage increases with age, while public transport usage decreases with it. Trip duration also monotonically decreases with age from 18 onwards. This could be related to older individuals having higher sensitivity to travel time.

[13]The value of the deflator comes from the French National Institute of Statistics and Economic Studies. See https://www.insee.fr/fr/statistiques/2122401.

Car usage is at least ten percentage points lower for the two lowest income categories than for the rest of the population. Meanwhile, public transport is popular across low and middle-level income categories. The lowest public transport usage corresponds to individuals with an income between €3,500 and €4,500. Across SPC, we see large heterogeneity in the share of trips made during peak hour, with less than half of qualified workers traveling at peak, while almost all students at high school or below travel during peak hours.

Table 1: Summary statistics by demographic groups.

		Mean		Mode & period shares		
	Freq.	**Dist.**	**Duration**	**Car**	**Pub. trans.**	**Peak**
Age						
Age $\leq$ 18	31.6	4.1	24.4	19.9	35.1	90.6
Age $\in$]18, 30]	17.3	15.3	39.7	22.4	67.4	70.7
Age $\in$]30, 40]	17.2	16.1	37.3	37.5	49.5	66.5
Age $\in$]40, 50]	17.6	16	36.3	41.4	46.6	70.7
Age $\in$]50, 60]	14	15.7	35.1	43.6	43.8	71.8
Age $>$ 60	2.27	12.8	32.7	44.5	41.7	72.3
Income						
Income $\leq$ 800	10.5	8.08	32.1	16.9	47.1	77.3
Income $\in$ [800, 1200[	12.69	10.05	32.53	23.84	48.72	75.76
Income $\in$ [1200, 1600[	15.6	11.8	31.8	35.5	41.5	74.2
Income $\in$ [1600, 2000[	15.3	13.4	33.5	36.3	46.4	73.6
Income $\in$ [2000, 2400[	14.2	13.5	34.6	33.4	47.1	75.1
Income $\in$ [2400, 3000[	11.4	13.6	34.6	32.1	51.5	75.7
Income $\in$ [3000, 3500[	8.62	12.3	33	29.1	50.6	79.9
Income $\in$ [3500, 4500[	7.56	13	32.8	35.5	43.8	81.6
Income $>$ 4500	4.18	14.5	34.5	37.9	48.3	77.6
Socio-professional category						
Farmers	0.11	14.2	32.7	36.4	29.4	82.3
Craftspersons	0.698	19.8	31	81.2	12.3	54.1
Shopkeepers	0.517	15.7	34.6	46.7	30.9	50.2
Entrepreneurs	1.45	13.4	32.6	36.2	37.8	66.9
Public executives	6.96	13.8	35.6	31.2	53.8	72.7
Private executives	12.9	17.2	38.9	31.8	58.3	76.7
Education, health	8.25	13.3	33	42	43.1	76.6
Administrative professions	7.21	17.1	38.8	32.5	59.6	74.8
Technicians	3.54	18.3	38.1	48	41.4	62.3
First-line supervisors	1.24	19.1	40.5	50.8	40.8	61.3
Public employees	5.55	13.3	35.6	37.6	45.2	71.1
Private employees	4.69	18.7	38.8	34.9	58.5	80.3
Retail employees	1.16	15.3	36.6	38.2	49.7	59.9
Services	1.71	9.76	33.2	17.4	59.6	60.3
Qualified Workers	5.27	15.8	34.4	55.6	36.2	47.3
Unqualified Workers	1.6	12.8	34.4	37.3	48.9	48.1
Students $\leq$ high school	31.6	3.89	23.9	20.4	33.6	91
Students in higher education	5.59	15.1	43.7	9.73	80.7	73.5
Average		12.1	33.2	30.9	47.1	76.2

Note: Durations in minutes, distances in km, monthly income in € per consumption unit. Frequencies and mode shares are in %. Distance and duration are those of the chosen transportation modes. All statistics are for the pooled 2010-2020 sample and are computed using survey weights.

Across socio-professional categories, we see a large variation in the usage of car and public

transport. We also observe large variation in the share of trips done at peak hours. Workers (qualified and unqualified), and individuals working in services have a lower rates of departure at peak hours than the average. In contrast, executives and individuals working in health have higher rates of departure during peak hours. We take this as evidence of differences in schedule flexibility across socio-professional categories. Mode availability, as well as the distribution of durations and costs by mode, are given in Appendix C.7.

One possible concern with using the 2010 and 2020 waves of the EGT survey together is that transportation patterns could have changed in the ten years between the surveys. The last panel of Table 20 in Appendix C.7 provides the availability and mode shares. We do not observe major changes across the two survey waves, with the difference between shares of most modes being less than two percentage points.

3.4 Estimation results

We estimate the transportation choice model by maximizing the log-likelihood defined by Equation (10). Only differences in utilities are identified in this discrete choice model. Thus, we consider walking at peak hours as the baseline option and normalize its intercept to 0. Note that the mean utility of an individual walking at peak hours is not normalized to 0 because the utility contains the trip duration. In the estimation, we impose that the sensitivities to duration and trip cost are always negative.

We present in Table 2 the results from four different specifications. The first corresponds to our main specification with stochastic schedule constraints governing departure time substitution. We use a control function in the second specification to deal with duration endogeneity. In the third one, all individuals can substitute across departure periods. Finally, in the last specification, individuals cannot substitute across departure periods. The last two specifications make extreme assumptions regarding the ability of individuals to substitute across periods. The differences between them and our preferred model are informative of the role of incorporating stochastic schedule constraints. All specifications include a rich set of fixed effects: the zones of origin and destination interacted with driving.

The table also provides the median value of travel time (or opportunity cost of time) in €/hr. The VOT represents how much an individual should receive (in €) to compensate for the decrease in utility related to an increase in travel time by an hour. Given our functional form assumptions and the unit for duration (ten minutes), the VOT is simply the ratio between the sensitivity to duration and the sensitivity to the trip monetary cost multiplied by six. The sensitivity to duration depends on individual specific demographic characteristics and trip distance.

Baseline sensitivities to duration and cost are very similar across specifications (1), (2) and (4). In specification (3), individuals in the base category appear to be more price-sensitive and more sensitive to travel time. This is intuitive because the model, without schedule constraints, rationalizes the fact that only 76.2% of individuals choose to commute during peak hours by a high sensitivity to duration. We take the results from specification (3) as evidence of a possible bias from assigning the option to substitute across departure times to individuals who cannot. However, we note that the median VOT remains very close to our baseline estimate.

Furthermore, all four specifications suggest qualitatively the same heterogeneity in preferences. When looking at the estimates from our preferred specification, the interactions between the trip duration and individual characteristics reveal that the sensitivity to trip duration is more heterogeneous across age than across income categories. Older and higher income individuals are more sensitive to trip duration. Older individuals are also less sensitive to trip's cost. We find little heterogeneity across income brackets on the cost sensitivity and the heterogeneity suggests a u-shaped curve: individuals with middle incomes (€2,000-3,000) are the most sensitive to the cost of the trip.

Our baseline specification suggests a preference shock correlation between periods of 0.82, indicating that leaving at peak and off-peak hours are subject to relatively independent shocks and thus constitute imperfect substitutes. Yet, the coefficient is lower than one, confirming the relevance of the nest to represent substitution patterns between different transportation modes and departure times. With the control function, the estimated σ is slightly higher (0.87). Meanwhile, the full flexibility model estimates a σ equals to 0.60, which suggests greater correlation of preferences within modes.

Finally, the included residuals from the first stage of the control function are not significant. Due to these factors, we prefer to use specification (1) as our main specification for the remaining analysis. Overall, the results from the different specifications are reassuring that our assumptions about the presence or absence of schedule constraints, as well as the control function, do not have large impacts on the estimated coefficients.

The transportation mode dummies reveal significant differences in the stand-alone preferences for different transportation alternatives. Consistently across transportation modes, we find that peak hours are always preferred to off-peak hours. The public transport controls have the expected signs: the number of layovers and overcrowding reduce the utility of public transport. The railway dummy is positive but not significant. The overcrowding has a small impact on the choice. Indeed, the average willingness to pay to decrease the overcrowding level by 10% during peak hours is 6.4 cents. In contrast, the average willingness to pay to

reduce the trip duration by 10% is 97 cents.

Table 2: Estimation results for the utility parameters

Coefficients	**(1)**		**(2)**		**(3)**		**(4)**	
Duration	-0.538**	(0.033)	-0.537**	(0.033)	-0.9**	(0.089)	-0.531**	(0.033)
Cost	-0.53**	(0.049)	-0.533**	(0.049)	-0.871**	(0.102)	-0.533**	(0.049)
Bicycle, peak	-3.47**	(0.075)	-3.46**	(0.076)	-5.8**	(0.429)	-3.47**	(0.076)
Public transport, peak	-1**	(0.062)	-0.995**	(0.063)	-1.79**	(0.157)	-0.994**	(0.062)
Motorcycle, peak	-3.43**	(0.112)	-3.43**	(0.113)	-5.66**	(0.406)	-3.49**	(0.113)
Car, peak	-2.68**	(0.527)	-2.71**	(0.528)	-4.54**	(0.935)	-2.72**	(0.528)
Car, off-peak	-3.88**	(0.544)	-3.95**	(0.563)	-6.27**	(0.95)	-3**	(0.535)
Public transport, off-peak	-1.9**	(0.174)	-1.94**	(0.221)	-2.96**	(0.164)	-1.16**	(0.098)
Walking, off-peak	-0.737**	(0.154)	-0.779**	(0.195)	-1.81**	(0.055)	0	(0)
Bicycle, off-peak	-4.15**	(0.16)	-4.18**	(0.188)	-7**	(0.438)	-3.37**	(0.133)
Motorcycle, off-peak	-3.73**	(0.162)	-3.75**	(0.18)	-6.31**	(0.412)	-2.74**	(0.164)
Duration × income ∈ [800, 1,200[	-0.03	(0.03)	-0.03	(0.03)	-0.036	(0.05)	-0.036	(0.03)
Duration × income ∈ [1,200, 1,600[	-0.115**	(0.032)	-0.115**	(0.032)	-0.158**	(0.053)	-0.116**	(0.032)
Duration × income ∈ [1,600, 2,000[	-0.072*	(0.031)	-0.071*	(0.031)	-0.083	(0.051)	-0.073*	(0.031)
Duration × income ∈ [2,000, 2,400[	-0.075*	(0.032)	-0.075*	(0.032)	-0.1†	(0.052)	-0.08*	(0.032)
Duration × income ∈ [2,400, 3,000[	-0.083*	(0.034)	-0.084*	(0.034)	-0.09†	(0.054)	-0.088**	(0.034)
Duration × income ∈ [3,000, 3,500[	-0.102**	(0.035)	-0.103**	(0.036)	-0.102†	(0.057)	-0.118**	(0.036)
Duration × income ∈ [3,500, 4,500[	-0.141**	(0.041)	-0.143**	(0.042)	-0.134*	(0.063)	-0.169**	(0.042)
Duration × income ≥ 4,500	-0.169**	(0.058)	-0.174**	(0.06)	-0.139†	(0.082)	-0.241**	(0.061)
Duration × age ∈ [18, 30]	-0.138**	(0.025)	-0.137**	(0.025)	-0.257**	(0.046)	-0.136**	(0.025)
Duration × age ∈]30, 40]	-0.311**	(0.029)	-0.308**	(0.03)	-0.54**	(0.058)	-0.291**	(0.03)
Duration × age ∈]40, 50]	-0.26**	(0.029)	-0.259**	(0.029)	-0.446**	(0.054)	-0.262**	(0.03)
Duration × age ∈]50, 60]	-0.327**	(0.033)	-0.326**	(0.033)	-0.532**	(0.06)	-0.322**	(0.034)
Duration × age > 60	-0.38**	(0.073)	-0.38**	(0.074)	-0.598**	(0.113)	-0.35**	(0.074)
Duration × distance	0.223**	(0.023)	0.223**	(0.023)	0.356**	(0.048)	0.22**	(0.023)
Duration × (dist-d_2) × (dist≥d_2)	-0.265**	(0.041)	-0.262**	(0.041)	-0.426**	(0.071)	-0.239**	(0.042)
Duration × (dist-d_3) × (dist≥d_3)	-0.031	(0.062)	-0.035	(0.063)	-0.048	(0.092)	-0.042	(0.064)
Duration × (dist-d_4) × (dist≥d_4)	0.099	(0.114)	0.105	(0.115)	0.104	(0.171)	0.118	(0.113)
No. layovers in Pub. transport	-0.486**	(0.041)	-0.488**	(0.041)	-0.778**	(0.09)	-0.49**	(0.041)
Railway only	0.015	(0.063)	0.011	(0.063)	0.143	(0.095)	-0.011	(0.065)
Pub. transport overcrowding	-0.066*	(0.033)	-0.064†	(0.033)	-0.199**	(0.041)	-0.046	(0.036)
Cost × income ∈ [800, 1,200[	-0.013	(0.036)	-0.014	(0.036)	-0.016	(0.059)	-0.012	(0.036)
Cost × income ∈ [1,200, 1,600[	-0.059†	(0.036)	-0.059†	(0.036)	-0.085	(0.06)	-0.055	(0.036)
Cost × income ∈ [1,600, 2,000[	-0.023	(0.034)	-0.024	(0.034)	-0.025	(0.057)	-0.015	(0.034)
Cost × income ∈ [2,000, 2,400[	-0.093**	(0.036)	-0.094**	(0.036)	-0.146*	(0.06)	-0.088*	(0.036)
Cost × income ∈ [2,400, 3,000[	-0.085*	(0.037)	-0.086*	(0.037)	-0.126*	(0.062)	-0.079*	(0.037)
Cost × income ∈ [3,000, 3,500[	-0.07†	(0.039)	-0.071†	(0.039)	-0.095	(0.064)	-0.061	(0.039)
Cost × income ∈ [3,500, 4,500[	-0.059	(0.04)	-0.06	(0.04)	-0.065	(0.066)	-0.056	(0.04)
Cost × income ≥ 4,500	0.017	(0.043)	0.016	(0.043)	0.064	(0.07)	0.016	(0.043)
Cost × age ∈ [18, 30]	0.301**	(0.044)	0.304**	(0.044)	0.459**	(0.078)	0.306**	(0.044)
Cost × age ∈]30, 40]	0.384**	(0.043)	0.389**	(0.044)	0.606**	(0.083)	0.391**	(0.044)
Cost × age ∈]40, 50]	0.45**	(0.043)	0.455**	(0.044)	0.717**	(0.088)	0.451**	(0.044)
Cost × age ∈]50, 60]	0.408**	(0.044)	0.412**	(0.045)	0.655**	(0.087)	0.407**	(0.045)
Cost × age > 60	0.385**	(0.063)	0.389**	(0.064)	0.616**	(0.113)	0.398**	(0.063)
σ	0.816**	(0.16)	0.87**	(0.217)	0.603**	(0.043)		
Residual control function duration peak			-0.006	(0.008)				
Residual control function duration off-peak			-0.013	(0.016)				
Log-likelihood	-17,441		-9,664		-17,923		-14,513	
Median VOT (in €/hr)	15.6		15.7		15.2		15.6	

*Notes: (1): Baseline specification, with stochastic schedule constraints. (2): Stochastic schedule constraints and control function for duration. (3): Full flexibility, all individuals can substitute across departure periods. (4): No substitution across departure periods. In this specification the mode dummies are identical across periods. Walking at peak hours is the baseline alternative. "income" represents the monthly individual income, "dist" is the distance, in 10 km and d_2, d_3 and d_4 are the inner values that split the distance interval equally in five. The reference categories are individuals with age < 18, with an income below €800. Duration measured in 10 minutes. Cost in €. Significance levels: **: 1%, *: 5%, †: 10%.*

Table 3 presents the estimated probabilities of being constrained (obtained from the workforce survey) and those for being able to travel at peak-hour only when constrained (calculated from the estimated parameters according to Equation (9)). The least constrained socio-professional categories are craftspersons, entrepreneurs, and private sector executives. The most constrained workers are public and retail employees and unqualified workers. When workers are constrained, we find that 78% of the time, they have to commute during peak hours. However, craftspersons, shopkeepers always have to make their trip during off-peak hours when constrained. The other categories which constraints make them commute during off-peak hours are entrepreneurs and self-employed individuals and qualified and unqualified workers. In contrast, constrained private executives always have to commute during peak hours. We also find that farmers, private employees, and students in high school or below are most likely to have only peak-hour travel available.

Table 3: Estimated probabilities of being constrained and having only peak-hour available.

Socio-professional category	**Prob. of being constrained** ($\hat{\phi}_c$)	**Std. error**	**Prob. only peak hour available** ($\hat{\pi}^*_c$)	**Std. error**
Farmers	0.302	0.011	0.991	0.031
Craftspersons	0.109	0.007	0	0
Shopkeepers	0.143	0.009	0	0
Entrepreneurs, self-employed	0.13	0.008	0.338	0.075
Public executives	0.382	0.008	0.732	0.017
Private executives	0.135	0.004	1	0
Education, health	0.636	0.006	0.785	0.006
Administrative professions	0.447	0.008	0.784	0.013
Technicians	0.473	0.01	0.515	0.013
First-line supervisors	0.527	0.014	0.519	0.011
Public employees	0.849	0.004	0.707	0.002
Private employees	0.624	0.009	0.852	0.007
Retail employees	0.884	0.006	0.581	0.002
Services	0.738	0.007	0.556	0.004
Qualified workers	0.793	0.005	0.406	0.003
Unqualified workers	0.869	0.006	0.444	0.003
Students $\leq$ high school	0.884	0.006	0.932	0.002
Students in higher education	0.109	0.007	0.748	0.088
Average	0.579		0.779	

Notes: $\hat{\phi}_c$ corresponds to the empirical share of respondents with constrained work schedules according to the workforce survey. $\hat{\pi}^*_c$ are estimates from our preferred specification, specification (1). Standard-errors for $\hat{\phi}_c$ correspond to the standard-error for the mean. Standard-errors for $\hat{\pi}^*_c$ computed using the delta-method and takes into account the variance of $\hat{\phi}_c$.

We further test the sensitivity of our estimation results to alternative model assumptions. These additional robustness checks and their results are presented and discussed in Appendix D.2. To account for the possible role of unobservables correlated with the trip's duration, we check that adding weather variables or a measurement of travel time reliability as controls does not affect our estimates. We study the effect of using a different cost definition for motorized vehicles and the impact of not including the correction to the public transport

cost. We also provide the estimation results when we use the two periods as nests. Finally, we check that our estimates are robust to alternative choice set definitions.

3.5 Values of travel time and substitution across modes and periods

Table 4 presents detailed information about the distribution of the VOT across individuals. We present the VOT distribution for the 2010 sample, which is used for the policy analysis. Due to the low number of observations in the 2020 survey, we limit counterfactual analysis to the 2010 data. We obtain an average value of travel time of €18.3/hr, which is higher than the median value of €16.6/hr. The mean value represents 77% of the mean wage in 2012 in the Paris metropolitan area (€23.9/hr).[14] This is very close to the ratio found by Goldszmidt et al. (2020) of 75% using natural field experiments on 13 U.S. cities. Barwick et al. (2024) finds a ratio of 95.6% for commuters in Beijing. Buchholz et al. (2024) finds an average VOT of $13.21/hr which represents 139% of the hourly wage. This value is rather specific because it is estimated on a sample of cab riders in Prague. Finally, our estimate aligns with Almagro et al. (2024), who find an average of $15/hr for Chicago, and with Kilani et al. (2012), who estimate an average of €17/hr for a working father in Paris.

We observe substantial heterogeneity in how individuals value their time in transport, reflected by the extreme minimum and maximum opportunity costs of time (€1.58/hr and €92.7/hr). Figure 9 of Appendix D.3 shows the distributions of VOT as functions of age, income, and distance. We find important heterogeneity in terms of age. Young individuals have the lowest VOT, and the VOT rapidly increases until 45. Regarding income, we see little heterogeneity for incomes below €3,000. Then, the VOT increases quickly with income due to the lowest sensitivity to the trip cost. Finally, the VOT is not monotonic in distance; the lowest VOTs are for very short and middle-length trips (20 km).

We compute the own and cross elasticities to driving duration and cost to better understand the substitution across departure periods for driving. These elasticities are crucial to predict individuals' reactions to tolls. Table 4 presents the distributions of these elasticities in the population for 2010. The duration elasticities for driving are highly heterogeneous across individuals. For instance, the duration elasticity at peak hours is between -7.1 and -0.01. The heterogeneity partly reflects the differences in the trip distance, which is highly correlated to duration. It is also the consequence of the heterogeneity in preferences, schedule constraints, and availability and characteristics of the substitutes for driving. We obtain an average of -1.01, slightly lower than the value obtained by Almagro et al. (2024) (-1.44 for peak hours).

[14] Source for the average hourly wage in Paris: https://www.lemonde.fr/les-decodeurs/article/2016/11/28/en-ile-de-france-le-salaire-horaire-depasse-de-41-celui-des-autres-regions_5039717_4355770.html.

The driving cost elasticities at peak hours are even more dispersed, between -13 and -0.004. The cost elasticities with values close to zero correspond to individuals with electric cars, who only pay the depreciation, maintenance, and insurance costs and have zero fuel costs. The cost elasticities are, on average, -0.58 at peak hours, very similar to the -0.55 found by Almagro et al. (2024).

Table 4: Distribution of the VOT and the driving duration and cost elasticities.

	Min	p1%	Mean	Median	p99%	Max
Value of travel time	1.58	2.75	18.3	16.6	53.8	92.7
Own elasticities						
$\mathcal{E}^{\text{duration}}_{t_1,t_1}$	-7.13	-4.93	-1.01	-0.54	-0.07	-0.01
$\mathcal{E}^{\text{duration}}_{t_2,t_2}$	-6.07	-3.74	-0.84	-0.57	-0.1	-0.03
$\mathcal{E}^{\text{cost}}_{t_1,t_1}$	-12.99	-3.97	-0.58	-0.28	-0.02	-0.004
$\mathcal{E}^{\text{cost}}_{t_2,t_2}$	-12.82	-4.12	-0.65	-0.35	-0.03	-0.005
Cross elasticities						
$\mathcal{E}^{\text{duration}}_{t_1,t_2}$	0.0004	0.0008	0.1	0.05	0.71	2.23
$\mathcal{E}^{\text{duration}}_{t_2,t_1}$	0.005	0.01	0.28	0.15	1.54	3
$\mathcal{E}^{\text{cost}}_{t_1,t_2}$	0.0001	0.0007	0.06	0.02	0.45	1.36
$\mathcal{E}^{\text{cost}}_{t_2,t_1}$	0.0004	0.003	0.15	0.07	0.93	3.33
Cross elasticities, conditional on $\mathcal{T}_{12}$						
$\mathcal{E}^{\text{duration}}_{t_1,t_2}$	0.004	0.009	0.24	0.18	1.32	2.63
$\mathcal{E}^{\text{duration}}_{t_2,t_1}$	0.03	0.08	0.68	0.55	2.49	5.55
$\mathcal{E}^{\text{cost}}_{t_1,t_2}$	0.0009	0.004	0.15	0.11	0.8	1.76
$\mathcal{E}^{\text{cost}}_{t_2,t_1}$	0.003	0.01	0.36	0.25	1.93	7.72

Note: Value of travel time in €/ hr. Elasticities in %. "t_1" represents peak hours and "t_2" off-peak hours. All statistics computed using survey weights for 2010 sample. Cross elasticities, conditional on $\mathcal{T}_{12}$ correspond to individuals who can substitute across departure periods.

In the bottom panel, we provide the cross elasticities with and without conditioning on the ability to do intertemporal substitution. Individuals are more elastic to changes in duration at peak hours than at off-peak hours, indicating strong preferences for driving at peak hours. The cross elasticities of driving at peak hours to the trip duration at off-peak hours are very low (0.1 on average), indicating low inter-temporal substitution. This is the consequence of important schedule constraints that limit inter-temporal substitution. We obtain average elasticities almost three times larger when conditioning on the ability to substitute across departure times. This highlights the critical role of schedule constraints in limiting individuals' responses to duration and cost changes.

3.6 Individual speed shocks

The last primitives of the transportation mode choice model to recover are the individual and time-specific driving speed shocks that are the ρ_{nt} in Equation (5). We take the logarithm of Equation (5):

$$\log(\text{duration}_{nt}) = \log\left(\sum_{a=1}^{A} \frac{k_n^a}{v_t^a}\right) + \tilde{\rho}_{nt}.$$

where $\tilde{\rho}_{nt} = \log(\rho_{nt})$. We use the TomTom durations and trip distances by area to estimate the inverse of the initial speeds, v_t^a. We use the non-linear least squares method. The individual speed shocks $\tilde{\rho}_{nt}$ are the residuals of this regression. This regression also provides us with the initial speeds by area, which are provided in Table 5. Speeds are always higher during off-peak hours than peak hours. They are also much higher on the highways, followed by the ring roads, far suburbs, close suburbs, and finally, in the city center.

Table 5: Estimated average speeds from TomTom data.

	Peak hours		Off-peak hours	
Area	**Average speed**	**Std. error**	**Average speed**	**Std. error**
Highways	58.6	0.82	84.6	1.06
City center	13.2	0.13	17.4	0.148
Ring roads	28.5	0.565	48.8	0.899
Close suburb	15.9	0.101	20.1	0.11
Far suburb	24.6	0.126	28.6	0.127

Note: Speeds in km/hr. Standard errors are computed using the delta-method from the estimates of the inverse of speeds.

4 Estimation of the road traffic congestion technologies

4.1 Overview of the data

We split the Paris area into five areas: the city center, the ring roads, the close suburb, the far suburb, and the main highways that connect the city center to the suburbs. We estimate the congestion technology for the city center, ring roads, and highways. Due to the absence of data, we cannot directly estimate a congestion technology for the suburbs. However, we still allow for adjustment of the equilibrium speeds in the suburbs but make additional functional form assumptions on their congestion technologies. More specifically, we assume the congestion technology in the suburbs is a convex combination of those on the highways and the city center. We provide the map that shows the areas and the locations of road traffic sensors in Appendix D.4.1.

To estimate the road congestion technologies, we rely on hourly data on traffic conditions from 1,242 road traffic sensors for 2016 and 2017. We use 2016 and 2017 data from traffic sensors since it is the earliest year available for highways.[15] The road traffic sensors typically record up to four variables: the traffic flow (in vehicles per hour), the traffic density (in vehicles per kilometer), the occupancy rate, i.e., the percentage of time during which the

[15]We use data from 2010 for the city center and the ring roads to evaluate the differences in traffic between the two periods. We find that the average speed decreased by only 5.5% and 5.1% at peak and off-peak hours in the city center between 2010 and 2016. In the ring roads, we find an increase of 0.7% at peak hours and a decrease of 3.7% during off-peak hours.

sensor detects a car (in percentage per hour), and the speed (in km/hr). We provide more details about these variables and their theoretical relationships in Appendix D.4.2. We rely on two key variables: speed (in km/hr) and road occupancy rate. We use the occupancy rate to represent the traffic level since it seems more appropriate because we aggregate different roads. We use these two variables to estimate the relationship between speed and occupancy rate denoted $\tilde{f}^a$. Note that this function differs from the speed function f^a defined in Equation (7) because the latter requires the number of kilometers driven as an argument. Section 4.4 defines a mapping between the occupancy rate and the number of kilometers driven K_t^a.

4.2 Speed-occupancy rate relationship

For the estimation, we observe a sample of $i = 1, ..., I$ independent observations of speed v_i^a and occupancy rate τ_i^a. There are unobserved speed shocks ν_i^a, so that we can write the speed as:

$$v_i^a = \tilde{f}^a(\tau_i^a) + \nu_i^a.$$

We make minimal functional form assumptions on $\tilde{f}^a$ by relying on basis polynomials. More specifically, we use Bernstein basis polynomials of degree Q^a:

$$v_i^a = \sum_{q=0}^{Q^a} c_q^a B_q(\tau_i^a) + \nu_i^a. \tag{11}$$

The coefficients c_q^a are the parameters of interest, and B_q are the Bernstein basis polynomials given by:

$$B_q(\tau) = \binom{Q^a}{q} \tau^q (1-\tau)^{Q^a - q}.$$

Since the occupancy rate τ_i^a and speeds are simultaneously determined in equilibrium, τ is correlated to the speed shock ν. We thus rely on instruments and use the general method of moments to estimate the parameters $(c_q^a)_{q=0,...,Q^a}$ in Equation 11. In addition, we impose that the speed functions are weakly decreasing. This can be imposed by restricting that $c_q^a \geq 0$ and $c_{q+1}^a \leq c_q^a \quad \forall q \in \{0, ..., Q^a - 1\}$.

The order of the Bernstein polynomial approximation, Q^a, is selected to minimize the mean squared forecast error (MSFE). We follow Hansen (2014) and use the leave-one-out estimator of the MSFE, which can be summarized by the following cross-validation criteria:

$$Q^a = \underset{1 \leq p \leq \bar{Q}}{\arg\min} \left\{ \frac{1}{I^a} \sum_{i=1}^{I^a} \frac{\hat{e}_{ip}^2}{\left(1 - h_{ip}^a\right)^2} \right\},$$

where $\bar{Q}$ is the maximum degree of the polynomial considered and I^a is number of observations in area a. $\hat{e}_{ip}^2$ is the squared prediction error for observation i under a polynomial basis of order p. h_{ip}^a is the leverage value for observation i given by the i^{th} diagonal element of the projection matrix $\mathcal{B}_p^a \left(\mathcal{B}_p^{a\prime} \mathcal{B}_p^a\right)^{-1} \mathcal{B}_p^{a\prime}$ where $\mathcal{B}_p^a = (B_0^a, ..., B_p^a)$ is a matrix containing the values of the Bernstein basis polynomials $B_p(\tau)$ for all observations.

To mitigate the concern about the traffic level being correlated with the speed shocks, we first exclude from our sample the observations with extreme weather conditions. For instance, snow may discourage individuals from driving and reduce their speed. Extreme weather conditions are defined by either snow, temperatures below the 5% percentile or above the 95% percentile of the entire temperature distribution, or wind or rain intensity above the 95% percentile of the entire wind or rain distribution. To be conservative, we drop the observations with an extreme weather event during the hour or up to three hours before or after.

Then, we construct instruments to estimate the parameters of the Bernstein polynomial. Valid instruments are variables uncorrelated with speed shocks but affect the traffic level. We use the following dummies: hour, day-of-the-week, school holidays, bank holidays, low public transport (number of daily passengers below the 25% quantile), days with a driving restriction in place, an accident in a 1.5 km radius donut (5 km on the highways), an accident in a 1.5 km radius (5 km on the highways) during the previous hour, a temperature between 19 and 25°celsius, temperatures between 4 and 9°celsius. All these variables presumably shift the traffic level exogenously and are not correlated with speed shocks. For instance, cold weather is likely to induce more car usage. However, driving speeds are affected only by changes in the level of traffic and not directly by low temperatures. Kreindler (2023) also uses hour and day-of-the-week dummies. In the same spirit, we use bank holidays and school holidays. The low number of public transport passengers represents a proxy for a strike event. An accident close to the road sensor is likely to affect traffic level and speed simultaneously. This is why we use a donut around the sensor to capture changes in traffic due to re-routing and accidents in the previous hour. Finally, we also use the interactions between the dummies if there are more than 500 observations with positive values. Ultimately, we use 391 instruments for the highways, 380 for the ring roads and 390 for the city center, and implement the two-step GMM to use the efficient weighting matrix.

The relationship between speed and traffic is identified from the local variation in traffic conditions in the data, conditional on the instruments. Since our instruments are all dummy variables, interpreting the orthogonality conditions is straightforward. We exploit several dimensions of variation between observations in the traffic data. We observe data for different

roads, at different hours, on different days, and with different exogenous shifters of traffic level.

We make several assumptions to estimate the congestion technologies in the close and far suburbs, where we do not have detailed traffic data. First, we assume the close and far suburbs share the same congestion technology. Second, we assume this technology is a convex combination of the congestion technologies of the city center and highways. We pin down the parameter of the convex combination by relying on a limited dataset we obtained from the Seine-Saint-Denis department, one of the four departments composing the close suburbs. The data contains one week of hourly observations for road traffic sensors in 2023. Instead of providing speed measurements, the data assigns each car to intervals such as 0 to 30 km/hr. These large intervals do not allow us to estimate a speed-traffic curve like in the other areas. We still use this dataset to compute peak and off-peak hours' average speeds and occupancy rates. We calibrate the parameter of the convex combination to be the closest to the two speed-occupancy rate data points. The parameter reflects a weight of 17.7% for the highways technology and 82.3% for the city center technology.

4.3 Summary statistics and estimation results

We explain how we construct the final sample to estimate the congestion technologies in Appendix D.4.3. It contains 1.2 million hourly observations for the ring roads recorded from 117 stations. We have 599 measurement stations recording 5.12 million observations for the city center. Finally, we use 643 stations and 3.84 million observations for the highways.

Table 6: Road traffic conditions by area.

		Peak	**Off-peak**	**All sample**		
	Area	**Mean**	**Mean**	**Mean**	**Median**	**Std. dev.**
Speed	Highways	41.7	66.7	67.7	76	33.3
	City center	19.8	29.4	22.8	17.8	17.7
	Ring roads	30.5	56.7	44.1	44.6	21.1
Occupancy	Highways	24.6	14	15	10.7	11
rate	City center	18.9	6.7	14.2	10.1	11.6
	Ring roads	32.5	15.6	22.6	20.6	12.1

Note: Speed is in km/hr, and occupancy rate is in %. Averages at peak and off-peak hours are computed using our final sample and weighted by the average traffic flow of the traffic sensor. Peak hours are between 8:00 and 8:59 a.m., and off-peak hours are between 6:00 and 6:59 a.m.

Table 6 provides the summary statistics for the speeds and occupancy rates in the different areas. We focus on 8:00 to 8:59 a.m. for peak hours and on 6:00 to 6:59 a.m. for off-peak hours to be comparable with the time used to do the TomTom queries. We observe significant heterogeneity across areas, suggesting that our partition is relevant. Speeds at peak and off-peak hours significantly differ, supporting our differentiation across periods. In addition

to providing evidence of heterogeneity across areas, the traffic speeds and occupancy rates are highly variable; we leverage these variations to estimate flexible road congestion technologies, given that the variability is still important after conditioning on the instruments.

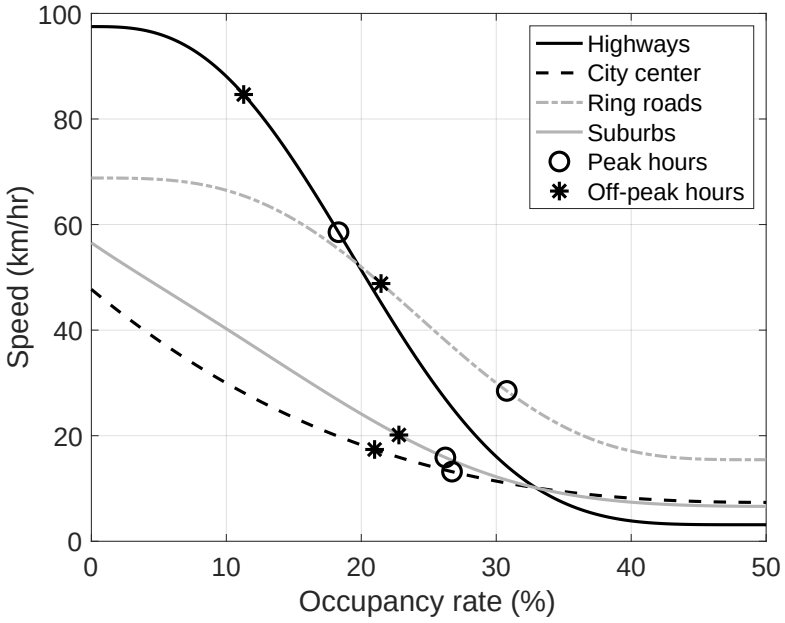

Figure 1: Estimated congestion technologies and initial traffic conditions.
Note: Initial conditions are average speeds at peak and off-peak hours from TomTom predicted durations. We provide the initial conditions in the close suburbs on the suburbs congestion technology curve.

In Figure 1, we provide the congestion technologies for the different areas (note that the close and far suburbs have the same technology, but they do not have the same equilibrium traffic conditions). The initial traffic conditions are obtained from the average speeds obtained from TomTom trip durations (see Table 5). From the initial speeds, we back out the initial occupancy rates by inverting the congestion technologies:

$$\tau_t^a = \left(\tilde{f}^a\right)^{-1}(v_t^a).$$

Note that τ_t^a is unique since $\tilde{f}^a$ is monotonically decreasing in speed at the initial speed value. Understanding which occupancy rates reflect a congested road helps interpret the congestion technology graph. The authorities consider the traffic fluid if the occupancy rate is below 15%, pre-saturated if between 15% and 30%, and saturated if it is above. According to this definition, the traffic is pre-saturated during peak and off-peak hours in all areas except on the highways (fluid during off-peak hours) and the ring roads (saturated at peak hours).

As Figure 1 shows, the estimated values of the maximal speeds are very much in line with the maximum speed limits in each area. We estimate it to be 97.5 km/hr for highways

compared to speed limits that vary between 90 and 130 km/hr depending on the road and the location. The speed limit is typically 70 km/hr on the ring roads, which is very close to our 68.8 km/hr estimate. Lastly, the speed limit is usually between 30 and 50 km/hr in the city center, close to our estimate of 47.7 km/hr. In the suburbs, the maximal speed is 56.5 km/hr. Therefore, our estimates of maximal speeds across areas show high consistency. We provide the R^2 and the polynomial degrees of the models for each area in Appendix D.4.4. The fits are particularly good for the highways and ring roads (with R^2 of 0.65 and 0.69, respectively), and the degree of the polynomial is high (8). In contrast, we select a polynomial of degree 3 in the city center and explain only 21% of the variance.

Our congestion technologies show heterogeneity across areas. Clearly, our estimates reject the assumption of a single, city-wide congestion technology and show that congestion technologies do not follow simple functional forms. We have a high speed for low traffic levels on highways, but it becomes slower than ring roads for occupancy rates above 19.7%, and slower than any other area for occupancy rates above 32.9%. This can be explained by the role of interchanges, entries, and exits on highways, which may slow down driving speeds quickly when the traffic increases. We also obtain a critical difference of 26.1 km/hr in speeds between peak and off-peak hours.

The congestion curve for ring roads remains flat initially: the slope remains higher than -0.72 until an occupancy rate of 10%. In contrast, the speed in the city center displays a convex relation, with speeds decreasing faster for lower occupancy rates than for larger ones. In the suburbs, speeds are higher than in the city center for occupancy rates below 32.9%. Then, the suburbs' speeds become only slightly below those of the city center.

4.4 Mapping between occupancy rate and kilometers driven

To estimate f^a, we need a mapping from the number of kilometers driven to the occupancy rate τ_t^a in each area. We assume an affine relation between the occupancy rate and the total number of kilometers driven. Formally, we introduce a scale parameter ϕ^a such that :

$$\tau_t^a = \phi^a \times (K_t^a + K_{0t}^a). \tag{12}$$

where K_t^a is the number of kilometers driven in the area a at time t predicted by our transportation choice model and K_{0t}^a represents the rest of traffic that we do not model (irreducible traffic). We can thus obtain f^a as:

$$f^a = \tilde{f}^a \left(\phi^a \times (K_t^a + K_{0t}^a)\right).$$

We can only identify two parameters per area because we observe individual choices and speeds for only two periods.[16] We impose that the irreducible traffic level is identical at peak and off-peak hours: $K^a_{0t} = K^a_0$. We could, alternatively, impose some restrictions across areas and let the irreducible traffic level vary with the period. However, given that the areas have very different sizes and may be subject to different levels of irreducible traffic, our assumption seems more appropriate.

With two linear equations and two unknowns, we can find a unique pair of parameters for each area. We further impose that irreducible traffic implies occupancy rates between 0 and 50% and use the constrained least-squares method that minimizes the sum of square deviations from Equation 12. The calibrated parameters are presented in Table 7. We obtain a relatively sizeable irreducible share of traffic in the suburbs (76.6% and 78.7% of traffic for the close and far suburbs, respectively). At the same time, we estimate lower levels of irreducible traffic for the city center and the ring roads (36.6% and 33.4%, respectively). Finally, we estimate a tiny share of 1.11% on the highways.

Table 7: Calibrated parameters of the mapping between occupancy rates and driven distances.

Area	**Scale parameter** ($\phi^a \times 10{,}000$)	**Irreducible traffic** ($K^a_0/10,000$)	**Irreducible traffic share (%)** ($K^a_0/(K^a_0 + K^a_{t_2}) \times 100$)
Highways	0.036	5.57	1.11
City center	0.426	23	36.6
Ring roads	0.361	28.2	33.4
Close suburb	0.043	465	76.6
Far suburb	0.01	1,491	78.7

Notes: The share of irreducible traffic is in % of the distance driven at peak hours.

4.5 Fit of the model

We now evaluate the fit of the model. By construction, our model almost exactly predicts the average speeds that rationalize TomTom's expected trip durations. The imperfect prediction comes from the constraint of bounding the traffic below 50% when estimating the mapping parameters. This implies that the equilibrium speeds differ slightly from those obtained in Table 5. The individual trip durations are thus going to be slightly different from the TomTom ones. We can see from the difference between columns 2 and 3 of Table 8 that the difference is negligible for the mode shares. This Table also suggests a good prediction of aggregate shares. Indeed, all the differences between observed and predicted shares are at most 0.7 percentage points. These results give us confidence in the ability of the model to predict equilibrium transportation mode shares.

[16] We only use the 2010 EGT sample. The 2020 EGT sample has too few observations, which compromises the sample representativity at the area level.

Table 8: Shares of transportation modes observed and predicted by the model.

	Observed	**Predicted with TomTom durations**	**Predicted with Equilibrium speeds**
Bicycle, peak	1.59	1.89	1.88
Pub. transport, peak	34	33.9	33.8
Motorcycle, peak	1.35	1.29	1.28
Walk, peak	15.2	14.9	14.9
Car, peak	24.4	23.9	24
Car, off-peak	8.46	8.35	8.46
Pub. transport, off-peak	11.7	11.7	11.6
Walk, off-peak	2.11	2.77	2.77
Bicycle, off-peak	0.446	0.568	0.566
Motorcycle, off-peak	0.644	0.763	0.756

Note: in %. All shares computed using survey weights for 2010.

We further assess the fit of our model by comparing the distances driven in each area. If our model predicts the total number of individuals driving well, the distance analysis reveals whether we can also predict well who is driving. Table 9 shows that we get very close estimates across all areas during peak hours, with the difference being smaller than 4.1% in all locations. We obtain slightly more extensive differences during off-peak hours. In particular, we underpredict distances in the highway and the city center but overpredict the amount of driving through the ring roads. We do not consider these differences large enough to signal the model's inability to predict counterfactual equilibrium outcomes.

Table 9: Observed and predicted distances driven.

	Peak hours		**Off-peak hours**	
Area	**Observed**	**Predicted**	**Observed**	**Predicted**
Highways	502	495	307	267
City center	39.7	39.8	26.2	21.7
Ring roads	57.1	56.3	31.3	33.8
Close suburbs	148	142	67.9	65.5
Far suburbs	418	404	170	161

Note: in 10,000 of kilometers.

Table 10 compares the average speeds from road sensor traffic data and those predicted from the model equilibrium (for the highways, city center, and ring roads where we have the data). This comparison constitutes an external validity check since the average speed data from road traffic sensors are not directly used in the estimation. We find that our estimates are not perfectly aligned with the average speeds but are pretty similar. Our estimates are optimistic for the highways but conservative for ring roads and the city center, particularly during off-peak hours. Nevertheless, we predict speeds in the same order of magnitude as those recorded by the sensor data, and we correctly predict the speed ranking between areas for both periods.

Table 10: Predicted equilibrium speeds and average speeds from traffic data.

Area	Peak hours		Off-peak hours	
	Traffic data	**Eq. speeds**	**Traffic data**	**Eq. speeds**
Highway	46.9	59.6	68.4	88.4
City center	22.5	13.1	31.4	19.1
Ring roads	31.8	29	57.5	46.8
Close suburb		16.2		20.3
Far suburb		24.9		28.8

Note: in km/hr.

4.6 Check of the equilibrium uniqueness

We now apply the method developed in Section 2.3 to verify that our algorithm is a contraction. Given the estimated model parameters, we check that the model has a unique equilibrium. We provide in Appendix D.5.1 the analytical formula for the Jacobian of $\mathbf{g}(.)$.

We compute the Lipschitz coefficients for values of the algorithm tuning parameter κ between 0 and 0.99 with a step of 0.01. We solve for these coefficients at the equilibrium speeds without policy and under different policy environments we consider in section 5. We calculate:

$$\max_{a\in A}\max_{t\in T}\max_{a'\in A}\max_{t'\in T}\left|\frac{\partial g_t^a(\mathbf{v}^*,\kappa)}{\partial v_{t'}^{a'}}\right|,$$

where $\mathbf{v}^*$ denotes the vector of equilibrium speeds. Panel (a) of Figure 2 shows that only when κ is equal to 0, i.e., when we only iterate on the speed function, the algorithm is not a contraction. We also find that the policies decrease the Lipschitz coefficients of the algorithm so that the no-policy environment requires the highest κ to have a contraction.

We also check for which values of the tuning parameters our algorithm is a contraction in the entire set of possible speed values in their interval $[\underline{\mathbf{v}}, \overline{\mathbf{v}}]$. This time we calculate:

$$\max_{a\in 1,\dots,A}\max_{t\in 1,\dots,T}\max_{a'\in 1,\dots,A}\max_{t'\in 1,\dots,T}\max_{\mathbf{v}\in[\underline{\mathbf{v}},\overline{\mathbf{v}}]}\left|\frac{\partial g_t^a(\mathbf{v},\kappa)}{\partial v_{t'}^{a'}}\right|.$$

Since this optimization is intense, we do a coarser grid search over the values of κ between 0 and 0.95 with a step of 0.05. Panel (b) of Figure 2 shows that there are values of $\kappa < 1$ for which the function is a contraction on the entire space of the speeds. From $\kappa = 0.55$, the algorithm is a contraction under all policies. This time again, the no-policy environments is associated with the smallest set of κ that ensures our algorithm is a contraction. The lowest value of κ that corresponds to the lowest Lipschitz coefficients under the different policy environments is thus 0.55. We use 0.65 to solve the equilibrium speeds in the different counterfactual simulations.

We show in Appendix D.5.2 the number of iterations and the computation time needed to solve the model for different values of κ in the no-policy environment. We can see it increases exponentially with the tuning parameter. We obtain the highest speed for $\kappa = 0.55$. However, the value we choose, $\kappa = 0.65$, increases the convergence time by only around 50%.

Figure 2: Lipschitz coefficients at the equilibrium speed and for any speed.

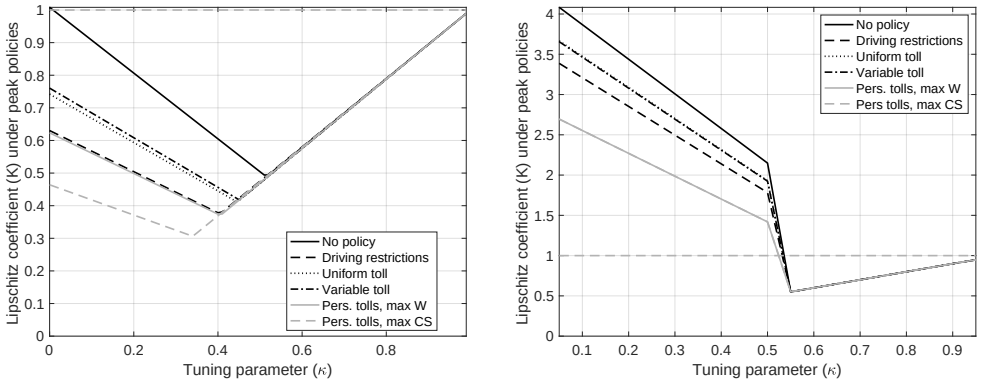

(a) At the equilibrium speeds.

(b) In the space of all possible speeds.

5 Quantifying the welfare consequences of the regulations

Our model predicts individual probabilities of choosing each transportation mode and the equilibrium driving speeds at peak and off-peak hours in the five areas. Thus, we do not predict counterfactual choices but individual choice probabilities, which we use to compute the expected number of individuals choosing each transportation mode and departure period. Before analyzing policy interventions, we evaluate how severe congestion problems are. We also quantify the role of scheduling constraints on congestion.

5.1 Value of driving, and marginal costs of congestion

We measure the value of driving at the initial equilibrium speeds by relying on consumer surplus changes when we remove the driving option or modify the speeds. We provide in Appendix E.1 the formula for the consumer surplus. If individuals could not take their cars at peak hours, they incur a surplus loss of €6.84 million, corresponding to €2.3 per trip for each potential driver.[17] Second, we measure the value of driving at peak hours under maximum speeds, given the irreducible portion of traffic in each area. The speed improvements lead to a

[17] A potential driver is an individual who owns a car.

total surplus increase of €9.9 million, corresponding to €3.28 per potential driver. The value of driving at peak hours at maximum speeds is 1.45 times that of driving at initial speeds, highlighting the detrimental effect of congestion in the Paris metropolitan area. Congestion generates a total increase in travel time of 202 thousand hours, equivalent to an average additional 4 minutes per driver (12.6% of the average trip durations for potential drivers).

We define the marginal costs of congestion for an area, at a given period, as the total surplus losses associated with one additional kilometer driven or an extra driver in that area. For the case of an extra driver, we add the average number of kilometers driven by a potential driver in that area. Adding one kilometer or a driver marginally decreases the area speed, which in turn increases car trip durations by a small amount for everyone driving in that area. We calculate the surplus variation from these marginal changes at the individual level. The society marginal cost thus corresponds to the sum of all surplus variations.

Table 11 shows area-specific marginal costs for an additional kilometer are between 0.2 and 129 cents. The highways and the far suburbs have the lowest marginal costs. The costs are particularly small during off-peak hours on those areas. This is the effect of area size; one additional kilometer has a very small impact on the traffic level. In addition, the speeds are relatively high in these areas during off-peak hours.

The costs associated with an additional driver are between 27 cents (for the far suburbs during off-peak hours) and €4.29 (for the highways at peak hours). The marginal costs are much higher at peak hours than at off-peak hours, with the average being 3.5 times larger. The differences between periods are quite heterogeneous across areas. The differences are smaller in the city center and the close suburbs, whereas the highways exhibit a much larger difference; the marginal cost of congestion per driver at peak hours is 6.5 times larger than during off-peak hours. The existence of schedule constraints that forces many individuals to commute during peak hours explains why the costs of congestion take much larger values at peak hours. Indeed, the slope of the congestion technology is almost two times higher (in absolute value) at peak hours than during off-peak hours on the highways. Finally, we also compute a marginal cost of congestion where we add an individual driving with the average itinerary (i.e., distance traveled in each area) among individuals owning a car. The average costs are €6.33 at peak hours and €1.81 at off-peak hours.

The most appropriate way to compare our results to results in the literature is to use our estimates of the marginal costs of congestion per kilometer. Making such a comparison puts our congestion values larger to Couture et al., 2018 (3.6 cents of $ for several U.S. cities), Akbar and Duranton, 2017 (10 cents of $ for Bogota), and Yang et al., 2020 (3 yuan or

approximately €0.36 for Beijing).[18] Our findings are closer to Koch et al. (2023) who estimate a marginal cost for an additional kilometer to be between 45 and 73 cents for Berlin between 6 and 10 a.m., and an average marginal cost of an additional average driver of €4.48.

Table 11: Estimated initial marginal costs of congestion by area.

	One kilometer (in cents)		One average driver (in €)	
Area	**Peak**	**Off-peak**	**Peak**	**Off-peak**
Highways	37.3	5.5	4.29	0.658
City center	129	54	4.24	1.79
Ring roads	97.7	27	4.24	1.2
Close suburb	55.2	22	1.62	0.626
Far suburb	14.7	0.2	0.882	0.268
Average			6.33	1.81

Note: "Average" is the marginal cost for the average driver's itinerary across areas.

Finally, we assess the importance of the schedule constraints. To do so, we recompute the new equilibrium if individuals are always able to substitute inter-temporally. We find that removing the constraints would increase the average individual surplus by €1.22. The share of individuals commuting during off-peak hours would raise by 2.92 percentage points. In contrast, if individuals can never substitute inter-temporally, the average surplus decreases by €1.02 and the share of individuals choosing peak hours goes up by 1.78 percentage point.

5.2 Main outcomes of interest and policy overview

Our estimated welfare effects of the policy are for one trip per person for the entire population of commuters in the Paris area.[19] We measure the policies' impacts on consumer surplus, tax revenue, and emissions. We define an aggregate welfare measure W that is the sum of the change in aggregate consumer surplus, tax revenues and the benefits from avoided emissions valued at standard levels.

We rely on a 2019 report from the European Commission (Van Essen et al., 2019) for the social costs of emissions (in €/ton) and use the values specific to urban areas in France. Table 12 contains the social cost of the different pollutants. Additional details on how we selected these costs can be found on Appendix E.2. On average, in our sample, the social cost of emissions per km for a gasoline car is €3.4 cents, while for a diesel car it corresponds to €4.5 cents (the detailed decomposition is provided in Table 25 in Appendix E.2).

[18] We use the average 2014 CNY-EUR exchange rate from https://www.exchangerates.org.uk/CNY-EUR-spot-exchange-rates-history-2014.html.

[19] There are, on average, 224 working days annually and two commuting trips per day, so we should multiply the costs by 448 to convert them into annual terms.

Table 12: Social costs of emissions.

	CO_2	NO_X	HC	PM
Social cost (€/ton)	189	27,200	1,500	407,000

We study the welfare effects of three policies: (1) driving restrictions banning a fraction of cars randomly, (2) uniform tolls, and (3) variable tolls linear in the trip's distance (or per-km toll). We focus on policies applicable at peak hours only so that driving during off-peak hours is never constrained or charged. For robustness, we present the results of the same analysis with policies applicable during both peak and off-peak periods and show that the results are qualitatively similar. We choose to focus on peak-hour policies in the main analysis for three reasons. First, congestion is most severe at peak hours, leading to high pollution levels and exacerbated congestion effects. So, targeting peak hours is very relevant. The second reason is that our model includes substitution across periods. This is a model feature that is rarely covered in the literature and is particularly relevant when regulations are period-specific. Finally, there are several real-life examples of congestion charges, with greater tolls during peak hours.[20]

We compare the different policies at all stringency levels. To make a fair comparison across policies, we compare policies that achieve the same traffic reduction during peak hours. Traffic reduction is likely to be the main objective of introducing a transportation policy. Note that the comparison results would be very similar if instead of considering the traffic reduction outcome we used the the emissions cost reduction.[21]

Since 0.07% of the individuals in our sample do not have an alternative to cars, they would have an empty choice set when simulating driving restrictions under schedule constraints. To overcome this issue, we assign these individuals a very bad public transport option. Its duration is calculated using the 10% percentile of the distribution of public transport speeds.

5.3 Comparison of simple instruments across policy levels

Figure 3 presents the welfare losses, surplus losses, and tax revenues associated with the three policies. Panel (a) shows that the two types of tolls have positive welfare impacts for moderate stringency levels. In sharp contrast, driving restrictions always generate welfare losses. Second, we can see that the per-kilometer toll is always superior to the uniform toll for welfare. The variable toll has also a broader range of welfare-enhancing policies. The

[20]Some examples of currently applied congestion pricing schemes with prices specific to peak hours are Santiago, Stockholm, Oslo, and Singapore.

[21]Panel(a) of Figure 4 below indeed suggests that the policies have very similar effects on the emissions cost reductions.

uniform toll generates welfare gains for reductions in the driving distance below 30.7%, while the variable toll can reach 51.7% of traffic reduction without welfare loss. Welfare-enhancing policies are uniform tolls below €5.4 or per-km tolls below €0.455/km. The optimal uniform and variable tolls maximizing total welfare are €2.3 and 20 cents/km, respectively. The optimal variable toll reduces traffic much more than the optimal uniform toll (25.7% against 14.1%). The welfare difference is significant: the optimal variable toll leads to €239,000 more than the optimal uniform toll.

Panel (b) and (c) help understand where the welfare gains come from. There are two key insights from Panel (b), which provides the changes in consumer surplus. First, we can see that all policy instruments and all the policy stringency levels generate consumer losses. This means that even if the policies relax the congestion problems, the speed improvements for individuals who drive never compensate for the costs of the tolls or the driving restrictions. There are two reasons for that. First, the speed improvements are modest, particularly in the city center and the suburbs as showed by Figure 12 in Appendix E.3.1. Second, the valuation of travel time savings does not compensate for the toll cost or the cost of being restricted a fraction of the time.

Secondly, the ranking of the policies in terms of surplus change is different from the ranking in terms of welfare. The uniform toll is always the policy that generates the largest surplus losses, followed by the driving restrictions and the variable toll. This is in part the consequence of needing to impose very high uniform tolls to trigger traffic reductions. Indeed, Panel (b) of Figure 4 shows that the average variable toll is always significantly lower than the uniform toll.

The variable toll has the property of targeting individuals with long-distance commutes. Indeed, Panel (c) of Figure 4 shows the average distances driven at peak hours under the regulations are quite different. The average distance only slightly increases under driving restrictions; it increases under uniform toll and decreases under the variable toll. This is helpful to understand who is targeted by each type of regulation. Driving restrictions force all individuals to contribute to traffic reductions. But, by nature, this policy targets randomly; this explains why we observe a relatively constant average trip distance across stringency levels. The uniform toll discourages short-distance trips, making this policy inefficient at reducing traffic. In contrast, by pricing based on the distance, the variable toll discourages long-distance individuals from driving and thus efficiently decreases traffic.

Panel (c) of Figure 3 shows that the welfare gains come from the ability of the tolls to generate extensive tax revenues. The toll revenues are substantial; they are the reasons for welfare improvements from the policies. The tolls can only improve welfare if the tax revenues

are redistributed. The uniform toll is, most of the time, better at generating revenue than the variable toll. This is because the uniform toll is set at a high level, as explained in the previous paragraph. In addition, we obtain Laffer curves as the total tax revenue decreases from certain policy stringency levels. The maximum tax revenues occur under very stringent policies, indicating again that it takes high toll values to discourage individuals from driving at peak hours. Panel (a) of Figure 4 shows that the emissions gains are modest since they are below €0.35 million, while the consumer surplus decreases by up to €7 million.

Figure 3: Change in welfare, consumer surplus, and tax revenue.

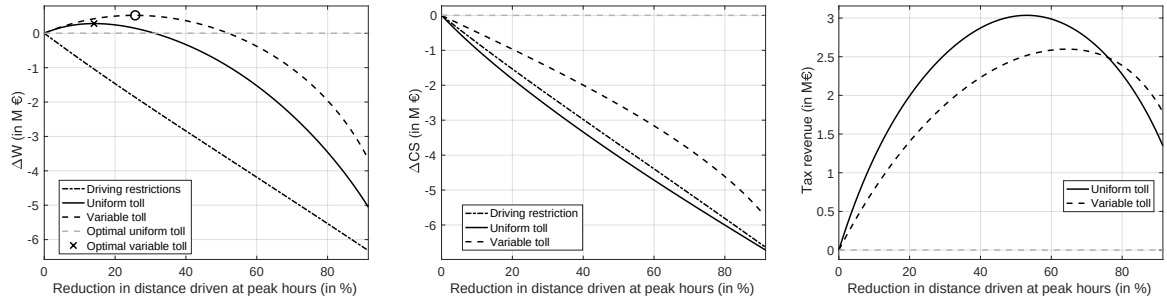

(a) Welfare. (b) Consumer surplus. (c) Tax revenues.

Figure 4: Additional policy outcomes.

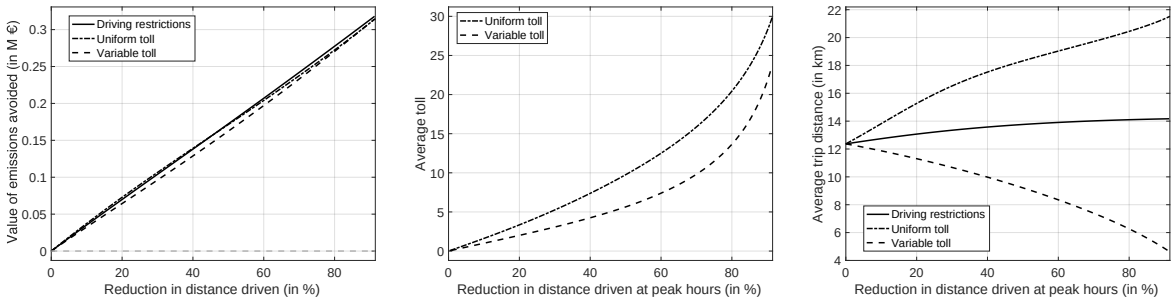

(a) Value of emissions. (b) Average toll. (c) Average distance conditional on driving at peak hours.

Figure 5 presents the total consumer surplus losses using distributional weights (the inverse of income), the range of surplus changes (difference between maximum and minimum surplus changes), and the difference in surplus changes between the top and bottom 10% of the income distribution. First, we can see that using distributional weights does not affect the policy ranking nor the consumer surplus loss magnitudes, as seen in Panel (a).

From Panel (b), we see that the differences between the maximum and minimum consumer surplus changes are similar across policies for mild stringency levels (up to 20%). After this,

policies diverge, with large differences for the uniform toll and smaller ones for the variable toll. Overall, we do not see major differences in the change of surplus ranges across policies.

Finally, Panel (c) shows the difference in changes in consumer surplus between the top and bottom deciles of the income distribution. All policies are always progressive as they generate more losses to high-income individuals. Second, we can see that progressivity increases with the stringency level. The driving restriction generates the largest differences between deciles, while the variable toll leads to the smallest ones. The analysis of the distributional effects shows that the three policies are all progressive and have similar distributional consequences. The driving restriction appears slightly more progressive than the two other regulations.

Figure 5: Change in distributional outcomes.

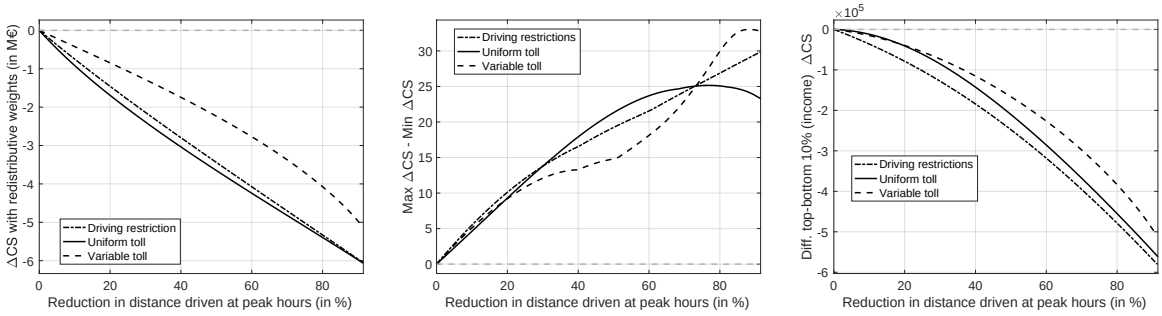

(a) ΔCS with distributional weights.

(b) ΔCS range.

(c) Difference in ΔCS between the top and bottom 10% of the income distribution.

Figure 6 presents how the welfare changes from the policies are distributed across the areas of origin of the individuals. Panel (a) shows that the ranking of the areas in terms of welfare changes remains constant across stringency levels for driving restrictions. The far suburbs are the most affected, followed by the close suburbs and, finally, the city center. This is consistent with suburban individuals having longer commutes and less access to public transport.

Panel (b) shows the distribution of welfare under uniform tolls. For mild stringency levels, the welfare gains are higher in the far and close suburbs than in the city center. When the stringency levels become high (around 22%), the ranking reverts, and the individuals living in the far suburbs are again the most affected. Large speed gains indeed compensate for the toll costs for long-distance drivers under mild stringency levels. Under higher toll values, the speed gains are insufficient to compensate for the toll cost. In contrast, we can see that the uniform toll is welfare-improving in the city center for traffic reduction levels of up to almost 60%.

Finally, Panel (c) shows the results for the variable toll. As for the uniform toll, for

moderate policy stringency levels, welfare gains are higher in the far and close suburbs. This highlights that the speed improvements are more valuable for individuals living in the suburbs, with typically longer commutes. However, when the stringency becomes very high, the individuals in the suburbs experience high welfare losses because they do not have good alternatives to driving. In the city center, individuals are almost always better off. This is because substituting other modes, particularly public transport, is not very costly.

Figure 6: Change in welfare by area.

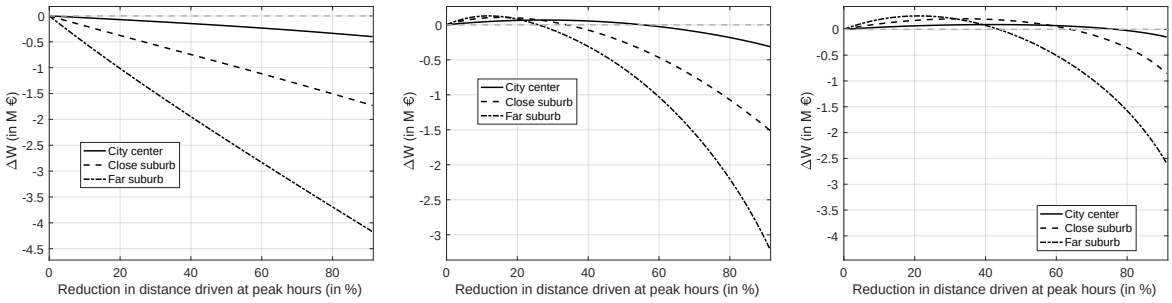

(a) Driving restrictions. (b) Uniform tolls. (c) Variable tolls.

We also study the importance of accounting for speed adjustments to accurately predict the transportation policies' effects. In Appendix E.3.2 we compare the congestion levels and driving rates predicted by our model against those obtained under a simpler model with constant speeds. The comparison highlights the importance of considering the policies' effects on speeds, as they influence substitution patterns between transportation modes and departure periods.

5.4 Comparison with optimal policies

We now compare the performance of the simple policy instruments with optimal policies that lead to the first-best equilibrium. We define first-best as a situation where the social planner sets personalized road tolls to maximize an objective subject to a traffic-level constraint. In our analysis the objective is either the welfare W or the aggregate consumer surplus CS.[22] We write here the problem of a social planner maximizing welfare as:

$$\begin{aligned} & \max_{\mathbf{p}} \mathrm{W}(\mathbf{p}) \\ \text{such that} \quad & \textstyle\sum_{n=1}^{N} \omega_n k_n s_{n\mathbf{d}t_1}(p_n) = \bar{K}_{t_1}, \end{aligned}$$

[22]We could consider alternative objectives for the social planner, such as sum of consumer surplus with redistributive weights or assign different weights to the different components of the welfare.

where $\mathbf{p} = (p_1, ..., p_N)$ is the vector of personalized tolls. We assign an objective of traffic reduction to the social planner, so we can compare the optimal policies with simple instruments on the basis of the traffic reduction outcome. This objective is represented by the total number of kilometers driven at peak hours that should meet the objective, $\bar{K}_{t_1}$. Because tolls influence individuals' decisions to drive and thus equilibrium speeds, we need to recompute traffic equilibrium for each toll vector along the optimization procedure. The traffic equilibrium generates links between an individual's utility and the other individuals' tolls. We overcome this challenge by rewriting the problem. The new formulation considers speeds as parameters and introduces the congestion technologies as additional non-linear constraints (in the spirit of the MPEC formulation of the BLP estimation of Dubé et al., 2012). This leads to the following problem to solve:

$$\begin{aligned} & \max_{\{\mathbf{v},\mathbf{p}\}} W(\mathbf{v}, \mathbf{p}) \\ \text{such that} \quad & \sum_{n=1}^{N} \omega_n k_n s_{n\mathbf{d}t_1}(\mathbf{v}, p_n) = \bar{K}_{t_1} \\ & v_t^a = f^a\left(K_t^a(\mathbf{v}, \mathbf{p}) + K_0^a\right) \quad \forall a = 1, ..., A, \quad \forall t = t_1, t_2. \end{aligned}$$

Note that this problem is still a high-dimension non-linear optimization problem. However, the dependencies across individuals occur only through the constraints (the speed functions). Additionally, we put some bounds on the toll values: tolls must be positive and below or equal €100. We provide the Lagrangian of the problem and interpret the optimality conditions in Appendix E.3.3.

Figure 7 shows the difference in outcomes between the simple regulations (driving restrictions, uniform and per-kilometer tolls) relative to the optimal welfare-maximizing policies.[23] Panel (a) provides the differences in welfare, the maximized outcome under the optimal tolls. We see that the difference in welfare is very large under the driving restrictions. The difference in welfare increases until a very high stringency and then decreases. The uniform tolls display large differences in welfare relative to the optimal policies, albeit lower than the driving restriction.

In contrast, the per-kilometer toll leads to very low differences in welfare. These differences are high for low stringency levels and decrease with the policy stringency level. When the policy stringency level is high, the shadow cost of letting individuals drive is very high, and the optimal toll becomes almost equal to the shadow cost multiplied by the distance. In contrast, under a low policy stringency level, the shadow cost of the traffic constraint is low, and the individual-specific terms that define the optimal personalized tolls have more

[23]To calculate the differences in outcomes across policies, we need the same policy outcome grid. We approximate the welfare, surplus, and tax revenue curves by Bernstein polynomials of degree eight.

importance. The social planner can improve welfare by reorganizing traffic, letting individuals with the lowest emissions costs, the lowest diversion to driving during off-peak, and the lowest contributions to traffic in areas with potential high-value speed improvements drive.

As before, we decompose welfare into the main components: consumer surplus and tax revenue. We see in Panel (b) that the difference in consumer surplus is particularly large for the uniform toll, while the variable toll sometimes achieves more consumer surplus than under welfare-maximizing tolls. In contrast, we see from Panel (c) that the uniform toll usually raises more revenues than welfare-maximizing tolls. Meanwhile, the per-kilometer tolls always raise lower tax revenue than optimal tolls. The under-performance in raising revenue explains the difference in welfare between welfare-maximizing and per-kilometer tolls.

We measure the performance of the simple instruments by looking at the welfare differences at the optimal policy level, represented by the vertical lines. We find that the variable toll achieves 85% of the potential gains while the uniform toll reaches 27.2%. These figures highlight the fact that the variable toll is an efficient second-best policy instruments.

Figure 7: Differences in welfare, consumer surplus and tax revenues relative to welfare-maximizing personalized tolls.

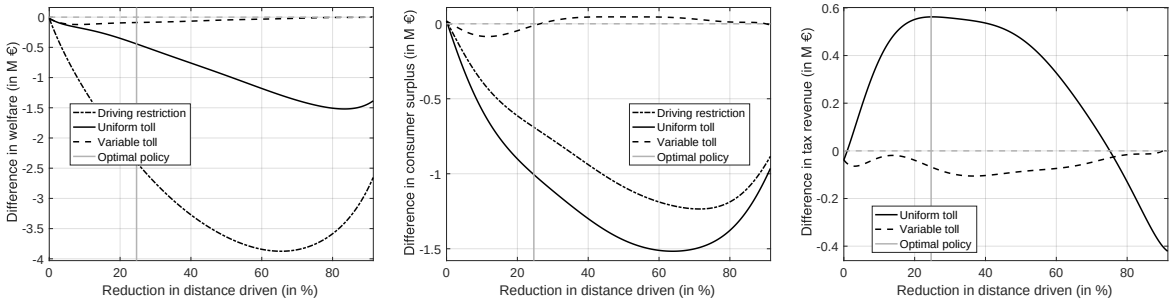

(a) Welfare. (b) Consumer surplus. (c) Tax revenue.

We turn to the difference between simple instruments and consumer surplus-maximizing tolls provided in Figure 8. From Panel (a), we can see that surplus-maximizing tolls always dominate driving restrictions in terms of welfare. However, the per-kilometer toll is always superior, in terms of welfare, to personalized tolls. The uniform tolls lead to similar welfare outcomes, especially when the policy stringency is moderate. The explanation comes from the absence of tax revenues when the social planner only cares about consumer surplus, as shown in Panel (c). We obtain the same tax revenue curves as in Panel (c) of Figure 3.

Indeed, to maximize surplus, the social planner sets nearly binary tolls: 0 for a fraction of individuals with the highest values of driving and very high values for individuals with low driving valuations. This means individuals taking the car do not pay any toll, as the

individuals targeted by large tolls never choose to drive. This is similar to imposing driving restrictions. However, the big difference is that the social planner targets efficiently the individuals allowed to drive. The heterogeneity in the valuation for driving at peak hours comes from different factors: travel time sensitivity, schedule constraints that limit the ability to do inter-temporal substitution, and the quality of the alternative transportation modes.

When looking at Panel (b), which provides consumer surplus, we see that the difference in surplus across policies is very important. Simple instruments are not suitable for improving consumer surplus. The worst policy is the uniform toll, which always generates high consumer surplus losses, reflecting bad targeting.

Figure 8: Difference of outcomes with respect to consumer surplus-maximizing personalized tolls.

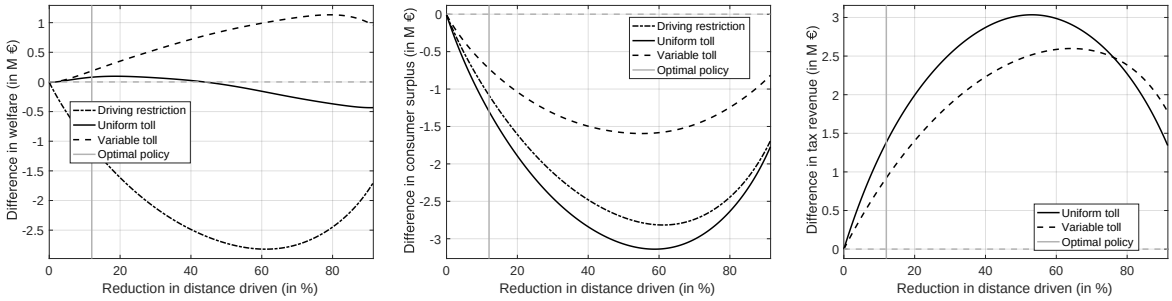

(a) Welfare. (b) Consumer surplus. (c) Tax revenue.

5.5 Comparison across policies at a benchmark level

To further analyze the effects of the previous policy instruments, we set a benchmark policy stringency level. The objective here is to analyze more outcomes of the policy and characterize the winners and losers under each type of policy. Because our model include many layers of heterogeneity (in preferences, in trip characteristics, in congestion technology), and all these dimensions of heterogeneity interact, it is difficult to precisely know which type of individual heterogeneity explains the results of the policy comparison.

We use the optimal policy level as benchmark level. This policy stringency level generates the highest welfare gains with personalized tolls. We calibrate the fraction of cars banned, the uniform toll, the variable road toll and the surplus-maximizing personalized tolls to achieve the same traffic reduction at peak hours. All five regulations reduce the number of kilometers driven by 24% at peak hours. Table 13 below provides the policy parameters. With two trips per day, the uniform toll implies a total cost of €8.2 per day, close to the London congestion charge in 2010.[24] The variable toll of €0.19/km implies an average cost of €2.42, much lower

[24]The London toll implemented in 2003 was initially £5/day and increased to £8 in 2005, £10 in 2011,

than the uniform toll. The maximum variable toll reaches €13 for the longest distance.

Table 13: Policy parameters for the benchmark stringency level.

Outcome matched	Driving restriction	Uniform toll	Variable toll	Av. pers. toll max W	Av. pers. toll max CS
Distance, peak hours	34.5%	4.09	0.19	3.37	21.3

Note: Uniform and average personalized tolls in €, and variable tolls in €/km.

Impacts on consumer surplus Table 14 presents the policies' impacts on consumer surplus. The ranking of policies by surplus losses and welfare changes follows the results from the previous section, and the policy costs are between €1.17 million and €2.14 million for the standard policies. As saw in the previous section, toll revenues are very large and cover 105% and 138% of the total surplus loss for the uniform and variable tolls, respectively. If we redistribute the entire tax revenue, the tolls generate benefits between €179,000 and €519,000. Under a shadow cost of public funds below 75%, both tolls outperform the driving restriction policy, which is very likely to be the case in reality. Personalized tolls maximizing welfare lead to a lower surplus loss and larger tax revenue. Interestingly, personalized tolls maximizing consumer surplus lead to a very small decrease in aggregate consumer surplus (€9,000) and generate almost no tax revenue (€460). However, thanks to the welfare gains from reducing emissions, the policy is welfare increasing (€82,000).

To better understand the role of the changes in speeds induced by the different policies, we decompose the total variation in consumer surplus into two terms: the variation in consumer surplus due to the policies while keeping speeds constant and the changes in surplus induced by the modification of the equilibrium speeds (see the formula for the decomposition in Appendix E.1). While speed improvements always create welfare gains, they are far from being sufficient to offset the welfare costs of most policies, as they only cover between 22% and 32% of the consumer surplus losses. Only the personalized tolls maximizing consumer surplus lead to surplus gains from improved speeds almost as large as the cost of the policy.

Across policies, there is a constant share of individuals with no change in their surplus. These are individuals without a car who are not affected by the regulations. Only the personalized tolls maximizing surplus lead to a large portion of individuals (54.9%) achieving surplus gains. Other policies only reach modest shares, with the driving restriction and the variable toll reaching shares where around 6% of individuals obtain surplus gains.

£11.5 in 2011, and £15 in 2020.

Table 14: Consumer surplus variation under the benchmark policies.

	Driving restriction	**Uniform toll**	**Variable toll**	**Personalized tolls, max W**	**Personalized tolls, max CS**
Total ΔCS (M€)	-1.83	-2.14	-1.17	-1.15	-0.009
ΔCS at constant speed	-2.36	-2.75	-1.71	-1.78	-0.687
ΔCS from speed	0.531	0.607	0.543	0.624	0.678
Total ΔwCS (M€)	-1.74	-1.98	-1.02	-1.03	-0.005
Tax revenue (M€)	0	2.24	1.61	1.68	0
Value emissions avoided (M€)	0.084	0.087	0.077	0.086	0.091
ΔW = ΔCS + Tax rev. - ΔE (M€)	-1.75	0.179	0.519	0.611	0.082
% ΔCS = 0	21.2	21.2	21.2	21.2	21.2
% ΔCS > 0	6.7	3.39	6.01	1.91	54.9
% ΔCS < 0	72.1	75.4	72.8	76.9	23.9

Note: "ΔE" are changes in emissions valued at standard levels.

Winners and losers We now characterize winners and losers by analyzing the surplus changes by demographic groups based on age, wealth, socio-professional activity, family size, and trip distance. We consider the surplus changes without tax revenue redistribution. Table 15 shows that the ranking of policies is identical for all subgroups of individuals except for the highest distance quantile, for which the mean surplus decreases the most under the variable toll. The category of individuals under 18, students in high school or below, and individuals with trips less than 1.89 km are the least affected under the variable toll. These subgroups lose less than €20 cents. This is due to the short distance of their trips, implying gains from improved speeds at peak hours and low toll costs.

Table 15: Average surplus variation by demographic group.

	Driving restriction	**Uniform toll**	**Variable toll**	**Personalized tolls, max W**	**Personalized tolls, max CS**
Age $\leq$ 18	-0.192	-0.499	-0.137	-0.151	-0.077
Age $\in$]18, 30]	-0.254	-0.485	-0.307	-0.332	-0.238
Age $\in$]30, 40]	-0.515	-0.613	-0.411	-0.402	-0.049
Age $\in$]40, 50]	-0.953	-0.599	-0.39	-0.364	0.286
Age $\in$]50, 60]	-0.705	-0.667	-0.403	-0.36	0.138
Age $>$ 60	-0.551	-0.57	-0.286	-0.242	0.177
Income $<$ 800	-0.311	-0.332	-0.132	-0.15	0.019
Income $\in$ [800, 1,200[	-0.509	-0.498	-0.243	-0.248	0.043
Income $\in$ [1,200, 1,600[	-0.51	-0.651	-0.329	-0.315	-0.016
Income $\in$ [1,600, 2,000[	-0.652	-0.621	-0.351	-0.342	0.035
Income $\in$ [2,000, 2,400[	-0.389	-0.628	-0.366	-0.363	-0.158
Income $\in$ [2,400, 3,000[	-0.414	-0.618	-0.392	-0.38	-0.13
Income $\in$ [3,000, 3,500[	-0.434	-0.614	-0.355	-0.354	-0.005
Income $\in$ [3,500, 4,500[	-0.406	-0.57	-0.345	-0.35	-0.058
Income $\geq$ 4,500	-0.755	-0.268	-0.088	-0.047	0.704
Farmers	-1.97	-1.51	-0.557	-0.466	-0.066
Craftspersons	-0.576	-0.749	-0.463	-0.349	0.192
Shopkeepers	-0.372	-0.515	-0.375	-0.268	-0.01
Entrepreneurs, self-employed	-0.41	-0.522	-0.352	-0.319	-0.086
Public executives	-0.468	-0.536	-0.314	-0.32	0.061
Private executives	-0.447	-0.518	-0.416	-0.361	0.078
Education, health	-0.942	-0.856	-0.424	-0.405	0.066
Administrative professions	-0.535	-0.525	-0.388	-0.384	-0.008
Technicians	-0.634	-0.68	-0.52	-0.446	-0.089
First-line supervisors	-0.794	-0.649	-0.633	-0.496	0.107
Public employees	-0.804	-0.655	-0.313	-0.362	0.112
Private employees	-0.742	-0.651	-0.395	-0.422	0.059
Retail employees	-0.8	-0.63	-0.34	-0.361	0.057
Services	-0.509	-0.425	-0.142	-0.152	0.076
Qualified workers	-0.722	-0.568	-0.391	-0.387	0.075
Unqualified workers	-0.608	-0.439	-0.265	-0.291	0.009
Students $\leq$ high school	-0.205	-0.515	-0.147	-0.163	-0.076
Students in higher education	-0.151	-0.343	-0.235	-0.249	-0.228
Couple, families	-0.491	-0.586	-0.318	-0.313	-0.015
Singles	-0.409	-0.421	-0.238	-0.235	0.064
Distance $\leq$ 1.89 km	-0.207	-0.407	-0.032	-0.046	0.009
Distance $\in$]1.89, 4.97] km	-0.433	-0.628	-0.09	-0.13	0.053
Distance $\in$]4.97, 10.7] km	-0.639	-0.706	-0.21	-0.268	0.112
Distance $\in$]10.7, 21.4] km	-0.663	-0.658	-0.44	-0.451	0.036
Distance>21.4 km	-0.449	-0.4	-0.753	-0.611	-0.222
Average	-0.478	-0.56	-0.305	-0.301	-0.002

Note: in €/trip.

Across policies, the most affected individuals tend to be those between 30 and 60 years old, those with a family, and the longest distance commuters. Under tolls, the highest income category individuals are on average better-off after the policies, which is due to their lower cost sensitivity. Among employed individuals, workers in education, health, public, and private employees are the most affected by the policies. Except for individuals with short

commutes, there is little heterogeneity in the policies' effects across trip distance for the driving restriction and the uniform toll. The heterogeneity of the policies' effects according to trip distance is more pronounced for the variable toll.

Environmental impacts The results in Table 16 below show the differences between policy instruments' efficiency in reducing carbon and local pollutant emissions. The three policies have roughly the same impact: they reduce carbon emissions by 288 to 325 tons of CO_2 emissions while the decreases in local pollutant emissions lie between 0.84 and 93 tons of equivalent NO_X emissions. As a robustness check, we measure the policy effects on emissions using our alternative estimates of car local pollutant emissions that depend on driving speeds (see Appendix C.4.2). We obtain more emissions avoided, but the heterogeneity patterns across pollutants and policies remain identical. Overall, the speed improvements are responsible for a small share of the total decrease in emissions, representing at most 23.2% for HC emission changes and 10.2% for equivalent NO_X emissions.

Table 16: Changes in emissions under the different policies.

	Driving restriction	**Uniform toll**	**Variable toll**	**Personalized tolls, max W_2**	**Personalized tolls, max CS**
Main emissions estimates					
ΔCO_2	-309	-325	-288	-323	-343
ΔNO_X	-0.41	-0.411	-0.37	-0.412	-0.428
ΔHC	-0.103	-0.11	-0.097	-0.11	-0.116
ΔPM	-0.034	-0.034	-0.031	-0.034	-0.035
ΔEq. NO_X	-0.929	-0.924	-0.836	-0.929	-0.965
Alternative emissions estimates (Copert)					
ΔNO_X	-1.13	-1.19	-0.98	-1.1	-1.1
ΔHC	-0.073	-0.082	-0.063	-0.076	-0.07
ΔPM	-0.051	-0.053	-0.045	-0.05	-0.05
ΔEq. NO_X	-1.9	-1.99	-1.66	-1.86	-1.86
Relative importance of speed changes (Copert)					
NO_X	10.9	11.6	10.9	10.5	8.41
HC	20.5	20	23.2	21.5	22.8
PM	7.33	8.07	6.92	6.85	4.8
Eq. NO_X	9.47	10.2	9.3	9.03	6.97

Note: Δ emissions in tons. "Eq. NO_X" aggregates the local pollutants into equivalent NO_X emissions. Relative importance in %.

In Appendix E.4, we analyze more outcomes: the substitution patterns across transportation modes, travel time variations, speed changes and the marginal costs of congestion.

5.6 Robustness and additional policies

We also study the welfare consequences from implementing the policies across all periods. We provide the results in Appendix E.5.1. The ranking across policies remains the same, but the

regulations are costlier for individuals, as inter-temporal substitution is no longer possible.

Our analysis holds the quality of public transport constant. In Appendix E.5.2, we check the sensitivity of the results to changes in the overcrowding levels in public transport. We consider the benchmark variable toll and two scenarios where overcrowding levels increase by 15% and 30%. These assumptions are rather extreme since public transport usage at peak hours increases by 11% in our benchmark. We find minimal changes in the transportation mode shares and equilibrium speeds. The total surplus loss would be 9% and 18% higher in the two scenarios, highlighting the small role of public transport overcrowding.

Finally, we lift the schedule constraints and allow all individuals to choose their departure time. The results, available in Appendix E.5.3 show that removing schedule constraints actually lowers the welfare gains from the policies. The variable toll generates lower surplus losses but the tax revenue and the emissions avoided become also lower due to more substitution to driving during off-peak hours.

We choose to focus on predicting the impacts of simple policy instruments that have been implemented in practice. However, our model could analyze more policies. Here, we outline a few counterfactuals for which we include results in Appendix F. We investigate more flexible yet feasible road toll schemes: location-specific tolls (inside and outside of the city center) and tolls composed of a fixed and a variable (kilometer-based) part in Appendix F.1. We find little potential gains upon the variable toll. In Appendix F.2, we study an auction resembling Shanghai's vehicle license regulation (see Li, 2018). This policy decreases welfare since individuals have to purchase the license before receiving their preference shocks, making them unable to react in case of high unexpected utility for driving during peak hours. In Appendix F.3, we compare the standard driving restrictions against two attribute-based policies: one banning older vehicles and one banning diesel cars. The diesel-based policy performs better than standard driving restrictions mainly because it generates less surplus losses. We also provide insights on how improvements to public transport can mitigate consumer surplus losses in Appendix F.4. Finally, additional scenarios are discussed briefly on Appendix G.

6 Conclusion

Combining data from a detailed survey, Google Maps, TomTom, and passenger flow in railway public transit, we estimate a nested logit model to represent the transportation decisions of individuals for their daily trips to work or places of study in the Paris metropolitan area. The estimated parameters confirm the importance of trip duration for individual decisions and reveal profound schedule inflexibility making it challenging to discourage individuals from

driving at peak hours. We combine this transportation mode choice model with a flexible reduced-form congestion model that predicts how road speeds vary when the number of drivers changes in the different parts of the city. We simulate the effects of simple transportation policies and measure their welfare effects on individuals and their impacts on emissions. We find that all the regulations are costly for individuals. Still, simple driving restrictions are not more costly for individuals than uniform road tolls because they force everyone to contribute to traffic reduction. As a result, it generates fewer surplus losses than uniform tolls on aggregate. However, variable tolls are better than driving restrictions because they target individuals with long distances and are thus efficient at reducing the total number of kilometers driven. In contrast, driving restrictions do not raise revenue, unlike tolls. If the toll revenue is entirely redistributed to individuals, moderate toll values may improve the total welfare.

References

Agarwal, N. (2015). An empirical model of the medical match. *American Economic Review 105*(7), 1939–1978.

Akbar, P. and G. Duranton (2017). Measuring the cost of congestion in highly congested city: Bogota. *CAF – Working paper*.

Allen, T. and C. Arkolakis (2022). The Welfare Effects of Transportation Infrastructure Improvements. *The Review of Economic Studies*.

Almagro, M., F. Barbieri, J. C. Castillo, N. G. Hickok, and T. Salz (2024). Optimal urban transportation policy: Evidence from chicago. Technical report, National Bureau of Economic Research.

Anderson, M. L. (2014). Subways, strikes, and slowdowns: The impacts of public transit on traffic congestion. *American Economic Review 104*(9), 2763–96.

Anderson, M. L. and L. W. Davis (2020). An empirical test of hypercongestion in highway bottlenecks. *Journal of Public Economics 187*, 104197.

Arnott, R., A. De Palma, and R. Lindsey (1990). Economics of a bottleneck. *Journal of Urban Economics 27*(1), 111–130.

Arnott, R., A. D. Palma, and R. Lindsey (1993). A structural model of peak-period congestion: A traffic bottleneck with elastic demand. *The American Economic Review 83*(1), 161–179.

Barahona, N., F. A. Gallego, and J.-P. Montero (2020). Vintage-specific driving restrictions. *The Review of Economic Studies 87*(4), 1646–1682.

Barwick, P. J., S. Li, A. R. Waxman, J. Wu, and T. Xia (2024). Efficiency and equity impacts of urban transportation policies with equilibrium sorting. Working paper, National Bureau of Economic Research.

Basso, L. J. and H. E. Silva (2014, November). Efficiency and substitutability of transit subsidies and other urban transport policies. *American Economic Journal: Economic Policy 6*(4), 1–33.

Batarce, M. and M. Ivaldi (2014). Urban travel demand model with endogenous congestion. *Transportation Research Part A: Policy and Practice 59*, 331 – 345.

Bento, A., K. Roth, and A. R. Waxman (2020). Avoiding traffic congestion externalities? The value of urgency. Working paper, National Bureau of Economic Research.

Berry, S., J. Levinsohn, and A. Pakes (1995). Automobile Prices in Market Equilibrium. *Econometrica 60(4)*, 889–917.

Bou Sleiman, L. (2021). Are car-free centers detrimental to the periphery? Evidence from the pedestrianization of the Parisian riverbank. Technical report, Center for Research in Economics and Statistics.

Buchholz, N., L. Doval, J. Kastl, F. Matějka, and T. Salz (2024). The value of time: Evidence from auctioned cab rides. Technical report, National Bureau of Economic Research.

Cardell, N. S. (1997). Variance components structures for the extreme-value and logistic distributions with application to models of heterogeneity. *Econometric Theory 13*(2), 185–213.

Carstensen, C. L., M. J. Hansen, F. Iskhakov, J. Rust, and B. Schjerning (2022). A dynamic equilibrium model of commuting, residential and work location choices. *Topics in Urban Economics: Non-Market Valuation and Location*, 35.

Cook, C. and P. Z. Li (2023). Value pricing or lexus lanes? the distributional effects of dynamic tolling. Technical report.

COPERT methodology report (2020). Emep/eea air pollutant emission inventory guidebook 2019 - update oct. 2021. *EEA*.

Couture, V., G. Duranton, and M. A. Turner (2018). Speed. *Review of Economics and Statistics 100*(4), 725–739.

Crawford, G. S., R. Griffith, and A. Iaria (2021). A survey of preference estimation with unobserved choice set heterogeneity. *Journal of Econometrics 222*(1), 4–43.

Davis, L. W. (2008). The effect of driving restrictions on air quality in Mexico City. *Journal of Political Economy 116*(1), 38–81.

De Palma, A. and R. Lindsey (2006). Modelling and evaluation of road pricing in Paris. *Transport Policy 13*(2), 115–126.

De Palma, A., R. Lindsey, and G. Monchambert (2017). The economics of crowding in rail transit. *Journal of Urban Economics 101*, 106–122.

De Palma, A., F. Marchal, and Y. Nesterov (1997). Metropolis: Modular system for dynamic traffic simulation. *Transportation Research Record 1607*(1), 178–184.

Dubé, J.-P., J. T. Fox, and C.-L. Su (2012). Improving the numerical performance of static and dynamic aggregate discrete choice random coefficients demand estimation. *Econometrica 80*(5), 2231–2267.

Dubois, P., R. Griffith, and M. O'Connell (2018). The effects of banning advertising in junk food markets. *The Review of Economic Studies 85*(1), 396–436.

Engelson, L. and M. Fosgerau (2016). The cost of travel time variability: Three measures with properties. *Transportation Research Part B: Methodological 91*, 555–564.

Galdon-Sanchez, J. E., R. Gil, F. Holub, and G. Uriz-Uharte (2021). Benefits and costs of driving restriction policies: The impact of Madrid Central on congestion, pollution and consumer spending. Working paper.

Gale, D. and H. Nikaido (1965). The jacobian matrix and global univalence of mappings. *Mathematische Annalen 159*(2), 81–93.

Gallego, F., J.-P. Montero, and C. Salas (2013). The effect of transport policies on car use: Evidence from Latin American cities. *Journal of Public Economics 107*, 47 – 62.

Geroliminis, N. and C. F. Daganzo (2008). Existence of urban-scale macroscopic fundamental diagrams: Some experimental findings. *Transportation Research Part B: Methodological 42*(9), 759 – 770.

Goldszmidt, A., J. A. List, R. D. Metcalfe, I. Muir, V. K. Smith, and J. Wang (2020). The value of time in the United States: Estimates from nationwide natural field experiments. Working paper, National Bureau

of Economic Research.

Hall, J. D. (2018). Pareto improvements from lexus lanes: The effects of pricing a portion of the lanes on congested highways. *Journal of Public Economics 158*, 113–125.

Hall, J. D. (2021). Can tolling help everyone? estimating the aggregate and distributional consequences of congestion pricing. *Journal of the European Economic Association 19*(1), 441–474.

Hall, J. D. and I. Savage (2019). Tolling roads to improve reliability. *Journal of urban economics 113*, 103187.

Hang, D., D. McFadden, K. Train, and K. Wise (2016). Is vehicle depreciation a component of marginal travel cost?: A literature review and empirical analysis. *Journal of Transport Economics and Policy 50*(2), 132–150.

Hanna, R., G. Kreindler, and B. A. Olken (2017). Citywide effects of high-occupancy vehicle restrictions: Evidence from "three-in-one" in Jakarta. *Science 357*(6346), 89–93.

Hansen, B. E. (2014, 02). 214215Nonparametric Sieve Regression: Least Squares, Averaging Least Squares, and Cross-Validation. In *The Oxford Handbook of Applied Nonparametric and Semiparametric Econometrics and Statistics*. Oxford University Press.

Haywood, L. and M. Koning (2015). The distribution of crowding costs in public transport: New evidence from Paris. *Transportation Research Part A: Policy and Practice 77*, 182–201.

Herzog, I. (2022). The city-wide effects of tolling downtown drivers: Evidence from London's congestion charge. Working papers.

Hintermann, B., B. M. Schoeman, J. Molloy, T. Götschli, A. Castro, C. Tchervenkov, U. Tomic, and K. W. Axhausen (2021). Pigovian transport pricing in practice. Technical report, WWZ Working Paper.

Jia, Z., C. Chen, B. Coifman, and P. Varaiya (2001). The PeMS algorithms for accurate, real-time estimates of g-factors and speeds from single-loop detectors. In *ITSC 2001. 2001 IEEE Intelligent Transportation Systems*, pp. 536–541. IEEE.

Kilani, M., S. Proost, and S. Van der Loo (2012). Tarification des transport individuels et collectifs à Paris. rapport final de recherche PREDIT. In *Technical Report*.

Kilani, M., S. Proost, and S. Van der Loo (2014). Road pricing and public transport pricing reform in Paris: Complements or substitutes? *Economics of Transportation 3*(2), 175–187.

Koch, N., N. Ritter, A. Rohlf, and B. Thies (2023). Machine learning from big gps data about the heterogeneous costs of congestion. *Available at SSRN 4526796*.

Kreindler, G. (2023). Peak-hour road congestion pricing: Experimental evidence and equilibrium implications. Technical report, National Bureau of Economic Research.

Li, S. (2018). Better lucky than rich? Welfare analysis of automobile licence allocations in Beijing and Shanghai. *The Review of Economic Studies 85*(4), 2389–2428.

Loder, A., L. Ambühl, M. Menendez, and K. W. Axhausen (2017). Empirics of multi-modal traffic networks–using the 3D macroscopic fundamental diagram. *Transportation Research Part C: Emerging Technologies 82*, 88–101.

Mangrum, D. and A. Molnar (2020). The marginal congestion of a taxi in new york city. Technical report.

McFadden, D. (1974). The measurement of urban travel demand. *Journal of public economics 3*(4), 303–328.

Ostermeijer, F., H. Koster, L. Nunes, and J. van Ommeren (2022). Citywide parking policy and traffic: Evidence from amsterdam. *Journal of Urban Economics 128*, 103418.

Petrin, A. and K. Train (2010). A control function approach to endogeneity in consumer choice models. *Journal of marketing research 47*(1), 3–13.

Reynaert, M. and J. M. Sallee (2021). Who benefits when firms game corrective policies? *American Economic*

Journal: Economic Policy 13(1), 372–412.

Rosaia, N. (2020). Competing platforms and transport equilibrium: Evidence from new york city. Technical report.

Russo, A., M. W. Adler, F. Liberini, and J. N. van Ommeren (2021). Welfare losses of road congestion: Evidence from rome. *Regional Science and Urban Economics 89*, 103692.

Small, K. A. (2012). Valuation of travel time. *Economics of transportation 1*(1-2), 2–14.

Small, K. A., E. T. Verhoef, and R. Lindsey (2007). *The economics of urban transportation*. Routledge.

Small, K. A., C. Winston, and J. Yan (2005). Uncovering the distribution of motorists' preferences for travel time and reliability. *Econometrica 73*(4), 1367–1382.

Tarduno, M. (2022). For whom the bridge tolls: Congestion, air pollution, and second-best road pricing. Working papers.

Tassinari, F. (2022). Low emission zones and traffic congestion: evidence from Madrid Central. Technical report.

Train, K. E. (2009). *Discrete choice methods with simulation*. Cambridge university press.

Tsivanidis, N. (2022). The aggregate and distributional effects of urban transit infrastructure: Evidence from Bogota's TransMilenio. Working paper.

Van Den Berg, V. and E. T. Verhoef (2011). Winning or losing from dynamic bottleneck congestion pricing?: The distributional effects of road pricing with heterogeneity in values of time and schedule delay. *Journal of Public Economics 95*(7), 983–992.

Van Essen, H., L. Van Wijngaarden, A. Schroten, D. Sutter, C. Bieler, S. Maffii, M. Brambilla, D. Fiorello, F. Fermi, R. Parolin, et al. (2019). *Handbook on the external costs of transport, version 2019*. Number 18.4 K83. 131.

Yang, J., A.-O. Purevjav, and S. Li (2020). The marginal cost of traffic congestion and road pricing: Evidence from a natural experiment in Beijing. *American Economic Journal: Economic Policy 12*(1), 418–53.

Appendix (for online publication only)

A Index of mathematical notation

Table 17: Index of the mathematical notation used in the paper

Symbol	Description
	Indices
$n \in N$	Individual
$t \in T$	Departure time period
$t_1, t_2 \in T$	Peak hours and off-peak hours
$\mathcal{T}_n \subseteq T$	Set of all periods accessible by n
$\mathcal{T}_1, \mathcal{T}_2, \mathcal{T}_{12}$	Combinations of period available (peak hours, off-peak hours, both)
$j \in J$	Transportation mode
$\mathcal{J}_n \subseteq J$	Set of all transportation modes accessible by n
$\mathbf{d}$	Index for driving
$c, c(n) \in C$	Socio-professional category (for an individual n)
$\mathcal{C}$	Set of individuals with socio-professional category c
$k(n)$	Type of fuel of individual n's car
$a \in A$	Area (Highways, city center, ring roads, close suburbs, far suburbs)
$q \in Q$	Bernstein basis polynomials index
p	Polynomial index selected to minimise MSFE
$i \in I$	Observation of speed, occupancy rate and instruments
l	Public transit line
	Variables
X_{njt}	Mode and departure period characteristics
u_{njt}	Utility
ϵ_{njt}	Preference shock
$\tilde{\epsilon}_{njt}$	Period-specific preference shock
ζ_{nj}	Mode-specific preference shock
s_{njt}	Probability of choosing mode j and period t for individual n
D_{nj}	Expected utility of the mode (nest) j
ω_n	Weight of individual n
π_{nl}	Probability of being able to access combination of periods $\mathcal{T}_l$
k_n^a	Trip distance in area a for individual n
k_n	Trip distance for individual n
K_t^a	Kilometers driven in area a and time t
f	Congestion technology
κ	Tuning parameter for the equilibrium speed algorithm
v_t^a	Speed in area a and period t
$\mathbf{v}$	Speed vector
$\mathbf{g}$	Contraction function
K	Lipschitz coefficient
$\phi_{c(n)}$	Probability of being schedule constrained for individual n with SPC $c(n)$
$\pi_{c(n)}$	Conditional on being constrained, probability that peak hours only are available for individual n with SPC $c(n)$
$\boldsymbol{\pi}$	Vector of probabilities that only peak hours are available, conditional on being constrained
μ_c	Fraction of individuals with SPC c commuting during peak hours
y_{njt}	Indicator when mode j and period t are chosen by n
duration	Trip duration
ρ_{nt}	Individual and period-specific speed shocks
ν_i	Unobserved speed shock from road traffic data
τ_i	Occupancy rate for road traffic data
τ_t^a	Occupancy rate at period t in area a
B_q	Bernstein basis polynomials
$\hat{e}_i$	Prediction error for estimating congestion technology
h	Leverage value for estimating congestion technology
$\mathcal{B}$	Matrix containing Bernstein polynomials
$\mathbf{p}$	Vector of personalized tolls (for all individuals)
fc	Fuel consumption of car in litres/km
ft	CO_2 emissions per litre of fuel
CO_2	CO_2 emissions
c	Overcrowding level
Υ	Train capacity
ψ	Hourly number of passengers
ns	Number of train stations
$\xi_{n\mathbf{d}t}$	Mode-specific preference shock for driving (for the control function specification)
$\hat{\epsilon}$	Residual independent of duration (for the control function specification)
$Z_{n\mathbf{d}t}$	Instruments for the control function specification
η_{nt}	Duration shock after projecting duration on the instruments for the control function specification
M	Mean effective car length
h	Length of traffic sensor
W	Welfare = consumer surplus + tax revenue + value of avoided emissions
CS_n	Individual consumer surplus
ΔCS_n	Change in individual consumer surplus
ΔCS	Change in aggregate consumer surplus
e_{nt}	Emissions per kilometer for individual n at period t
	Parameters
β_n	Mode and departure period characteristics
α_n	Sensitivity to trip cost
σ	Nest parameter
γ	Instrument parameter for the control function specification
θ	Set of parameters for demographic characteristics and the nest parameter
c_q^a	Coefficients of estimated congestion technology
ϕ^a	Scale parameter for the mapping between distance and road occupancy rate
$\sigma^{\hat{\epsilon}}$	Variance of $\hat{\epsilon}$ for the control function specification
$\boldsymbol{\lambda}$	Lagrange multipliers vector for road speed constraint
μ	Lagrange multiplier for total distance driven constraint

B Additional details on the model

B.1 Uniqueness of the model equilibrium case with one period and one area

We consider here the case of only one endogenous speed in the model. The equilibrium speed v is given by:

$$v - f\left(\sum_{n=1}^{N} \omega_n k_n s_{n\mathbf{d}}(v) + K_0\right) = 0$$

We define $g(v) := v - f\left(\sum_{n=1}^{N} \omega_n k_n s_{n\mathbf{d}}(v) + K_0\right)$. If the non-linear equation admits a solution, the solution is unique if the function is monotonic, i.e., if $|g'(v)| > 0 \; \forall v \in [\underline{v}, \overline{v}]$. The derivative is:

$$g'(v) = 1 - \underbrace{f'\left(\sum_{n=1}^{N} \omega_n k_n s_{n\mathbf{d}}(v) + K_0\right)}_{\leq 0} \times \sum_{n=1}^{N} \omega_n k_n \underbrace{\frac{\partial s_{n\mathbf{d}}(v)}{\partial v}}_{\geq 0},$$

which is always positive for $v \in [\underline{v}, \overline{v}]$ as long as the speed function is weakly decreasing in the occupancy rate and the probability of driving increases with speed. Note that the assumption that K_0 is fixed is not crucial, but the result is still valid if K_0 increases in speed.

B.2 Uniqueness of the model equilibrium case with multiple periods and one area

Now, we consider a model with a single area but multiple time periods which are substitutes for individuals. In this setting we have a system of T non-linear equations, $\mathbf{g}(\mathbf{v}) = 0$, where:

$$g_t(\mathbf{v}) := v_t - f\left(\sum_{n=1}^{N} \omega_n k_n s_{n\mathbf{d}t}(\mathbf{v}) + K_{0t}\right)$$

We want to show that the Jacobian of the system is a Leontieff matrix, i.e. the diagonal terms are positive and the off-diagonal terms are non-positive. First we compute the diagonal terms, which is the same as the previous derivative and is always greater than 1:

$$\frac{\partial g_t}{\partial v_t} = 1 - \underbrace{f'\left(\sum_{n=1}^{N} \omega_n k_n s_{n\mathbf{d}t}(\mathbf{v}) + K_{0t}\right)}_{\leq 0} \times \sum_{n=1}^{N} \underbrace{\omega_n k_n \frac{\partial s_{n\mathbf{d}t}(\mathbf{v})}{\partial v_t}}_{\geq 0}.$$

Then, we compute the off-diagonal terms, which are always negative due to the substitutability between the different time periods:

$$\frac{\partial g_t}{\partial v_{t'}} = \underbrace{-f'\left(\sum_{n=1}^{N}\omega_n k_n s_{n\mathbf{d}t}(\mathbf{v}) + K_{0t}\right)}_{\leq 0} \times \sum_{n=1}^{N} \underbrace{\omega_n k_n \frac{\partial s_{n\mathbf{d}t}(\mathbf{v})}{\partial v_{t'}}}_{\leq 0}.$$

The Jacobian of $\mathbf{g}(\mathbf{v})$ is thus a Leontieff matrix and by Theorem 5 from Gale and Nikaido (1965) it is a P-matrix. We can then apply the main theorem of Gale and Nikaido (1965) (Theorem 1) that states that if the Jacobian of a system of non-linear equations is a P-matrix, the system has a unique solution in its bounded support.

C Additional information on data and sample construction

C.1 Information about the EGT data

The EGT constitutes publicly available data upon request on ADISP.[25] The 2010 survey was conducted from 2009 to 2011 between October and May, excluding school holidays. Due to the COVID crisis, the 2020 survey was stopped and only contains observations collected in 2019. Instead of relying on a trip diary where surveyed individuals self-report their trips, the EGT relies on pollsters visiting households and recording the information of the trips performed the previous day.

The 2010 survey initially contains 35,175 individuals and 124,262 trips, while the 2020 survey contains 10,470 individuals and 35,656 trips. In our final sample, we keep the first work or study-related trip. We drop trips if one of the variables we need for the model is missing (origin, destination, departure time, professional activity, residence location, or income class). We also drop trips using less common transportation modes that are not included in our choice set (e.g., taxis, boats). We also drop individuals who took their first work or study trip outside the morning time window (defined as 5:45-10:15 a.m.). Finally, we exclude trips with distances lower than 700 meters or higher than the 99$^{\text{th}}$ percentile of the distance distribution (72.7 km). Our final sample consists of 15,480 individuals, of which 12,359 are from the 2010 survey and 3,121 from the 2020 survey.

The 2010 survey maps the Paris region into a grid with 1,489,347 squares to locate individual trips' origins and destinations. The size of the square edge is 100 meters. Thus, we use the

[25] Enquête Globale Transport (EGT) - 2010 and Enquête Globale Transport (EGT) - 2020, DRIEA, ADISP, see http://www.progedo-adisp.fr/.

GPS coordinates of the centroids of the grid squares. This approach limits any trip geocoding inaccuracy to a maximum of 70 meters. The 2020 survey provides GPS coordinates with three decimals, equivalent to an accuracy of 100 meters. The 2010 survey divides the region into 112 zones, where 400 and 500 individuals are interviewed to have representativity at the zone level. However, such zones are not used in the 2020 survey, leading to some zones with very few trips. We thus regroup some zones according to the following algorithm. In each iteration, we aggregate the zone with the smallest number of observations with the neighboring zone with the smallest number of observations. We iterate until no zone has less than 50 departing trips (pooling both survey waves). After this process, the region is divided into 93 zones.

C.2 Details about TomTom and Google Maps queries

Google Maps and TomTom Directions APIs provide directions and expected travel times associated with a given origin and destination pair of GPS coordinates at a specified departure time. The data from these API services have been used previously in the transportation literature (see Kreindler, 2023, Hanna et al., 2017, Akbar and Duranton, 2017, Tarduno, 2022, and Almagro et al., 2024). The public transport queries were done on November 9th, 2023, setting all trips to take place on Tuesday, November 21st, 2023, with a departure time at 9:30 a.m. We use TomTom data for driving times because this API gives 2,500 free queries daily. The car queries were done in November 2023, setting the trips to take place on Thursday 19th of September 2024 at 8:30 a.m. for peak hours and 6:30 a.m. for off-peak hours. For both modes, we winsorize the top and bottom 1% of the implied speeds from the queries. This allows us to avoid situations where the returned information from the APIs implies unrealistic speeds for the transportation modes.

TomTom queries for future dates use historical trip data and not the live conditions. We may be worried that TomTom modified its prediction algorithm after Covid. To study concerns regarding the impact of Covid on traffic and TomTom's predictions, we study a subsample of the queries that we also did before Covid, in August 2019 (for the future date of 19/11/2020) with Google maps. We find that, on average, TomTom predicts trip speeds 8.5% lower than Google maps. These differences translate into TomTom queries having on average speeds lower than Google maps by 4.2 km/hr. The results suggest that the Covid crisis did not significantly decrease trip duration predictions. Furthermore, the mild difference between the two APIs is reassuring about TomTom's reliability.

C.3 Additional information on the workforce survey

The workforce survey data is publicly available upon request on ADISP.[26] For the 2019 data, the information regarding employment starting and ending time flexibility comes in the additional survey module "Organisation du travail et Aménagement du temps de travail". For the 2022 survey, the information regarding work-hour flexibility appears in the primary survey data. We consider individuals to have a flexible starting time if they state that they fully decide their working hours or if they can decide their working hours within a specific time interval. We regroup several SPCs to have larger samples to estimate the probability of being flexible by SPC. In particular, we regroup farmers with agricultural workers, public executives with professors and information professions, intermediate professions across public and private sectors, civil employees with police and army officers, qualified workers across public and private sectors, unqualified workers across public and private sectors, and entrepreneurs with self-employed. This procedure reduces the number of SPCs from 32 to 16. We also have students in high school or below and students in higher education, so our final sample contains 18 SPCs.

C.4 Car fuel consumption and emissions

C.4.1 Baseline estimation method

The EGT data does not include the information for car fuel consumption. Since fuel consumption and car emissions are linked through the formula:

$$fc_n = \frac{\mathrm{CO}_{2n}}{ft_{k(n)}},$$

where fc_n is the fuel consumption (in liter/km) for car n and $ft_{k(n)}$ reflects the quantity of CO_2 emissions (in gram) in a liter of fuel k (diesel or gasoline).[27] We thus estimate CO_2 emissions as well as local pollutants of each car in the EGT data with a prediction model. We rely on additional car registration data in the Paris metropolitan area from 2003 to 2018 that contain the main car characteristics, sales, and the value of CO_2 emissions.[28] We complement the car registration data with local pollutant emissions data by car model from the UK Vehicle Certification Agency.[29] Note that all the emissions datasets are from official

[26] "Module ad-hoc de l'enquête Emploi: organisation du travail et aménagement du temps de travail - 2019, INSEE, ADISP" and "Enquête Emploi en continu (version FPR) - 2022, INSEE, ADISP".

[27] It is equal to 2,287 g/L for gasoline cars and 2,686 g/L for diesel cars.

[28] These are proprietary data obtained from the French Car Manufacturers syndicate "CCFA" (for 2003-2008) and AAAData (for 2009-2018).

[29] Source: https://carfueldata.vehicle-certification-agency.gov.uk/downloads/archive.aspx.

car manufacturer tests and may be different from real-time driving emissions, as pointed out by Reynaert and Sallee (2021).

We first match the French car registration data to the UK emissions data so that we can weigh each car model in the UK emissions data by their sales in the Paris metropolitan area in the prediction model. We rely on the following matching algorithm. (1) We aggregate the French car data at the year, brand, model name, fuel type, and CO_2 emissions. (2) We merge them with the UK emissions data by year, brand, model name, and fuel type. Since there are several versions for the same combination in the UK data, we select the closest neighbor based on cylinder capacity and CO_2 emissions. We drop observations for which either the percentage difference in CO_2 emissions or cylinder capacity between the two matches is larger than 10%. (3) For each pollutant, we drop car models for which the emission levels are above the corresponding Euro standard limit. We also drop cars whose emissions are lower than a tenth of the Euro norm value.

For hybrid cars and other fuel types (liquefied petroleum or natural gas), we observe that the top-selling models in France are not available in the UK emissions data. Thus, we rely on another dataset that provides car emissions data from 2012 to 2015. The data comes from the French environment agency ("ADEME").[30] We follow the same procedure described above but allow for more discrepancy between the potential matches by dropping observations only if the percentage difference in CO_2 emissions or cylinder capacity between the two matches is above 30%. We also rely on these ADEME data to obtain estimates of PM emissions for gasoline cars since the UK data only provides PM emissions for diesel cars.

With the final sample of car models with their corresponding sales and emissions, we estimate the prediction model. We specify the emissions level of a specific pollutant as a linear function of the horsepower, a linear time trend, and dummies for the years of changes in the emissions standard of this particular pollutant. We allow all the parameters to be different by fuel type. Finally, we regress the logarithm of the emission levels on car characteristics for PM emissions because PM data has more outliers. All regressions are weighted by the car model sales in Paris metropolitan area. Given the small sample size (91 observations) for hybrid cars and other fuels, we do not estimate a prediction model and instead use the sales-weighted average emission levels by fuel type. Emissions for electric vehicles are set to zero for all pollutants. For some individuals in EGT data, the car vintage and horsepower is missing. In such cases, we attribute the average vintage or horsepower values in the EGT sample conditional on the fuel type.

[30] Source: https://www.data.gouv.fr/fr/datasets/emissions-de-co2-et-de-polluants-des-vehicules-commercialises-en-france/. We prefer not to use it for conventional fuel cars because the sample period is limited.

C.4.2 Alternative method for emissions estimates

We follow an alternative method to estimate car emissions of local pollutants that depend on driving speed. We rely on Copert emissions factors for cars published in the COPERT methodology report (2020).[31] This report provides emission functions that link a car's emissions of local pollutants with its speed depending on fuel type, emission standard, and car segment (in four categories: mini, small, medium, and large).

The EGT data does not directly provide the car segments, so we predict them from the fiscal horsepower. We use our proprietary car data containing the horsepower and segment from 2003 to 2018. We specify and estimate an ordered logit model to predict the car segment from its horsepower.

Finally, we assign cars to an emission standard from their vintage: cars with a vintage before 2000 are under Euro 2 standards. From 2000 to 2005 they are under Euro 3 standards. From 2005 onward, they are subject to Euro 4 standards. Since both the Copert emissions data and the EGT data include information on fuel types, we can directly match survey cars to the correct set of emission function parameters by fuel type. The Copert methodology also assumes electric vehicles do not emit pollutants.

Table 18 compares average observed and predicted emissions under both prediction methods. Our baseline method finds similar average CO_2 values to the observed ones. We find higher values for PM than observed, but this might be related to the fact that the observations are for much more recent car models than in the EGT data. However, our baseline method and the Copert methodology provide similar estimates. Our method predicts lower NO_X than observed, while the alternative Copert method predicts higher values. It is the reverse for HC. Despite some differences at the pollutant level related to the emission prediction method, we do not think the benefits of reducing emissions will drastically differ.

[31] See https://www.emisia.com/utilities/copert/documentation/.

Table 18: Fit of the prediction models and comparison between average observed and predicted emissions.

Pollutant	R^2	Gasoline			Diesel		
		Observed	Predicted	Predicted Copert	Observed	Predicted	Predicted Copert
CO_2	0.84	203	167		171	148	
NO_X	0.91	100	53	87.8	369	278	568
HC	0.47	100	81.1	29.3	110	36	14.2
CO	0.35	617	525	441	223	223	104
PM	0.9	0.4	2.2	1.9	3.2	23.9	30.1

Note: We obtain the same R^2 for diesel and gasoline since the estimation is performed on pooled data. "Observed" emissions are calculated on the CCFA data for the year 2003 (the average car vintage in the EGT sample) except for PM. We use the earliest years with available data for PM emissions: 2012 for gasoline and 2005 for diesel. For the Copert methodology, we assume a 45 km/hr speed. CO_2 in g/km. NO_X, HC, and PM in mg/km. All predicted values correspond to the weighted average of the final sample's observations from the 2010 survey.

C.5 Cost estimation

C.5.1 Driving costs for cars and motorcycles

We estimate the cost of using a car or a motorcycle by combining the trip distance from the itinerary provided by TomTom, estimates of the fuel consumption of household vehicles, and average fuel prices in 2011 from the National Survey Institute ("Insee").[32] For motorcycles, we assign the average fuel consumption by the number of cylinders, which is the only motorcycle characteristic we observe in the EGT data.[33] When a household has multiple vehicles, we assume the trip uses the most fuel-efficient one. We also assume each individual pays the total cost of the trip, regardless of the number of passengers.

Both for cars and motorcycles, we estimate additional costs related to vehicle depreciation, insurance, and maintenance. To decide which element to include and how, we follow the methodology from the American Automobile Association (AAA), which produces yearly reports on the cost of driving for several countries, including France. While their estimates have been directly used in other studies (Almagro et al., 2024), we leverage the detailed information we have on individuals' cars, costs, and driving intensity to build our own estimates. This allows us to have more precise costs that are heterogeneous across individuals. From the list of non-fuel-related driving expenses suggested by the AAA, we account for the car depreciation, maintenance, and insurance.[34] To estimate the depreciation cost, we exploit the same data used for the emissions predictions to estimate the price of each car in the EGT sample. For cars, we follow Hang et al. (2016) and assume a 12-year, uniform depreciation

[32]Source for fuel prices: https://www.prix-carburants.developpement-durable.gouv.fr/petrole/se_cons_fr.htm.

[33]Source: French Energy Agency ("ADEME"). See https://www.statistiques.developpement-durable.gouv.fr/les-deux-roues-motorises-au-1er-janvier-2012.

[34]In the EGT, individuals report their "additional expenses including maintenance and insurance".

rate to obtain the yearly depreciation cost. For motorcycles, we assume a price of €1,500 and the same depreciation length and rate.[35] For the yearly maintenance and insurance costs, the EGT only provides six cost intervals at the household fleet level. We divide the values of the middle of the intervals by the size of the household's vehicle fleet.[36]

The EGT data contains the annual number of kilometers driven. To control for misreporting and extreme values, we assign each household to three possible values for cars: 7,500 km driven if the reported distance is below that value, 12,000 km if the reported distance is between 7,500 km and 17,500 km, and 17,500 km if the reported distance is larger than 17,500 km.[37] Since the average reported yearly distance driven with motorcycles is roughly half the one driven with cars, we divide by two these thresholds for motorcycles. Finally, we divide the sum of the yearly depreciation, maintenance, and insurance costs by the assigned number of kilometers driven to obtain a cost per kilometer. We winsorize the top and bottom one percent of this cost per kilometer distribution. We obtain an average cost of depreciation, maintenance and insurance of €0.22 for 2010 and €0.27 for 2020. Finally, we obtain the total cost of driving by adding the fuel costs. We find an average cost per-kilometer of €0.31 in 2010 and €0.34 in 2020. For comparison, the 2010 AAA report finds a per-kilometer cost before taxes of €0.45 for gasoline cars. Our estimate is slightly below the AAA estimate because we do not include potential loan repayments and parking costs (we do not have the information in the EGT data). Our average is also likely to be lower than the national average since Parisians tend to drive smaller cars, that are cheaper.

C.5.2 Public transport cost

The public transport network in Paris is operated by two companies: "RATP" mainly covers the public transport inside Paris and close suburbs, while "SNCF" operates trains connecting Paris to the suburban areas. During the period of the 2010 survey, the RATP pricing system relies on five pricing zones of the trip's origin and destination. We use the prices stated in the price guide of RATP for July 2011 and April 2020.[38] The ticket price using the SNCF network

[35]The average ownership length of a motorcycle in France is 12.2 years: https://www.onisr.securite-routiere.gouv.fr/etudes-et-recherches/vehicules/parc-des-vehicules/le-parc-deux-roues-motorises-des-menages#:~:text=L'%C3%A2ge%20moyen%20du%20parc,6%2C5%20ans%20en%202020.

[36]For households than own both cars and motorcycles, we count motorcycles as 0.8 cars, the value of the ratio between the reported cost for owners of a single motorcycle and a single car.

[37]In the 2010 report for France, the AAA uses an average of 9,363 km per year for conventional fuel cars. See https://www.automobile-club.org/actualites/la-vie-de-l-aca/budget-de-l-automobiliste-juin-2010.

[38]Source: "Guide tarifaire", July 2011, https://www.slideshare.net/quoimaligne/guide-tarifaire-ratp-sncf-ile-de-france-2011 and April 2020, https://www.iledefrance-mobilites.fr/medias/portail-idfm/9ae5b132-467f-404c-ac33-a6a5ffa679a8_16340_IDFM_guide_tarifaire_10x21_WEB.pdf.

depends on the exact stations of origin and destination rather than zones. Since there is no exhaustive data on the prices for all combinations of origin and destination train stations, we rely on a sample of ticket prices for 36 origin and destination pairs and estimate the train ticket price as a square function of the distance between stations. This regression has a good fit with an R^2 of 0.77. We use this function to predict prices for all origin-destinations pairs in the SNCF network. For 186 individuals, Google Maps does not provide a public transport route, yet they report using public transport. We impute the driving distance to compute their train ticket cost and use their reported travel times in the survey. For all train tickets, if the distance is larger than the maximum trip distance in the sample of SNCF tickets, we cap the distance to be the same as the maximum of the ticket sample (41 km). We thus avoid predicting the ticket price for distances that lie outside the ticket sample used for estimation.

For individuals with a public transport subscription, we estimate a trip's average cost by dividing the daily price of the subscription (obtained by dividing the subscription price by the relevant number of working days after accounting for holidays and bank holidays: 224) by two, which is the average number of trips taken in a day conditional on using public transport. For individuals without a subscription, missing information about their subscription coverage, or taking a trip outside their subscription coverage, we assume they pay the regular ticket price. The survey includes information on whether individuals can buy subsidized or reduced-price tickets, we use this information when computing the cost of public transport without subscription. Some itineraries require layovers between different services. Without a subscription, layovers between bus and tramway, as well as those between subway and commuter trains are included within a single ticket. Meanwhile, layovers such as bus-subway require the payment of an additional ticket. We account for these differences in our cost imputation.

In our final sample, 40.5% have a public transport subscription. Conditional on using public transport the share increases to 86%. There could be a selection effect on the estimation stage due to assigning to individuals that do not use public transport a higher cost of public transport than public transport users because of the subscription. We avoid this issue by predicting a cost of public transport net of the rebate related to the potential subscription. For this, we estimate the price with potential subscription from the individual ticket price and some individual characteristics on the subsample of public transport users. The individual characteristics are age and distance, which are likely to affect the subscription rebate value and the likelihood of holding a subscription. We consider the deciles of the age and the trip distance distributions. The average public transport cost with subscription is €1.75 while the average cost without subscription is €3.21.

C.6 Public transport overcrowding

We compute a line-level measure of overcrowding in public railway transport. To do so, we rely on data provided by SNCF and RATP on the number of passengers at the metro or train station level. We use data for 2015, the oldest data available, and consider only the urban railway network, where overcrowding is the most problematic. The data only records validations from passengers that use an electronic metro card; there is no exhaustive data on passengers using tickets. Estimates suggest that the electronic validations represent two-thirds of the traffic for 2016; we expect the share to be even higher during morning peak and off-peak hours.[39] We exploit the variation in traffic between peak and off-peak hours across metro lines to estimate the role of overcrowding in transportation decisions. As long as traffic is homogeneously underestimated over the network and periods, omitting a portion of the traffic is not a major problem.

The data we use is composed of two separate datasets. The first contains daily entry flows of passengers at the railway station level. The second dataset contains "hourly profiles" at the station level: the distribution of validations (in %) across hours for different periods (business days outside holidays, business days during school holidays, and weekends).[40] By combining these datasets, we obtain daily and hourly estimates of the number of passengers in each metro station for regular business days. We exclude weekends, school holidays, public holidays, and two dates with a relatively low total number of entries.[41] Finally, we average traffic levels over 172 days. We use the passenger flow between 7:00-8:59 a.m. to represent peak hours and 6:00-6.59 a.m. for off-peak hours. We observe the number of passengers entering each station, but not the line they take. Thus, we allocate passengers to metro lines proportionally, using the annual traffic levels by lines as weights.

We also use schedule data that provides frequencies of trains at the station level for the second semester of 2015.[42] We count the average number of scheduled trains for each line (and direction) and for each hour. Additionally, we gather information about the passenger capacity of the train models used on each line.[43] The passenger capacity represents the number of passengers a train can carry, assuming four passengers per square meter. We

[39] See https://www.iledefrance-mobilites.fr/usages-et-usagers-des-titres-de-transport.

[40] We use the average profiles for the business days outside holidays for the second semester of 2015 since we noticed some problems with the data from the first semester 2015: the percentages did not sum to 100% for 20 stations.

[41] These record total daily traffic levels below a million, while the average is 7.5 million according to the official figures of the RATP. We interpreted this low number of passengers as indicating the occurrence of a strike.

[42] "General Traffic Feed Specification", see: https://transitfeeds.com/l/162-paris-france.

[43] We rely on Wikipedia and internal reports from the transport organization in the Paris area "STIF" containing information about the characteristics of the fleet of trains.

compute the total railway line capacity Υ_{lt} by multiplying the train's physical capacity by the number of trains per hour. Finally, the overcrowding level c_{lt} for line l, at period t is:

$$c_{lt} = \frac{\psi_{lt}}{2 \times \Upsilon_{lt} \times ns_l},$$

where ψ_{lt} is the hourly number of passengers in line l at time period t and ns_l is the number of stations. Since there are two directions, we multiply the total line capacity by two and use the total number of passengers going in both directions. We assume an uniform distribution of passengers entering and exit each line and thus divide the measurement by each line's number of stations. Finally, we obtain individual overcrowding levels by weighting the overcrowding level of each line used in a trip by the time spent in that line. Finally, we provide in Table 19 the estimates of the overcrowding levels in the different metro and train lines. On average, we estimate the overcrowding to be 0.73 at off-peak hours and 1.8 at peak hours. But these averages hide substantial heterogeneity across lines that provide key variations for estimating the sensitivity to overcrowding in public transport.

Table 19: Estimates of overcrowding levels in the railway public transit.

Metro			**Suburb trains**		
Line	**Off-peak**	**Peak**	**Line**	**Off-peak**	**Peak**
1	0.27	1.21	A	0.78	2.08
2	0.29	1.31	B	0.52	1.12
3	0.35	1.58	C	0.39	1.2
3B	0.17	0.92	D	0.81	1.52
4	0.61	1.95	E	0.56	1
5	0.75	2.14	H	0.79	0.95
6	0.24	1.28	J	0.36	0.57
7	0.53	1.54	K	4.42	7.3
7B	0.2	1.06	L	0.7	2.19
8	0.26	1.17	N	0.79	1.42
9	0.28	1.12	P	2.17	3.63
10	0.19	1.32	R	0.8	1.1
11	0.56	2.08	U	2.08	4.59
12	0.31	1.63			
13	0.54	1.8			
14	0.43	1.46			
Average	0.37	1.47		1.17	2.2

C.7 Additional descriptive statistics

Table 20 provides a comparison between the durations and costs for the transportation modes available to each individual, in the final sample. Taking the car is the fastest option available to the largest fraction of individuals. However, the relatively low initial shares suggest that the high monetary cost dissuades many from choosing it. Interestingly, public transport is not, on average, the fastest nor the cheapest alternative, yet it is the most used mode in

both periods. The public transport cost does not increase much with distance while the car or motorcycle costs linearly increase with distance. For this reason, the maximum price of public transport is lower than the maximum car and motorcycle costs.

The last panel of Table 20 presents the share of individuals with access to each transportation mode and the share of trips done with each one of the five modes, in each period. Across modes and periods, the differences between both years are at most two percentage points, confirming the similarity in transportation patterns across surveys. Car usage at peak hours in the 2020 survey has the largest decrease with respect to 2010, with a 2.47 percentage point decrease. This small reduction seems to go towards an increases in public transport and bike usage (1.39 and 0.66 percentage points respectively). This change could also be explained by a decrease of 4.88 percentage points on car availability between the two surveys.

Table 20: Average duration, cost and availability by transportation mode.

Variable	**Mean**	**Median**	**Std. dev.**	**Min**	**Max**
Duration					
Bicycle	48.7	35.6	40.4	5.1	150
Public transport	41.9	37.8	23.6	2.58	266
Motorcycle	18.1	16.2	12.3	1.63	69.8
Walk	59.9	49	40	12.4	170
Car, peak	26.9	20.9	21.8	1.08	111
Car, non-peak	20.2	16.2	15.9	1.03	108
Cost					
Bicycle	0.68	0	0.8	0	1.74
Public transport	1.77	1.64	0.73	0.43	7.69
Motorcycle	3.3	2.14	3.48	0.1	26.9
Car	4.03	2.49	4.27	0.12	41.9
	Mode availability			**Shares**	
	2010	2020		2010	2020
Peak					
Bicycle	78.8	79.4		1.59	2.25
Public transport	86.1	87		34	35.4
Motorcycle	12.9	9.48		1.35	1.05
Walk	53.1	54.7		15.2	15.2
Car	78.8	73.9		24.4	21.9
Off-peak					
Bicycle	78.8	79.4		0.446	0.71
Public transport	86.1	87		11.7	13
Motorcycle	12.9	9.48		0.644	0.605
Walk	53.1	54.7		2.11	2.9
Car	78.8	73.9		8.46	6.97

Note: Durations in minutes, costs in €. Mode availability and initial shares in %. All statistics computed using survey weights.

D Additional estimation results

D.1 Control function approach for car travel times

We consider that there might be some endogeneity problem for individual trip durations. To formalize this issue, we consider that the source of endogeneity is due to unobservable individual preference for driving that might be correlated to the trip duration. For instance, if individuals like driving, they may locate in an area where the travel time is low. This is modeled as follow:

$$u_{n\mathbf{d}t} = \tilde{\beta}_n' \tilde{X}_{n\mathbf{d}t} + \beta_n^{\text{duration}} \text{duration}_{n\mathbf{d}t} + \xi_{n\mathbf{d}t} + \epsilon_{n\mathbf{d}t}$$

where $cov(\boldsymbol{\xi}_{\mathbf{d}t}, \mathbf{duration}_{\mathbf{d}t}) \neq 0$, $cov(\tilde{\mathbf{X}}_{\mathbf{d}t}, \boldsymbol{\xi}_{\mathbf{d}t}) = 0$ and $cov(\boldsymbol{\epsilon}_{\mathbf{d}t}, \mathbf{duration}_{\mathbf{d}t}) = 0$, $cov(\boldsymbol{\epsilon}_{\mathbf{d}t}, \boldsymbol{\xi}_{\mathbf{d}t}) = 0$. In short, only car trip duration is endogenous and the preference shock for driving can be decomposed as an exogenous iid term and another term that generates the correlation with duration.

We specify a control function as a linear function of a matrix of instruments Z. This matrix includes excluded instruments and individual characteristics which are also used to parametrize the preference heterogeneity. We rely on two sets of excluded instruments. First, we construct functions of other individuals' trip characteristics (other than duration), and choice sets at the origin or destination of an individual. The intuition is that choice set and trip characteristics should affect other individuals' decisions to drive and, thus, equilibrium speeds. But these variables should not affect individuals directly because what matters for an individual decision is only his own choice set and his own trip characteristics. We construct six instruments for the origin and the destination of an individual. These variables are the sum of other individuals' costs, the sum of other individuals' overcrowding levels at peak hours and off-peak hours, the sum of other individuals' trip distances, the sum of other individuals' numbers of alternatives in the choice set and the share of individuals with a car. The free-flow car trip duration (measured as trip duration at 3 a.m.) is the second set of excluded instruments. Finally, we use individual characteristics that shift preferences (income dummies, age dummies, a local linear function of distance and the socio-professional activity).

We use the same instruments for the duration at peak and off-peak hours. Formally, we have:

$$\text{duration}_{n\mathbf{d}t} = Z_{n\mathbf{d}t}\gamma_t + \eta_{n\mathbf{d}t}.$$

The important assumption is that $cov(\xi_{\mathbf{d}t}|Z_{\mathbf{d}t}) \neq 0$ but $cov(\eta_{\mathbf{d}t}, \xi_{\mathbf{d}t}) = 0$. In economic terms,

the assumption is that once we condition the duration of individual trip on the instruments, the residual is uncorrelated with unobserved individual preferences. And we can express the unobserved individual preference term as:

$$\xi_{n\mathbf{d}t} = \rho_t \eta_{n\mathbf{d}t} + \hat{\epsilon}_{n\mathbf{d}t},$$

with $cov(\hat{\epsilon}_{\mathbf{d}t}, \text{duration}_{\mathbf{d}t}) = 0$. Then, we can re-write the utility function as:

$$u_{n\mathbf{d}t} = \tilde{\beta}_n' \tilde{X}_{n\mathbf{d}t} + \beta_n^{\text{duration}} \text{duration}_{n\mathbf{d}t} + \rho_t \eta_{n\mathbf{d}t} + \hat{\epsilon}_{n\mathbf{d}t} + \epsilon_{n\mathbf{d}t}$$

The standard assumption would be to consider the joint distribution of the error terms to be normal: $(\eta_{\mathbf{d}t}, \xi_{\mathbf{d}t}) \sim N(0, \Sigma)$ so that $\hat{\epsilon} \sim N(0, \sigma^{\hat{\epsilon}})$. As it has been done previously in the applied literature, we set $\sigma^{\hat{\epsilon}} = 0$ and ignore $\hat{\epsilon}_{n\mathbf{d}t}$.

Table 21 provides the results of the regressions of driving durations at peak and off-peak hours on the instruments. The R^2 are very high, indicating strong predicting power of the instruments.

Table 21: First-stage regressions.

	Peak hours		Off-peak hours	
	Parameter	**Std. error**	**Parameter**	**Std. error**
Intercept	20.9**	(2.19)	9.52**	(1.02)
Income ∈ [800, 1,200[	-0.057	(0.187)	-0.044	(0.09)
Income ∈ [1,200, 1,600[	-0.097	(0.187)	-0.059	(0.091)
Income ∈ [1,600, 2,000[	-0.157	(0.19)	-0.02	(0.094)
Income ∈ [2,000, 2,400[	0.067	(0.196)	-0.012	(0.099)
Income ∈ [2,400, 3,000[	-0.29	(0.212)	-0.199†	(0.108)
Income ∈ [3,000, 3,500[	-0.329	(0.216)	-0.238*	(0.107)
Income ∈ [3,500, 4,500[	-0.505*	(0.223)	-0.337**	(0.111)
Income ≥ 4,500	-0.185	(0.3)	-0.158	(0.153)
Age ∈]18, 30]	-0.929*	(0.379)	-0.486*	(0.195)
Age ∈]30, 40]	-1.08*	(0.427)	-0.693**	(0.219)
Age ∈]40, 50]	-1.26**	(0.425)	-0.808**	(0.218)
Age ∈]50, 60]	-1.21**	(0.428)	-0.718**	(0.22)
Age > 60	-1.45**	(0.52)	-0.971**	(0.261)
Distance	1.48**	(0.204)	-0.796**	(0.103)
(Dist-d_2) × (dist≥d_2)	0.876**	(0.277)	2.43**	(0.136)
(Dist-d_3) × (dist≥d_3)	-3.89**	(0.49)	-0.848**	(0.293)
(Dist-d_4) × (dist≥d_4)	-0.272	(1.01)	0.954	(0.826)
Craftspersons	-0.134	(1.85)	0.125	(0.882)
Shopkeepers	0.279	(0.906)	0.13	(0.435)
Entrepreneurs, self-employed	0.001	(0.801)	-0.052	(0.399)
Public executives	-0.262	(0.712)	-0.109	(0.343)
Private executives	0.363	(0.706)	0.079	(0.339)
Education, health	-0.111	(0.705)	0.097	(0.339)
Administrative professions	1.23†	(0.72)	0.561	(0.35)
Technicians	0.602	(0.743)	0.326	(0.361)
First-line supervisors	1.08	(0.848)	0.335	(0.413)
Public employees	0.194	(0.725)	0.231	(0.351)
Private employees	0.86	(0.73)	0.386	(0.356)
Retail employees	-0.528	(0.87)	-0.328	(0.43)
Services	1.4†	(0.786)	0.704†	(0.38)
Qualified workers	0.192	(0.727)	0.196	(0.35)
Unqualified workers	0.331	(0.816)	0.244	(0.379)
Students ≤ high school	-0.839	(0.802)	-0.381	(0.393)
Students in higher education	-0.397	(0.741)	-0.4	(0.364)
Sum of costs, at origin	0.261**	(0.061)	0.167**	(0.033)
Sum of overcrowding levels, peak, at origin	-2.19**	(0.454)	-2.08**	(0.237)
Sum of overcrowding levels, off-peak, at origin	2.45**	(0.612)	2.28**	(0.318)
Sum of distances, at origin	-4.44**	(0.581)	-1.36**	(0.29)
Sum of number of alternatives, at origin	-3.35**	(0.354)	-1.67**	(0.165)
Car ownership rate, at origin	15**	(0.813)	6.69**	(0.399)
Sum of costs, at destination	0.783**	(0.061)	0.375**	(0.028)
Sum of overcrowding levels, peak, at destination	10.9**	(0.483)	5.23**	(0.241)
Sum of overcrowding levels, off-peak, at destination	-15.4**	(0.783)	-7.16**	(0.384)
Sum of distances, at destination	-6.33**	(0.619)	-3.15**	(0.284)
Sum of number of alternatives, at destination	0.27	(0.337)	0.077	(0.153)
Car ownership rate, at destination	-18.2**	(1.01)	-8.02**	(0.49)
Free-flow duration	1.54**	(0.016)	1.25**	(0.009)
R^2	0.948		0.975	

*Note: The reference categories are individuals with age < 18, with an income below €800 and farmers. Duration and free-flow duration measured in 10 minutes. Significance levels: **: 1%, *: 5%, †: 10%.*

D.2 Robustness checks for the transportation mode choice model

We analyze the robustness of our estimates to several model assumptions. Table 22 provides the estimates of the average utility parameters, while Table 23 presents the implied values of travel time.

Weather controls We use historical hourly data from OpenWeather for the city of Paris to control for the possible role of weather on individual choices.[44] First, we match the OpenWeather data to the exact departure hour and date provided in the survey. Then, based on the distribution of temperatures in our sample, we construct temperature quintiles. For rain and snow, we create four categories based on the levels (in millimeter per hour): 0, less than 0.3, between 0.3 and 0.8, and more than 0.8. The weather dummies are then interacted with the bike and walk alternative constants, as these modes are the most susceptible to being affected by the weather shocks. The inclusion of weather controls has no significant impact on the average sensitivities to duration and cost and almost no impact on the distribution of valuations of travel time.

Travel time reliability Recent transportation literature has focused on the importance of the reliability of travel time for individual transportation decisions (Small et al., 2005, Engelson and Fosgerau, 2016, Hall and Savage, 2019, Bento et al., 2020). We study the role of preferences for travel time reliability in our model and how including this factor affects our estimates. We build a measure of travel time reliability by collecting real-time traffic data from TomTom for all trips in our sample that have car access, for every weekday between February 26$^{\text{th}}$, 2024, and March 22$^{\text{nd}}$, 2024. We query trip itinerary and durations at 6:30 a.m. (to represent off-peak hours) and at 8:30 a.m. (for peak hours). We construct a proxy of reliability by taking the standard deviation of the durations for each trip at each period.[45]. As seen from the estimation results, the average utility parameters remain close to the benchmark, and the distribution of the values of travel time is marginally lower.

Alternative model assumptions First, we consider a model where we modify the nest structure by allowing individuals to choose first between transportation modes and then peak and off-peak hours. This model allows for correlation in the preference shocks across departure times for a given mode. However, column (4) of Table 22 shows a high value for the

[44]Source for weather data: https://openweathermap.org/.

[45]We also consider another reliability measure given by the difference between the 80$^{\text{th}}$ and 50$^{\text{th}}$ percentiles as suggested by Small et al. (2005). We choose to rely on the standard deviation because we obtain a better fit

nest parameter (σ), almoost equal to 1, indicating that the options within nests are almost independent and suggesting that our nesting structure is more relevant.

Then we consider two specifications were we modify our assumptions regarding the cost of the trip. In column (5) of Table 22, we analyze the effect of not including the additional cost per km driven (depreciation, maintenance, and insurance). We find larger average sensitivities to cost, which translate into a large decrease in the mean VOT, reaching only €3.8. In the second specification, column (6) of Table 22, we do not perform the correction for the cost of public transport subscriptions. This implies that individuals without subscription pay the full price, while individuals with subscription pay the average trip cost of their subscription. We find a large decrease in the average sensitivity of cost, leading to a large increase in the distribution of valuation of travel time, with a mean VOT of €326. Such high VOT values are unrealistic, supporting the relevance of our correction

Finally, we consider two possible changes to our choice set definition. First, we allow every individual to drive, even those who do not own a car. For those without a car, we attribute the average car cost in the sample. Then, we query the TomTom service for those trips for the travel times, as with the rest of the sample. As expected, adding a non-available alternative changes the results by lowering the average utility of driving. As seen in column (7) of Table 22, this change leads to small changes in the average duration cost sensitivities. These changes lead to a small decrease in the average VOT, as seen in Table 23. The second change in the choice set definition corresponds to allowing only individuals who have a bike or a bike-sharing pass to use this mode. We see very small changes, in particular, the mean valuation for bicycling marginally increases. The distribution of valuations of travel time remains increases with respect to our benchmark and there is a significant increase in the nest parameter, implying less correlation between periods.

Table 22: Average estimated parameters under alternative model specifications.

Coefficients	(1)		(2)		(3)		(4)		(5)		(6)		(7)		(8)	
Duration	-0.61**	(0.014)	-0.611**	(0.014)	-0.609**	(0.014)	-0.611**	(0.02)	-0.618**	(0.013)	-0.591**	(0.013)	-0.5910	(0.013)	-0.6140	(0.014)
Cost	-0.312**	(0.016)	-0.312**	(0.016)	-0.333**	(0.017)	-0.313**	(0.017)	-1.01**	(0.043)	-0.121**	(0.012)	-0.3290	(0.016)	-0.2930	(0.016)
Bicycle, peak	-3.47**	(0.075)	-3.47**	(0.075)	-3.42**	(0.074)	-3.47**	(0.1)	-3.3**	(0.077)	-3.53**	(0.077)	-3.410	(0.074)	-3.340	(0.077)
Public transport, peak	-1**	(0.062)	-0.897**	(0.091)	-0.969**	(0.062)	-0.995**	(0.062)	-0.332**	(0.079)	-1.21**	(0.063)	-0.9040	(0.059)	-0.9880	(0.062)
Motorcycle, peak	-3.43**	(0.112)	-3.33**	(0.13)	-3.28**	(0.111)	-3.46**	(0.133)	-3.49**	(0.114)	-3.65**	(0.117)	-3.440	(0.109)	-3.420	(0.113)
Car, peak	-2.68**	(0.527)	-2.59**	(0.527)	-2.79**	(0.54)	-2.68**	(0.529)	-3.3**	(0.545)	-2.99**	(0.54)	-3.810	(0.457)	-2.550	(0.517)
Car, off-peak	-3.88**	(0.544)	-3.79**	(0.543)	-3.69**	(0.55)	-4.02**	(0.534)	-4.62**	(0.56)	-4.3**	(0.593)	-5.030	(0.474)	-3.850	(0.541)
Public transport, off-peak	-1.9**	(0.174)	-1.78**	(0.181)	-1.65**	(0.128)	-2.07**	(0.085)	-1.16**	(0.154)	-2.22**	(0.296)	-1.760	(0.148)	-1.980	(0.202)
Walking, off-peak	-0.737**	(0.154)	-0.743**	(0.152)	-0.541**	(0.108)	-0.888**	(0.092)	-0.86**	(0.151)	-0.847**	(0.255)	-0.7480	(0.139)	-0.8260	(0.181)
Bicycle, off-peak	-4.15**	(0.16)	-4.17**	(0.159)	-3.96**	(0.129)	-4.27**	(0.149)	-4.08**	(0.16)	-4.32**	(0.242)	-4.080	(0.148)	-4.060	(0.176)
Motorcycle, off-peak	-3.73**	(0.162)	-3.62**	(0.173)	-3.49**	(0.139)	-3.83**	(0.161)	-3.8**	(0.159)	-4.02**	(0.226)	-3.740	(0.153)	-3.760	(0.178)
No. layovers in PT	-0.486**	(0.041)	-0.485**	(0.041)	-0.453**	(0.041)	-0.484**	(0.042)	-0.252**	(0.039)	-0.265**	(0.038)	-0.5110	(0.038)	-0.4110	(0.039)
Railway only	0.015	(0.063)	0.014	(0.063)	0.032	(0.062)	0.014	(0.064)	0.131*	(0.065)	0.107†	(0.063)	-0.0290	(0.06)	0.0420	(0.063)
PT overcrowding	-0.066*	(0.033)	-0.066*	(0.033)	-0.06†	(0.031)	-0.065†	(0.034)	0.06†	(0.034)	-0.004	(0.034)	-0.050	(0.031)	-0.0680	(0.033)
σ	0.816**	(0.16)	0.807**	(0.153)	0.617**	(0.105)	0.999**	(0.058)	0.87**	(0.135)	0.978**	(0.299)	0.8130	(0.136)	0.9070	(0.192)
Reliability					0.069**	(0.014)										
Log-likelihood	-17,441		-17,417		-17,429		-17,441		-17,130		-17,600		-18,442		-17,416	

*Note: (1): Baseline model. (2): Weather controls. (3): Travel time reliability. (4): Departure periods as nests. (5): Only fuel cost for cars. (6): No public transport subscription correction for cost. (7): Car available to everyone. (8): Bicycle not widely availability. Walking at peak hours is the baseline alternative. Duration measured in 10 minutes. Cost in €. We provide the mean coefficients, the standard-errors are computed using the delta-method. Significance levels: **: 1%, *: 5%, †: 10%.*

Table 23: Values of travel time for the alternative specifications.

	Min	Q1	Mean	Median	Q99	Max
(1) Baseline	1.58	2.55	17.4	15.6	53.8	90.3
Alternative specifications						
(2) Weather controls	1.58	2.58	17.4	15.6	54.1	91.3
(3) Reliability measure	1.57	2.52	15.3	14.2	43.3	67.3
Alternative specifications						
(4)Periods as nests	1.58	2.56	17.4	15.6	53.3	86.9
(5) Only fuel costs	0	0.942	3.8	3.72	6.78	7.17
(6) No public transport subscription correction	0	8.03	326	31.8	2841	2,887
(7) Car widely availability	1.16	2.74	16.4	14	51	111
(8) Bicycle not widely availability	2.11	3.09	18.5	16.6	57	91.4

Note: in €/hr.

D.3 Additional results on the value of time

We present the distributions of the value of travel time by age, income, and trip distance in Figure 9 using second-order local polynomials. Young individuals are associated with the lowest values of the opportunity cost of time. The VOT then increases with age, reaching its highest value around 45 years old. After that age, the VOT starts decreasing, and it becomes around 20% lower than the maximum at age 70. We also see some heterogeneity in the VOT across income categories, but the heterogeneity is less pronounced. Poor individuals have the lowest valuations of time, on average, but the opportunity cost of time increases rapidly with income. The average VOT slightly decreases between incomes of 1,800 an income of 3,200, and then the average VOT increases. Regarding the VOT and distance, we see non-monotonic effects of distance. Short trips tend to be associated with a low valuation of travel time, which is consistent with the distribution of distances by age: the shortest commuters tend to be children in high-school or below. The VOT values rapidly increase with distance, decrease until 20 km, and rise again but more slowly.

Figure 9: Value of travel time and individual characteristics.

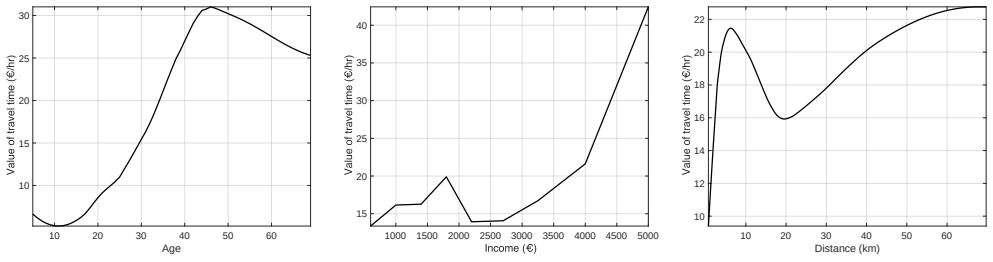

D.4 Traffic sensor data and congestion technology estimates

D.4.1 Definition of the areas

Figure 10 displays the locations of the traffic sensor stations (black dots) as well as the definitions of the five areas in our model: city center (light grey), ring roads (the circles around the city center, in white), the close suburbs (dark grey), the far suburbs (the part with no color) and the highways (the dots connecting the suburb to the city center). As we can see in Figure 10, there is no traffic sensor station in the suburbs outside of the highways. The data comes from two different sources. The highway traffic data comes from the regional road maintenance agency (DRIF). Traffic data for Paris and for the ring roads comes from the city of Paris.[46]

Figure 10: Traffic sensors' road coverage.

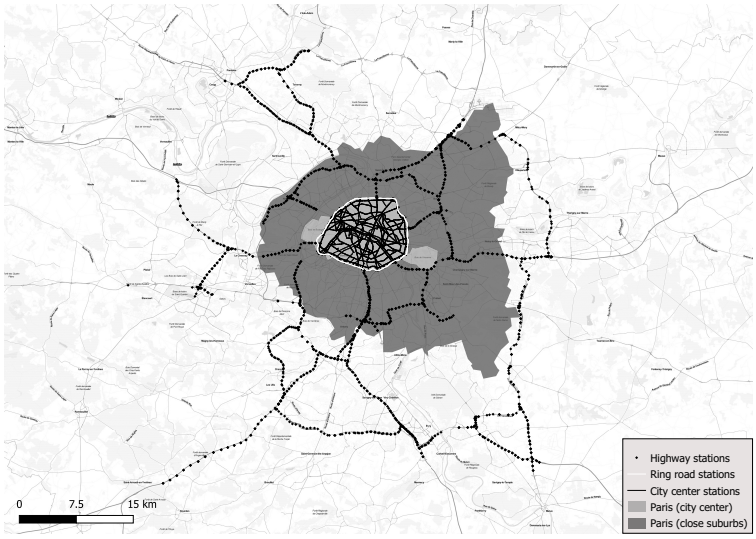

D.4.2 Fundamental equations of traffic

The traffic flow (number of vehicles passing per hour), traffic density (number of vehicles per kilometer and hour), and speed are related through the fundamental equation of traffic flow:

$$\text{traffic flow} = \text{speed} \times \text{traffic density}.$$

[46]Source: https://opendata.paris.fr/explore/dataset/comptages-routiers-permanents-historique/information/.

The road traffic density is related to the occupancy rate (the fraction of the road-lane occupied by a vehicle) using:

$$\text{traffic density} = \frac{\text{occupancy rate}}{M+h} \times \text{no. lanes}, \tag{13}$$

where M is the mean effective car length, representing the length of the car plus the space between two vehicles. h represents the length of a traffic sensor. The data on the highways contain all traffic variables but the data from the city center and the ring roads do not record speeds. We reorganize the fundamental equation above to obtain the speeds from occupancy rates and traffic flows:

$$\text{speed} = \frac{\text{traffic flow}}{\frac{\text{occupancy rate}}{M+h} \times \text{no. lanes}}. \tag{14}$$

D.4.3 Sample construction

For traffic observations from the highways connecting the far suburb to the city center, we restrict the sample to sensors that record traffic going in the direction of the city center. We drop outliers in speed (below 0 or greater than the maximum highway speed limit, 130 km/hr) and occupancy rates (below 0% and above 50%). An occupancy rate of 50% represents extreme traffic conditions: the traffic monitoring institute in Paris defines traffic as pre-saturated from 15% and saturated from 30%. We follow the same approach when cleaning the data from Seine-Saint-Denis. We also detect inconsistent observations using the fundamental relationship between traffic flow, occupancy rates, and speed. More specifically, we combine the Equations 13 and 14 to obtain the implied average car length plus sensor length from traffic flow, speed, and occupancy rate:

$$M + h = \frac{\text{occupancy rate} \times \text{speed} \times \text{no. lanes}}{\text{traffic flow}}.$$

We then drop observations in the top and bottom 1% of the implied length distribution, keeping 6.1 million observations.

The data on the city center traffic and the ring roads contain sensor measurements of traffic flows and occupancy rates only. Unfortunately, sensors cannot measure speed accurately because of traffic lights and multiple intersections.

Instead of relying on an assumption for the effective car length as often done in the literature (e.g., Geroliminis and Daganzo, 2008 or Loder et al., 2017), we rely on the highway data to predict the average car length plus sensor length in Paris. It has been documented by Jia

et al. (2001) that the traffic composition varies over time, making the uniform car length assumption inappropriate. We rely on a prediction model for the average car length plus sensor length that we estimate using the highway data. Then, we use this model to predict hourly lengths in the city center and the ring roads. Our prediction model specifies the length as a function of the distance to the city center and day-of-the-week interacted with hour fixed effects. Because the relationship between the length and the distance to the city center may not be constant as we get closer to the city center, we rely on a piecewise linear specification with six intervals. This prediction model is estimated using 4.8 million observations from highway data, for which we observe the GPS coordinates of the measurement stations and obtain an R^2 of 0.18. For predictions, we set the distance to the city center to 0. We then get expected lengths specific to the hour and the day of the week. We do not directly observe the number of lanes in the city center traffic data, so we rely on additional data from Open Street Map. Finally, we exclude outliers in occupancy rate and estimated speed following the same criteria as before for the highway data.

Additional data from Seine-Saint-Denis For the additional data used to calibrate the linear combination technology for the close suburbs, we received data from the Directorate of Roads and Travel of the Seine-Saint-Denis Department. The data for Seine-Saint-Denis has good coverage of that area of the close suburbs. However, measurements of traffic conditions are very noisy in the data (speed intervals such as 0 to 30 km/hr rather than exact speeds) and only covers one week of data per sensor. Therefore, it is not enough to directly estimate a congestion technology, which is why we do not include those sensors in Figure 10.

The additional data covers 71 sensors across the Seine-Saint-Denis department. For each sensor, data for one week of 2023 are provided (ranging from January 25$^{\text{th}}$ 2023 to April 20$^{\text{th}}$ 2023). For each sensor, the number of vehicles (cars and trucks) going at different speed intervals is recorded each hour. The first speed interval is 0-30 km/hr and then each interval has a 10 km/hr range. We compute the average hourly speed of a sensor by taking the average across the midpoints of each interval, weighted by the number of vehicles in the interval. However, this average hourly speed is a noisy measure of the actual speed, as the intervals are fairly large. In particular, the first interval from 0 to 30 km/hr is large enough to hide important speed variation during the most congested periods. The data includes roads lengths, average speeds, and flows, but no occupancy rate measure. We rearrange Equation 13 to express occupancy rate as a function of the observed variables and we assume a mean car length of 5.9 meters (the average car length we estimated for Paris). We drop observations following the same criteria as for the city center sensors.

Finally, we compute average speed and occupancy rates by weighting each sensor by the

average traffic flow of the sensor. We find an average speed of 34.9 km/hr and an occupancy rate of 14.1 % at peak hours, while we find a speed of 36.6 km/hr and an occupancy rate of 11.4 % at off-peak hours.

Additional data for the instrumental variables We use data on accidents recorded by the National interministerial road safety observatory (ONISR).[47] It contains the date and time of every accident that involved at least one vehicle and where at least one person required medical care. The information in the dataset comes from the corresponding police reports of the accidents. During the period 2016 to 2017, the dataset records 25,439 accidents in the Paris metropolitan area. Additional instruments rely on weather changes. We use data on weather conditions in Paris at the hourly level from OpenWeatherMap.[48]

D.4.4 Fit of the congestion technology models

Table 24 represents the number of observations used to estimate the congestion technologies for each area and the fit of the models, measured by the R^2. The three congestion technologies have good fits with R^2 between 0.21 for the city center and 0.69 for the ring roads. The lower R^2 in the city center probably reflects more idiosyncrasies in traffic speed: traffic lights and intersections generate heterogeneous traffic flows, implying heterogeneous speeds.

Table 24: Fit of the congestion technology by area.

Area	Number of observations	R^2	Degree
Highways	6,195,874	0.65	8
City center	8,013,979	0.21	3
Ring roads	1,907,088	0.69	8

Note: "Degree" represents the degree of the polynomial.

D.5 Additional results on checking the equilibrium uniqueness

D.5.1 Formula for the Jacobian

We provide here the analytical formula for the Jacobian of the contraction defined as:

$$g_t^a(\mathbf{v}, \kappa) = \kappa v_t^a + (1 - \kappa) f^a(\mathbf{v}).$$

We can identify, in the Jacobian, three types of derivatives: $\frac{\partial g_t^a(\mathbf{v},\kappa)}{\partial v_t^a}$, $\frac{\partial g_t^a(\mathbf{v},\kappa)}{\partial v_t^{\tilde{a}}}$ and $\frac{\partial g_t^a(\mathbf{v},\kappa)}{\partial v_{t'}^{\tilde{a}}}$.

[47] Source: https://www.data.gouv.fr/fr/datasets/bases-de-donnees-annuelles-des-accidents-corporels-de-la-circulation-routiere-annees-de-2005-a-2022/.

[48] See https://openweathermap.org/.

$$\frac{\partial g_t^a(\mathbf{v},\kappa)}{\partial v_t^a} = \kappa + (1-\kappa)\underbrace{f^{a'}\left(\sum_{n=1}^N \omega_n k_n^a s_{n\mathbf{d}t}(\mathbf{v}) + K_{0t}^a\right)}_{\leq 0} \times \sum_{n=1}^N \underbrace{\omega_n k_n^a \frac{\partial s_{n\mathbf{d}t}(\mathbf{v})}{\partial v_t^a}}_{\geq 0}$$

$$\frac{\partial g_t^a(\mathbf{v},\kappa)}{\partial v_t^{\tilde{a}}} = (1-\kappa)\underbrace{f^{a'}\left(\sum_{n=1}^N \omega_n k_n^a s_{n\mathbf{d}t}(\mathbf{v}) + K_{0t}^a\right)}_{\leq 0} \times \sum_{n=1}^N \underbrace{\omega_n k_n^a \frac{\partial s_{n\mathbf{d}t}(\mathbf{v})}{\partial v_t^{\tilde{a}}} \mathbb{1}\{k_n^{\tilde{a}} > 0\}}_{\geq 0}$$

$$\frac{\partial g_t^a(\mathbf{v},\kappa)}{\partial v_{t'}^{\tilde{a}}} = (1-\kappa)\underbrace{f^{a'}\left(\sum_{n=1}^N \omega_n k_n^a s_{n\mathbf{d}t}(\mathbf{v}) + K_{0t}^a\right)}_{\leq 0} \times \sum_{n=1}^N \underbrace{\omega_n k_n^a \frac{\partial s_{n\mathbf{d}t}(\mathbf{v})}{\partial v_{t'}^{\tilde{a}}} \mathbb{1}\{k_n^{\tilde{a}} > 0\}}_{\leq 0}$$

Given the functional form assumptions we make on the demand model, the derivatives of the probability of driving at period t_1 with respect to speeds at period t_1 and t_2 are given by:

$$\begin{aligned}
\frac{\partial s_{n\mathbf{d}t_1}(\mathbf{v})}{\partial v_{t_1}^a} &= \left[\phi_n \pi_n \sigma s_{n\mathbf{d}t_1|\mathcal{T}_1}(1 - s_{n\mathbf{d}t_1|\mathcal{T}_1}) + (1-\phi_n) s_{n\mathbf{d}t_1|\mathcal{T}_{12}} \left(1 - (1-\sigma)\frac{s_{n\mathbf{d}t_1|\mathcal{T}_{12}}}{s_{n\mathbf{d}t_1|\mathcal{T}_{12}} + s_{n\mathbf{d}t_2|\mathcal{T}_{12}}} - \sigma s_{n\mathbf{d}t_1|\mathcal{T}_{12}}\right)\right] \\
&\quad \times \left(-\frac{k_n^a}{(v_{t_1}^a)^2}\rho_{nt_1}\right) \times 6 \times \frac{\beta_n^{\text{duration}}}{\sigma} \\
\frac{\partial s_{n\mathbf{d}t_1}(\mathbf{v})}{\partial v_{t_2}^a} &= (1-\phi_n) s_{n\mathbf{d}t_1|\mathcal{T}_{12}} \left(-(1-\sigma)\frac{s_{n\mathbf{d}t_2|\mathcal{T}_{12}}}{s_{n\mathbf{d}t_1|\mathcal{T}_{12}} + s_{n\mathbf{d}t_2|\mathcal{T}_{12}}} - \sigma s_{n\mathbf{d}t_2|\mathcal{T}_{12}}\right) \\
&\quad \times \left(-\frac{k_n^a}{(v_{t_2}^a)^2}\rho_{nt_2}\right) \times 6 \times \frac{\beta_n^{\text{duration}}}{\sigma}
\end{aligned}$$

Note that the factor 6 corresponds to converting speeds in km/hr into tens of minutes, which is the unit of duration in the individual utility.

D.5.2 Additional results on the equilibrium solving algorithm

We show additional numerical results about the convergence by plotting the average number of iterations needed to converge for the possible values of κ between 0.55 and 0.95. More specifically, we draw ten different initial speed values from a uniform distribution over $[\underline{\mathbf{v}}, \overline{\mathbf{v}}]$ and solve for the speed equilibrium with different values for the tuning parameter. As expected, the number of iterations and the time increases exponentially from $\kappa = 0.55$ onward. Furthermore, we always converged to the same equilibrium speeds. This shows that the choice of setting $\kappa = 0.65$ is not too inefficient regarding convergence speed. Figure 11 indicates the number of iterations and the convergence time depending on the tuning parameter. The graphs are very similar when we introduce any policy.

Figure 11: Average number of iterations and convergence times (across 10 simulations).

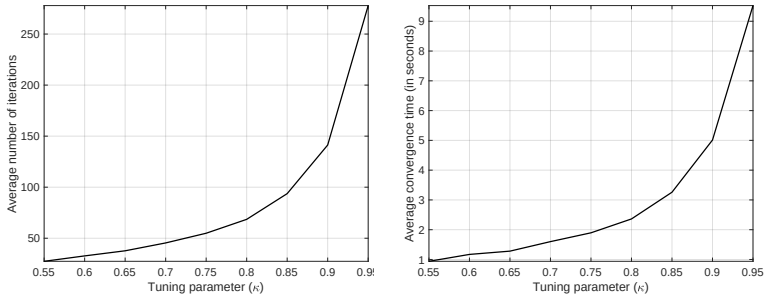

(a) Number of iterations. (b) Average convergence time.

E Additional results on the policy effects

E.1 Consumer surplus and welfare definitions

To evaluate the impacts of transportation policies on individuals, we rely on changes in consumer surplus, which measure compensating variations. The consumer surplus per trip for individual n is defined as the expected utility of the choice that maximizes the utility conditional on the set of periods available $\mathcal{T}_n$. It is:

$$CS_n|\mathcal{T}_n = \frac{1}{|\alpha_n|} \log\left(\sum_{j\in\mathcal{J}_n} \exp(\sigma \log(D_{nj}))\right),$$

where $D_{nj} = \sum_{t\in\mathcal{T}_n} \exp\left(\frac{\beta_n' X_{njt}}{\sigma}\right)$ is the expected utility of the best departure period within $\mathcal{T}_n$ for transportation mode j. α_n is the parameter of sensitivity to the trip cost, which converts the utility into monetary terms. Note that there is a constant utility term that cannot be identified and that is normalized to 0 in the expression above.

The variation of consumer surplus eliminates the constant and thus is identified and given by:

$$\Delta CS_n|\mathcal{T}_n = \frac{1}{|\alpha_n|}\left[\log\left(\sum_{j\in\mathcal{J}_n^1} \exp(\sigma \log(D_{nj}^1))\right) - \log\left(\sum_{j\in\mathcal{J}_n^0} \exp(\sigma \log(D_{nj}^0)\right)\right].$$

Where $\mathcal{J}_n^1$ and D_{nj}^1 represent respectively the choice set and the expected utility of transportation mode j under the counterfactual scenario, while $\mathcal{J}_n^0$ and D_{nj}^0 represent their initial values.

In our model with stochastic constraints, the change in individual surplus is thus:

$$\Delta CS_n = (1-\phi_n)\Delta CS_n|\mathcal{T}_{12} + \phi_n\pi_n\Delta CS_n|\mathcal{T}_1 + \phi_n(1-\pi_n)\Delta CS_n|\mathcal{T}_2.$$

We can further decompose the variation in consumer surplus into a partial policy effect which measures the policy effect at constant initial speeds, and an equilibrium speed effect under the implemented policy. To make the expression clearer, we make apparent the dependence between the driving speeds and the utilities associated with the transportation modes $D^0_{nj}(\mathbf{v_0})$ and $D^1_{nj}(\mathbf{v_1})$, where $\mathbf{v_0}$ and $\mathbf{v_1}$ represent the initial and final vectors of speeds. The decomposition is given by:

$$\Delta CS_n|\mathcal{T}_n = \frac{1}{|\alpha_n|}\Bigg[\underbrace{\log\left(\sum_{j\in\mathcal{J}^1_n}\exp\left(\sigma\log\left(D^1_{nj}(\mathbf{v_0})\right)\right)\right) - \log\left(\sum_{j\in\mathcal{J}^0_n}\exp\left(\sigma\log\left(D^0_{nj}(\mathbf{v_0})\right)\right)\right)}_{\text{policy effect at constant speed}}$$
$$\underbrace{+\log\left(\sum_{j\in\mathcal{J}^1_n}\exp\left(\sigma\log\left(D^1_{nj}(\mathbf{v_1})\right)\right)\right) - \log\left(\sum_{j\in\mathcal{J}^1_n}\exp\left(\sigma\log\left(D^1_{nj}(\mathbf{v_0})\right)\right)\right)}_{\text{equilibrium speed effect}}\Bigg]$$

Our welfare change outcome is simply the sum of consumer surplus change, the potential toll revenue and the monetary value of emissions avoided :

$$\Delta W = \sum_{n=1}^{N}\omega_n\left(\Delta CS_n + \sum_{t=\{t_1,t_2\}}\left(p_{nt}s^1_{n\mathbf{d}t} + \left(e^1_{nt}s^1_{n\mathbf{d}t} - e^0_{nt}s^0_{n\mathbf{d}t}\right)k_n\right)\right),$$

where p_{nt} is the toll for individual n and period t. e^0_{nt} represents the cost of emissions, per kilometer, for individual n and period t in the initial situation and e^1_{nt} in the counterfactual situation. The emission costs are function of the period and the policy environment because in some specifications the emissions levels depend on the speeds. $s^0_{n\mathbf{d}t}$ and $s^1_{n\mathbf{d}t}$ represents the probability to drive at period t under the initial situation, and the counterfactual policy respectively.

E.2 Social costs of emissions

All the values used for the social cost of emissions come from a 2019 report from the European Commission (Van Essen et al., 2019). The values for NO_X and PM correspond to the "transport city" and "transport metropole" values for those pollutants in Table 14 of the report. For hydrocarbons (HC), we take the value for non-methane volatile organic compound (NMVOC), which includes hydrocarbons. Finally, for CO_2 we use the "high" cost estimate from Table 24 in the report.

We use EGT survey data on each individual's car in order to estimate their emissions of pollutants per kilometer driven, details are available on Appendix C.4.1. As a robustness

check, we compute a second set of emissions estimates that depend on driving speeds, details can be found on Appendix C.4.2. Table 25 presents the average social cost in cents per km driven of the emissions for the vehicles in the final sample using the main emissions estimates. Gasoline cars have, on average, a lower social cost from emissions than diesel cars. For gasoline cars, CO_2 is the main driver of the cost of emissions with a 92.9% share. For diesel vehicles, CO_2 remains an important component of emissions costs, but NO_X and PM also represent important shares of the emissions social cost.

Table 25: Social costs of emissions per kilometer driven.

	Gasoline	Diesel
Average cost per km	3.4	4.53
Cost composition (in %)		
CO_2	92.9	62.3
NO_X	4.15	16.4
HC	0.36	0.12
PM	2.63	21.2

Note: Average cost in cents of euro per km. All statistics computed using survey weights, restricting the sample to the 2010 EGT survey, and using the baseline approach to estimate vehicles' emissions.

E.3 Additional results on the comparison across stringency levels

E.3.1 Additional outcomes of the policy effects

We provide the equilibrium speeds for three areas for all policy stringency levels in Figure 12. At peak hours, the speeds increase with the policy stringency level, while at off-peak hours, they decrease monotonically. This is the consequence of major shifts towards driving at off-peak hours. The speed at peak hours changes the most on the highways while there is much less speed improvement in the city center. At the same time, the off-peak hour speed in the city center is almost constant. This reflects that individuals driving in the city center have better alternatives to cars, while those who use the highways and the ring roads are more likely to substitute for driving during off-peak hours.

Figure 12: Speeds under the different policies and stringency levels.
Peak hours.

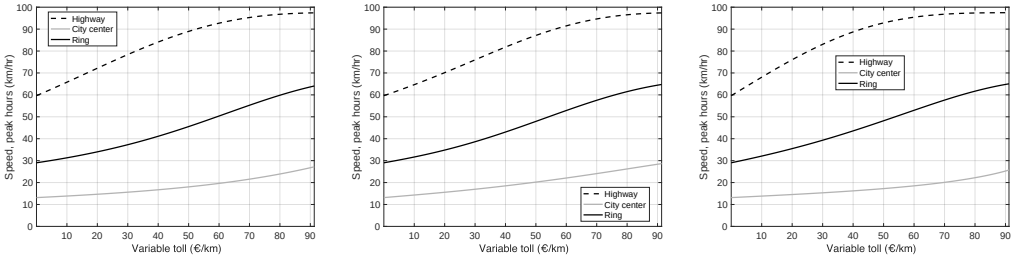

(a) Driving restrictions. (b) Uniform tolls. (c) Variable tolls.

Off-peak hours.

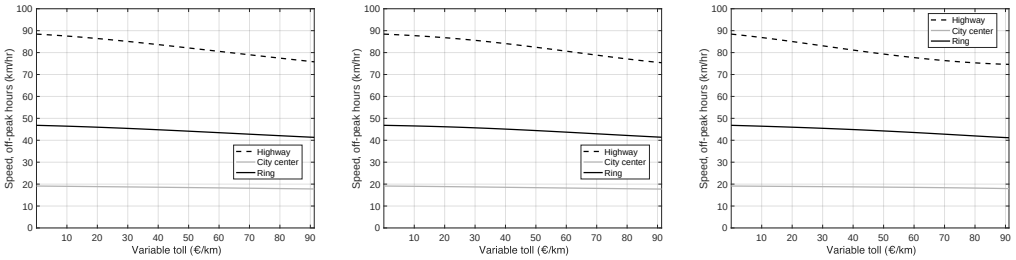

(d) Driving restrictions. (e) Uniform tolls. (f) Variable tolls.

E.3.2 Importance of endogenous speeds

In Figure 13, we compare our model's predictions for car shares with those from a naive model that would consider speeds and trip durations fixed. All scenarios and stringency levels deliver the same biases under exogenous speeds: we overestimate the number of individuals substituting away from using their cars at peak hours and underestimate those who choose to drive at off-peak hours. The equilibrium speed effects indeed dampen incentives to stop driving.

Figure 13: Predicted car shares as function of the policy stringency level.

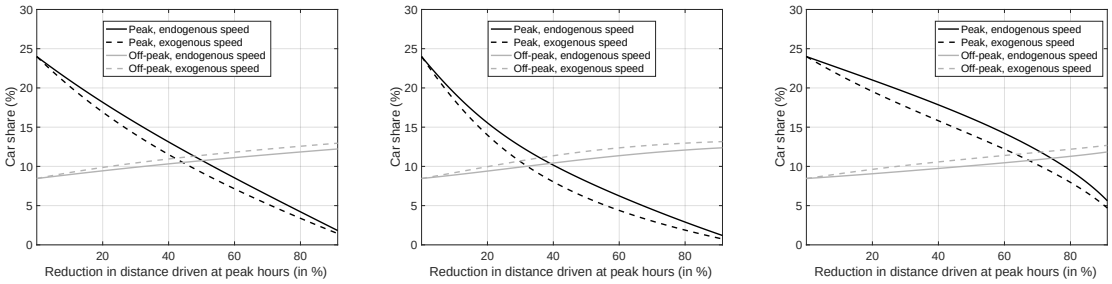

(a) Driving restrictions. (b) Uniform tolls. (c) Variable tolls.

To further highlight the importance of taking into account the equilibrium speed adjustments, we compare the tax revenues predicted under constant speeds with the predictions from our model. The results, in Figure 14 below, suggest that not accounting for the changes in speeds significantly underestimates the number of individuals paying the toll and the tax revenue. Moreover, the magnitude of the bias increases with the policy stringency levels, reflecting the increasing role of speed adjustments. In addition, we note that the tax revenues follow a Laffer curve under both toll types and decrease when the toll levels are too high. This maximum level is attained more rapidly for the uniform toll than the variable.

Figure 14: Predicted tax revenues under tolls at peak hours.

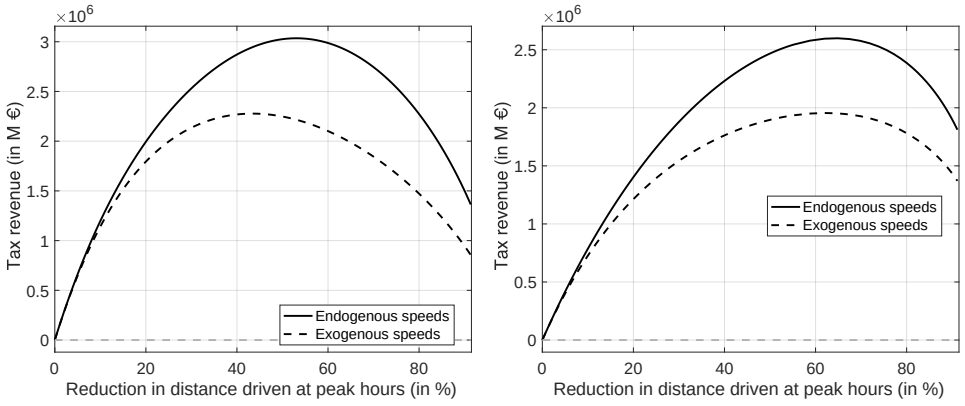

(a) Uniform tolls. (b) Variable tolls.

E.3.3 Social planner problem

The problem of the social planner maximizing welfare can be represented by the following Lagrangian:

$$\mathcal{L}(\mathbf{p},\mathbf{v},\mu,\boldsymbol{\lambda}) = W(\mathbf{v},\mathbf{p}) + \mu\left(\bar{K}_{t_1} - \sum_{n=1}^{N}\omega_n k_n s_{n\mathbf{d}t_1}(\mathbf{v},p_n)\right) + \sum_{t=\{t_1,t_2\}}\sum_{a=1}^{A}\lambda_t^a\left(v_t^a - f^a\left(K_t^a(\mathbf{v},\mathbf{p}) + K_0^a\right)\right)$$

where $W = \sum_n \omega_n CS_n + \sum_n \omega_n p_n s_{n\mathbf{d}t_1} - \sum_{t=t_1,t_2}\sum_n \omega_n e_n k_n s_{n\mathbf{d}t}$ The first-order conditions associated to the maximization of the welfare function are:

$$\frac{\partial\mathcal{L}(\mathbf{p},\mathbf{v},\mu,\boldsymbol{\lambda})}{\partial p_n} = 0 \quad \forall n, \quad \frac{\partial\mathcal{L}(\mathbf{p},\mathbf{v},\mu,\boldsymbol{\lambda})}{\partial v_t^a} = 0 \quad \forall t,\forall a, \quad \frac{\partial\mathcal{L}(\mathbf{p},\mathbf{v},\mu,\boldsymbol{\lambda})}{\partial\mu} = 0, \text{ and } \frac{\partial\mathcal{L}(\mathbf{p},\mathbf{v},\mu,\boldsymbol{\lambda})}{\lambda_t^a} = 0 \quad \forall t,\forall a$$

We write the expressions of the two first partial derivatives since the derivatives with respect to the multipliers are simply the constraints.

$$\frac{\partial\mathcal{L}(\mathbf{p},\mathbf{v},\mu,\boldsymbol{\lambda})}{\partial p_n} = \frac{\partial W}{\partial p_n} - \mu\omega_n k_n \frac{\partial s_{n\mathbf{d}t_1}}{\partial p_n} - \sum_t\sum_a \lambda_t^a f^{a\prime}(K_t^a) \times \omega_n k_n^a \frac{\partial s_{n\mathbf{d}t}}{\partial p_n}$$

And:

$$\frac{\partial\mathcal{L}(\mathbf{p},\mathbf{v},\mu,\boldsymbol{\lambda})}{\partial v_{t'}^{a'}} = \frac{\partial W}{v_{t'}^{a'}} - \mu\sum_{n=1}^{N}\omega_n k_n \frac{\partial s_{n\mathbf{d}t_1}}{\partial v_{t'}^{a'}} - \sum_t\sum_a \lambda_t^a f^{a\prime}(K_t^a) \times \sum_{n=1}^{N}\omega_n k_n^a \frac{\partial s_{n\mathbf{d}t}}{\partial v_{t'}^{a'}}$$

Because the tax revenue and the consumer surplus enter the welfare function with the same weight, the marginal welfare change due to a change of p_n is simply equal to the marginal increase in the tax revenue and the marginal benefits from emissions avoided:

$$\frac{\partial W}{\partial p_n} = \omega_n p_n \frac{\partial s_{n\mathbf{d}t_1}}{\partial p_n} - \sum_{t=\{t_1,t_2\}}\omega_n e_n k_n \frac{\partial s_{n\mathbf{d}t}}{\partial p_n}$$

So the optimal toll for individual n satisfies:

$$(p_n - e_n k_n - \mu k_n)\frac{\partial s_{n\mathbf{d}t_1}}{\partial p_n} - e_n k_n \frac{\partial s_{n\mathbf{d}t_2}}{\partial p_n} - \sum_{t=\{t_1,t_2\}}\sum_a \lambda_t^a f^{a\prime}(K_t^a) \times k_n^a \frac{\partial s_{n\mathbf{d}t}}{\partial p_n} = 0$$

This is a non-linear equation in p_n since p_n appears in the partial derivatives of the probability of driving. Note also that in this equation we also have the tolls of other individuals through K_t^a, the traffic levels in the different areas and periods. To gain intuition, we re-write the equation as follows:

$$p_n = (e_n + \mu)k_n + e_n k_n \frac{\frac{\partial s_{n\mathbf{d}t_2}}{\partial p_n}}{\frac{\partial s_{n\mathbf{d}t_1}}{\partial p_n}} + \frac{\sum_{t=\{t_1,t_2\}}\sum_a \lambda_t^a f^{a\prime}(K_t^a) \times k_n^a \frac{\partial s_{n\mathbf{d}t}}{\partial p_n}}{\frac{\partial s_{n\mathbf{d}t_1}}{\partial p_n}}$$

We have decomposed the optimal toll in three terms. The first term represents the social planner cost of letting individual n drive, which is equal to its emission cost $e_n k_n$ plus the shadow cost related to the traffic objective constraint μk_n. This term is linear in the distance driven by the individual. And when the reduction in traffic is large, we expect μ to be large and to dominate e_n. This implies that the heterogeneity of optimal personalized tolls across individuals is mostly related to distance.

The second term is negative and drives the optimal toll down. It is equal to the individual emissions costs multiplied by the diversion ratio between driving at peak and driving at off-peak hours. This term arises because the social planner benefits from reducing emissions at both periods.

The third term comes from the speed constraints. Discouraging individual n to drive by setting a high p_n relaxes the constraint on speeds at peak hours but intensifies those on speeds during off-peak hours. This term disappears if we consider speeds to be exogenous.

We now analyze the optimal tolls when the social planner maximizes the consumer surplus. The social planner that only cares about aggregate consumer surplus would set tolls to 0 absent of a traffic reduction constraint. Indeed, the marginal surplus is always decreasing since it is equal to:

$$\frac{\partial CS}{\partial p_n} = -\omega_n s_{n\mathbf{d}t_1}.$$

We also can see that the marginal surplus loss from toll is proportional to the probability of driving. However, the traffic reduction constraint forces the social planner to set positive tolls. The optimal toll p_n satisfies:

$$-s_{n\mathbf{d}t_1} - \mu k_n \frac{\partial s_{n\mathbf{d}t_1}}{\partial p_n} - \sum_{t=\{t_1,t_2\}} \sum_a \lambda_t^a f^{a\prime}(K_t^a) \times k_n^a \frac{\partial s_{n\mathbf{d}t}}{\partial p_n} = 0$$

From this equation, we can learn that the social planner targets individuals with low preference (with low $s_{n\mathbf{d}t_1}$), with long distance trips (high k_n) and with high sensitivity to tolls (high $\frac{\partial s_{n\mathbf{d}t_1}}{\partial p_n}$).

E.4 Additional results for the benchmark policy levels

Modal shift The aggregate shares of transportation modes are reported in Table 26. They indicate a significant inter-temporal modal shift towards driving at off-peak hours. The share of car users at peak hours drops under all policies, but the magnitudes differ. For example, while driving restrictions and uniform tolls decrease the number of car users by 6.9 to 9.7 percentage points, the variable toll only decreases it by 3.6 percentage points. This is because the variable toll discourages individuals with long distances from driving and keeps the

number of drivers relatively high. For the same reason, we also observe essential differences in the modal shifts across policies: driving restrictions and the uniform toll increase the fraction of individuals who walk and take public transport more than the variable toll.

Table 26: Predicted shares of the transportation modes under different policies.

	Initial	**Driving restriction**	**Uniform toll**	**Variable toll**	**Personalized tolls, max W**	**Personalized tolls, max CS**
Bicycle, peak	1.88	2.2	2.38	1.99	2.02	1.95
Pub. transport, peak	33.8	37.1	37.6	35.7	36.2	35.7
Motorcycle, peak	1.28	1.48	1.51	1.4	1.42	1.37
Walk, peak	14.9	16.4	18.3	15.3	15.4	14.9
Car, peak	24	17.1	14.3	20.4	19.8	21.4
Car, off-peak	8.46	9.62	9.61	9.19	9.08	8.68
Pub. transport, off-peak	11.6	11.9	12	11.9	12	11.8
Walk, off-peak	2.77	2.83	2.9	2.78	2.79	2.77
Bicycle, off-peak	0.57	0.58	0.6	0.57	0.58	0.57
Motorcycle, off-peak	0.76	0.79	0.8	0.79	0.79	0.78
Total car	32.5	26.7	23.9	29.6	28.8	30.1
Total pub. transport	45.4	49	49.7	47.6	48.1	47.5

Note: in %.

Impacts on individual trip durations We complement the analysis by looking at how the policies impact the expected travel times in Table 27 below. There is a large difference in the total travel time increase across policies: under the variable toll, it is only 11.3 thousand hours against 56.2 to 84.6 thousand hours under the driving restriction and the uniform toll. This reflects the extensive substitution for driving at off-peak hours under the variable toll. It further indicates that the surplus losses from the variable toll are mainly related to the surplus loss from driving outside peak hours and paying high tolls than an increase in travel time. The distribution of changes in travel time under all policies is skewed towards more extensive trips. For instance, the maximum time reductions are always lower than the maximum increases in travel time. Under the three policies, some individuals reduce their expected trip durations. The variable toll has the largest share of individuals with reduced travel times, with 42.3% of the individuals versus 27.2% and 30.7% under the two other policies.

Table 27: Trip duration variation under alternative policies.

	Driving restriction	**Uniform toll**	**Variable toll**	**Personalized tolls, max W**	**Personalized tolls, max CS**
Min Δduration	-4.72	-7.97	-8.36	-11.3	-13.7
Mean Δduration	0.881	1.33	0.177	0.189	-0.048
Max Δduration	26.6	45.2	41	38	80.2
Total Δduration (in 1,000 hrs)	56.2	84.6	11.3	12	-3.04
% Δduration > 0	51.6	48.1	36.5	39.2	13.5
% Δduration < 0	27.2	30.7	42.3	39.6	65.3

Note: Δ durations are in minutes, except "Total Δ duration".

Speed changes We analyze the speed changes for the different areas in Table 28. The variable toll most improves the speed on the highways at peak hours. The variable toll is also better than the driving restriction to improve the speed on the ring roads at peak hours. However, it raises speeds in the city center and the suburbs the least at peak hours. This occurs because the individuals who drive on the highways and ring roads have long distances and are discouraged from using their cars at peak hours. But since they do not have good transportation alternatives, they drive during off-peak hours. This is consistent with the highest speed reduction at off-peak hours under the variable toll. The uniform toll is the policy that enhances the speeds at peak hours in the city center, the ring roads, and the close suburb the most. Across the three regulations, the area with the smallest improvements is the far suburbs, revealing a lack of good car alternatives. For instance, public transport offers poor coverage in the distant suburb. The speeds at off-peak hours decrease in all areas but remain higher than the initial levels at peak hours. This reflects the imperfect substitution between driving at peak and off-peak hours, which avoids having a simple shift of the peak hour period.

Table 28: Predicted speeds under the different policies.

	Area	Initial	Driving restriction	Uniform toll	Variable toll	Personalized tolls, max W	Personalized tolls, max CS
Peak hours	Highways	59.6	74.7	72.5	79	77.7	80
	City center	13.1	15	16.1	14.8	17.6	16.6
	Ring roads	29	35.3	36.3	37	44	43.1
	Close suburb	16.2	18	18.5	17.4	18	17.5
	Far suburb	24.9	26.8	26.8	26.4	26.1	26
Off-peak hours	Highways	88.4	85.9	86.3	84.3	85.6	86
	City center	19.1	18.8	18.8	18.9	18.6	18.8
	Ring roads	46.8	45.7	46	45.8	45	45.7
	Close suburbs	20.3	19.9	19.9	20	19.9	20.1
	Far suburbs	28.8	28.3	28.4	28.3	28.5	28.6

Note: in km/hr.

Marginal costs of congestion Table 29 presents the marginal congestion costs for each area and period under the different policies. We provide the marginal costs associated with adding one average driver in each area to account for differences in area sizes. The driving restriction and uniform toll reduce the marginal congestion costs across all areas at peak hours. However, we observe an increase in the marginal costs of congestion in the city center and the close suburb at peak hours under the variable toll. The cost increases are lower than 8%, and we can observe the opposite pattern at off-peak hours, where the costs decrease in the same two areas and the far suburb. This occurs because the speed improvements make individual trip durations lower, increasing and in turn increase their marginal valuations of duration. Thus, having an additional driver on the road raises the surplus losses for

individuals. The marginal costs on the highways and the ring roads are the most reduced by the policies.

Table 29: Marginal costs of congestion under the different policies.

	Area	Initial	Driving restriction	Uniform toll	Variable toll	Personalized tolls, max W_2	Personalized tolls, max CS
Peak hours	Highways	4.29	1.97	2.41	1.58	1.8	1.89
	City center	4.24	3.28	3.12	3.64	2.62	3.21
	Ring roads	4.24	2.83	2.85	2.7	1.7	1.92
	Close suburbs	1.62	1.06	1.06	1.3	1.43	1.53
	Far suburbs	0.882	0.53	0.581	0.653	1.11	1.35
Off-peak hours	Highways	0.658	0.861	0.807	0.977	0.858	0.81
	City center	1.79	1.88	1.85	1.82	1.89	1.81
	Ring roads	1.2	1.32	1.26	1.28	1.35	1.25
	Close suburbs	0.626	0.666	0.649	0.633	0.638	0.605
	Far suburbs	0.268	0.385	0.358	0.369	0.345	0.263

Note: costs associated to adding an average driver, in €.

E.5 Robustness checks for the policy simulations

E.5.1 All-day policies

In this section, we analyze the impacts of policies applied during the whole day across stringency levels as we did in Section 5.3. For this exercise, the traffic is computed as the sum of kilometers driven at peak and off-peak hours. Figure 15 presents the main outcomes of interest across the three policies for all stringency levels. Panel (a) shows that the ranking between policies remains the same as in the peak period only policies. However, policies are welfare enhancing for a slightly smaller set of stringency levels, with the uniform toll stopping at around 25% and the variable toll at around 45%. Interestingly, Panel (b) reveals that in terms of aggregate consumer surplus loss the ranking remains the same between all day and peak policies. This highlights the role of departure time substitution on the aggregate effect of the policies. Finally, Panel (c) shows a similar trend in terms of tax revenue.

Figure 16 presents the change in emissions, average tolls paid, and average distance driven per trip across stringency levels for the all day policies. In terms of rankings across policies we find very similar results than for the peak-only policies presented in Figure 4. From panels (a) and (b) we see that gains form emissions reductions almost double and a significant increase in the average toll for both policies across stringency levels. However, from panel (c) we see that the average kilometers driven per trip remains similar between all-day and peak-only policies across all stringency levels. This result signals that the targeting of the policies does not vary depending on the periods targeted by the policies. Similarly, the rankings across policies remains constant across outcomes and departure periods targetted. We take

these results as evidence that the main results in the paper are not driven by individuals substituting across departure time period under the peak-only policies.

Figure 15: Change in welfare, consumer surplus, and tax revenue.

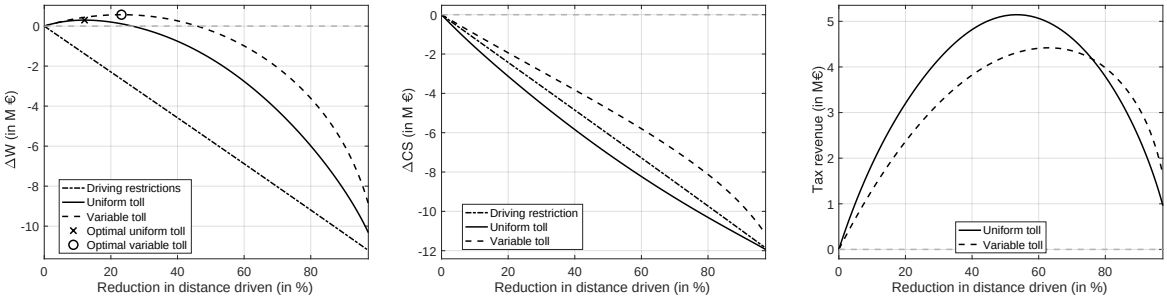

(a) Welfare. (b) Consumer surplus. (c) Tax revenues.

Figure 16: Additional policy outcomes under all-day policies.

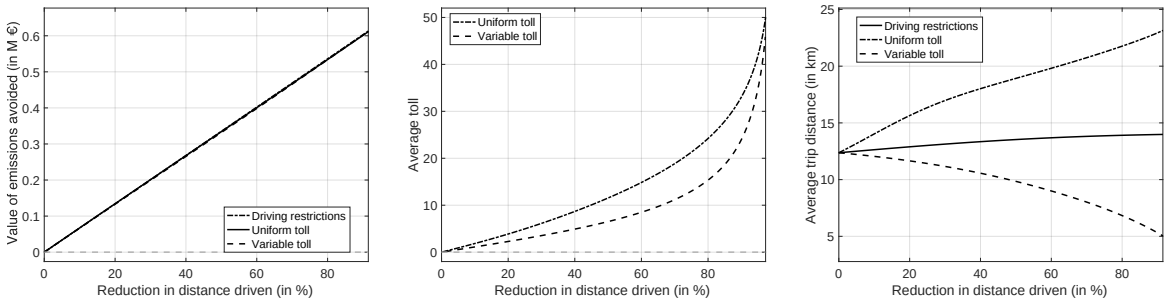

(a) Change in emissions costs. (b) Average toll. (c) Average distance conditional on driving at peak hours.

E.5.2 Increase in public transport overcrowding

We compare the benchmark variable toll and two scenarios where the policy is followed by a 15% or a 30% increase in the overcrowding levels in public transport. Table 30 presents the impact of these policies on consumer surplus and aggregate welfare. In the two scenarios, the total surplus loss would be 9% and 18% higher, highlighting the limited role of public transport overcrowding. Moreover, tax revenues remain almost constant under the three scenarios since the share of individuals driving is barely affected by the change in the overcrowding level. Finally, the welfare outcomes decrease by between 21% and 41%, mainly because of the larger surplus losses. Yet, we still obtain a positive effect from the variable toll.

Table 30: Policy effects with overcrowding level changes in public transit.

	Overcrowding constant	**Overcrowding +15%**	**Overcrowding +30%**
Total ΔCS (M€)	-1.17	-1.28	-1.39
ΔCS at constant speed	-1.71	-1.81	-1.92
ΔCS from speed	0.543	0.536	0.529
Total ΔwCS (M€)	-1.02	-1.12	-1.22
Tax revenue (M€)	1.61	1.62	1.62
Value emissions avoided (M€)	0.077	0.075	0.074
ΔW = ΔCS + Tax rev. + ΔE (M€)	0.519	0.412	0.306
% ΔCS = 0	21.2	9.19	9.19
% ΔCS > 0	6.01	3.18	2.27
% ΔCS < 0	72.8	87.6	88.5

E.5.3 Full flexibility in departure time choice

For this robustness check, we take the estimated model under our preferred specification and set the probability to be constrained to be equal to zero for all socio-professional categories. We then solve for the equilibrium under each one of the considered policies, calibrating them to reach the same traffic reduction than the first best personalized tolls under the benchmark specification. Table 31 presents compares the consumer surplus and welfare variation across policies. We see marginally lower aggregate consumer surplus losses and very similar welfare changes. These results confirm that departure time substitution is not the main reaction from individuals after the implementation of the toll, otherwise the results after lifting the constraints would vary more significantly.

Table 31: Welfare effects of the variable toll, with and without schedule constraints.

	Schedule constraints	**No schedule constraints**
Total ΔCS (M€)	-1.17	-1.13
ΔCS at constant speed	-1.71	-1.64
ΔCS from speed	0.543	0.51
Total ΔwCS (M€)	-1.02	-0.994
Tax revenue (M€)	1.61	1.56
Value emissions avoided (M€)	0.077	0.071
ΔW = ΔCS + Tax rev. + ΔE (M€)	0.519	0.507
% ΔCS > 0	6.01	6.3
% ΔCS < 0	72.8	72.5

Note: "ΔE" are the emissions avoided valued at standard levels.

F Additional policies examined with the model

F.1 Differentiated tolls

This section investigates the consequences of applying differentiated tolls. We consider tolls that depend on the areas where individuals drive and combinations of fixed and variable tolls.

Area-specific tolls We consider a toll that takes two different values: one for the city center and ring roads and one for the highways and the close and far suburbs. This policy instrument is similar to a cordon pricing mechanism. We determine all the toll combinations that imply the same objective traffic at peak hours and find the best toll combination for different objectives. When individuals drive through the two toll zones, we assume they only pay the highest toll.[49] Area-specific tolls might incentivize individuals to change their route choice. Still, we believe that the relatively large definition of areas in our setup considerably limits this potential effect.

Combination of fixed and variable tolls As well, we consider another way to define tolls, given by a fixed and a variable part. We allow for negative values of the two components of the toll. Interestingly, the best toll value for consumer surplus has the lowest fixed and highest variable parts. This means that individuals receive a fixed amount when taking their car but pay a high fee for each kilometer driven. Since individuals with short trips have higher valuations of travel time than individuals with more extended trips, their gains largely compensate for the losses of long-distance commuters and their high toll values, achieving the maximum consumer surplus. However, this combination of road tolls is not efficient at raising tax revenue. This is why the best combination, from a welfare perspective (defined as the sum of the aggregate surplus and the tax revenue minus the costs of emissions), is a toll with a smaller variable part than our benchmark variable toll (7 cents/km instead of 9 cents/km) and a moderate fixed amount of €0.73. This toll combination would improve the welfare gains by 13.3%. We could reach the maximum tax revenue with the high fixed value of €3.2 and a negative variable part (-0.2 cents/km). However, this combination of tolls would be welfare-decreasing, as Figure 17 (b) suggests.

[49] Alternatively, we could assume individuals driving through the two toll areas pay the sum of the tolls, but this situation would not nest the benchmark uniform toll.

Figure 17: Combination of fixed and variable tolls and their welfare effects.

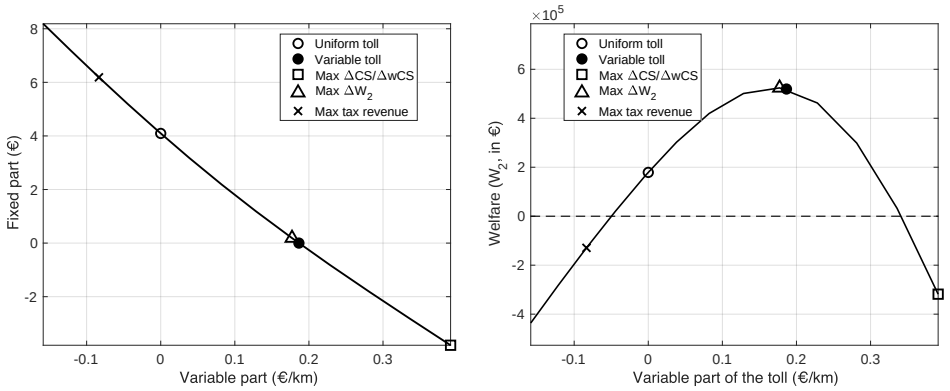

(a) Toll combinations.

(b) Welfare (W_2).

Efficiency of second-best instruments Table 32 below sumarizes the welfare gains achieved by the different second-best tolls, we compare policies that achieve the benchmark traffic reduction (34%). The two-part toll, with a fixed fee and variable part, achieves 85.8% of the welfare gains obtained under the welfare-maximizing personalized tolls. As well, the simple variable toll is very efficient since it generates 85.1% of the maximal welfare gains. The area-specific and uniform tolls have lower performances and generate 48.6% and 29.3% of the welfare gains under personalized tolls, respectively.

Table 32: Welfare effects of personalized tolls versus second-best instruments.

	ΔW (M€)	%ΔW w.r.t. personalized tolls
Personalized	0.611	100
Fixed and variable	0.524	85.8
Variable	0.519	85.1
Area-specific	0.297	48.6
Fixed	0.179	29.3

Figure 18: Differentiated tolls and their welfare impacts.

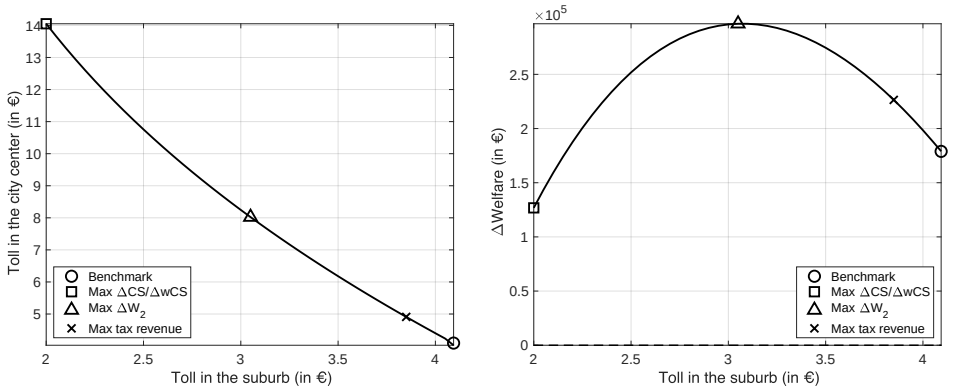

(a) Toll combinations.

(b) Welfare (W).

F.2 Auctioned driving license

We consider a simple uniform second-price auction format, which implies that individuals bid their true license valuation. The equilibrium price is the highest rejected bid associated with a fixed number of licenses. Individual valuations are equal to the difference between the expected utilities with and without the right to drive, and we assume individuals perfectly anticipate the speed improvements. However, they do not know their preference shocks before submitting their bids. Thus, the willingness to pay includes the gain in utility from better speeds at peak hours. We use an iterative algorithm to solve for the license price together with the equilibrium speeds for a given quota of driving licenses. Our algorithm cannot find a stable equilibrium for some values of the quota of driving licenses. This occurs when we consider stringent policies (i.e., with a low number of permits) where the speed gains are significant. We thus select the quota of driving licenses that implies the closest outcome to the one obtained in our main policies. Then, we re-calibrate the uniform toll to match the traffic reduction across policies. We thus analyze policies that identical to before since they trigger a decrease in traffic at peak hours of 24%. This policy seems more suited to a comparison with the uniform toll, as they both put a price on the right to drive. However, there is an essential difference from the perspective of individuals. Under the toll, individuals decide to drive and pay the toll after they receive their preference shocks for the transportation modes and departure times. While under the auction, individuals have to submit their bid for the license before receiving their preference shocks and lose the ability to react in case of extreme preference shocks. We provide the policy parameters in Table 33 below. We find a uniform toll of €4.09, higher than the license price of €3. Since individuals do not know their mode and departure period preference shocks when bidding, they have moderate valuations for the

driving license.

Table 33: Parameters for the driving license quota and equivalent uniform toll policies.

Policy type	**Parameter**	**Value**
License	Quota of licenses	29.3%
	License price	3
Uniform toll	toll	4.09

Note: License price and toll in €/trip.

Since individuals who get the license pay for it regardless of how often they decide to drive at peak hours, the policy generates considerably higher surplus losses. Individuals can no longer react to good or bad realizations of their preference shocks for driving. Indeed, the driving license regulation causes 72% more surplus losses than the uniform toll. The license generates higher tax revenue (€2.65 million). Under tax revenue redistribution, the quota of driving licenses causes a net welfare loss of €0.9 million, while the uniform toll is welfare enhancing.

However, we can see that the driving license quota is more effective than the toll to reduce emissions: we obtain 26% more benefits from reducing emissions. Despite the important environmental effect, in monetary terms, the emissions gains do not offset higher surplus losses from the quota of licenses since our second welfare measure is also higher under the uniform toll. Both with and without the redistribution of the tax revenue, the average cost of reducing emissions is lower under the uniform toll. From a distributional point of view, both policies seem to have similar effects, generating identical shares of losers and virtually no winners. The total consumer surplus losses are very similar with or without the redistributive weights, indicating that the driving license quota is not a regressive regulation.

Table 34: Driving license versus uniform toll.

	Uniform toll	**License**
Total ΔCS (M€)	-2.14	-3.68
ΔCS at constant speed	-2.75	-4.4
ΔCS from speed	0.607	0.722
Total ΔwCS (M€)	-1.98	-3.39
Tax revenue (M€)	2.23	2.65
Value emissions avoided (M€)	0.086	0.108
ΔW = ΔCS + Tax rev. + ΔE (M€)	0.179	-0.924
% ΔCS = 0	21.2	21.2
% ΔCS > 0	3.4	0.46
% ΔCS < 0	75.4	78.3

Note:"ΔE" are changes in emissions valued at standard levels.

F.3 Attribute-based driving restrictions

Low emission zone policies are widely used in Europe.[50] They impose driving restrictions based on combinations of fuel type and vintage to remove the most pollutant cars from the roads. Attribute-based policies are thus more cost-efficient at reducing emissions but generate greater distributional consequences than simple driving restrictions. We study the trade-off faced by policymakers by comparing the standard driving restrictions against two attribute-based policies: one banning all vehicles below a particular vintage and one banning diesel cars with a certain probability. While individuals are likely to change their cars in response to such policy, as shown by Barahona et al. (2020), we abstract from any effect on the fleet's composition.

As before, we calibrate the policies to reach the same traffic reduction as under the optimal personalized tolls. Since car vintage is a discrete variable, we cannot exactly match the expected number of kilometers at peak hours with this parameter only. We use the strictest vintage and assume that individuals are subject to the policy with a certain probability. For the diesel-based restriction, we assume all diesel cars have a probability of being affected. These technical assumptions can be interpreted as the frequency at which the policy is implemented. The calibrated parameters are as follows: the vintage selected is 2004, the average car vintage, and the policy should be applied 86.8% of the time. This regulation restricts 48.5% of the population. The diesel-based restriction should be applied 52% of the time and affects 59.4% of the people.

As Table 35 suggests, the vintage-based policy is slightly more costly for individuals, generating €2.05 million of surplus losses versus €1.83 million for the standard driving restriction. The diesel-based restriction causes lower surplus losses than the vintage one (€1.76 million). Under the vintage-based and diesel-based regulations, 40.6% and 32.3% of the population experience a surplus increase, highlighting the existence of distributional effects. Aggregate surplus losses measured using the redistributive weights are significantly higher for the vintage based restriction, pointing out that it hurts low-income individuals more.

The vintage-based restriction is also more efficient at reducing equivalent emissions, decreasing NO_X emissions 55% more than simple restrictions. The improved emission reduction balances the higher surplus losses through a lower implied average cost of regulation, reducing it by €125,000/ton. The targeting effectiveness is more nuanced for the diesel-based restric-

[50] For instance, in 2022, 82 German cites and 15 French cities are under low emission zone restrictions. Madrid, Barcelona, Milan, Rome, and Naples are additional examples of large cities with this type of policy. Source: https://urbanaccessregulations.eu/countries-mainmenu-147. Last accessed: 08/04/2022.

tion: CO_2 emissions decrease less than in the standard restriction, but we observe larger reductions of local pollutants. The net emission benefits are higher under the attribute-based restrictions than under the traditional driving restrictions (€0.28 million).

Table 35: Surplus changes under different driving restrictions.

	Standard	**Vintage-based**	**Diesel-based**
Total ΔCS (M€)	-1.83	-2.05	-1.76
ΔCS at constant speed	-2.36	-2.61	-2.26
ΔCS from speed	0.531	0.566	0.501
Total ΔwCS (M€)	-1.74	-2.41	-1.67
Value emissions avoided (M€)	0.084	0.108	0.095
ΔW = ΔCS + Tax rev. + ΔE (M€)	-1.75	-1.94	-1.66
% ΔCS = 0	21.2	21.2	21.2
% ΔCS > 0	6.7	40.6	32.3
% ΔCS < 0	72.1	38.2	46.5
Mean ΔCS (€)	-0.478	-0.535	-0.459
Median ΔCS (€)	-0.153	0	0
Max ΔCS (€)	1.57	7.09	5.77

Note:"ΔE" are emissions avoided valued at standard levels.

F.4 Improving public transport

While the main analysis focuses on traffic policies, we can provide insights on how improvements to public transport can mitigate consumer surplus losses. Public transport is the most used transportation mode in our data. In the first scenario, we improve public transport coverage by allowing the 13.9% individuals who initially don't have access to use a hypothetical public transport service. We use the median characteristics of public transport: a speed of 14.7 km/hr, a price of €1.63, and congestion levels of 120% at peak hours and 37% at off-peak hours, one layover and not using the railway system only.

In the second scenario, we decrease public transport travel times by 40%, similar to a frequency or speed improvement. Finally, in the third scenario, we make public transport free. We compare the effects of the variable toll applied before and after the implementation of the three different public transport improvements. The quality improvement and the free usage increase the total public transport usage by around 10%. In contrast, the coverage improvement increases use by almost 30%, indicating that improving coverage is the best instrument to increase public transit ridership.

Surplus changes are shown in Table 36. Public transport improvements reduce consumer surplus losses by up to 15%. The largest reduction corresponds to duration improvements. All policies reduce car usage and therefore imply lower tax revenues. Interestingly, improving coverage is the only improvement that has almost no effect on the outcomes from the toll. Moreover, reducing surplus losses does not compensate for the lower tax revenue, generating

lower welfare gains across all scenarios. However, this welfare measure does not include public transport revenue, which would increase in the first two scenarios. Across scenarios, the share of winners from the toll decreases after the improvements to public transport have been implemented.

Table 36: Consumer surplus variation under public transport improvements.

	(1)	**(2)**	**(3)**	**(4)**
Total ΔCS (M€)	-1.17	-1.17	-0.989	-1.12
ΔCS at constant speed	-1.71	-1.71	-1.24	-1.57
ΔCS from speed	0.543	0.545	0.248	0.448
Total ΔwCS (M€)	-1.02	-1.02	-0.862	-0.974
Tax revenue (M€)	1.61	1.61	1.06	1.44
Value emissions avoided (M€)	0.077	0.077	0.086	0.077
ΔW = ΔCS + Tax rev. + ΔE (M€)	0.519	0.523	0.16	0.401
% ΔCS = 0	21.2	21.2	21.2	21.2
% ΔCS > 0	6.01	6.01	3.34	4.68
% ΔCS < 0	72.8	72.8	75.4	74.1

Note: (1): Benchmark. (2): Coverage improvement. (3): Duration improvement. (4): Free access.

G Discussion about the scope of the model

Change in road congestion technology Recent urban policies consist of pedestrianization of specific roads, as well as their conversion into bike lanes. By reducing the road capacity for cars, such policies reduce speed for the same level of traffic. We can model such policies as changes in the congestion technologies, either through parallel shifts of the curves or a proportional decrease in speed along the curve. Alternatively, we could also model improvements of the road congestion technology, such as a road capacity increase or autonomous vehicles that would make traffic smoother.

Carpooling We have recently seen some initiatives to encourage carpooling. The U.S. has, for instance, a long tradition with high occupancy lanes in 27 metropolitan areas. While our model cannot predict the impacts of dedicating special lanes to carpooling and how individuals decide whether or not to carpool, we can still evaluate the benefits of carpooling under some simple assumptions. For instance, assuming that everyone has to carpool with three other people, a carpooling requirement amounts to considering that individuals are only driving one-fourth of their kilometers. Thus, it is equivalent to modifying the mapping parameter between individuals using their cars and the occupancy rate to $\tilde{\phi}^a = \phi^a/4$. The model can easily accommodate different cost-sharing assumptions and include detours that increase driving times.

Modifying work conditions We could consider policies incentivizing working from home a fraction of the time. We can model this similarly to carpooling. For instance, if we assume

individuals work from home one day per week, this is equivalent to reducing the expected number of kilometers driven by 20% or modifying the mapping parameter between the number of kilometers driven and the occupancy rate to $\tilde{\phi}^a = \frac{4}{5}\phi^a$. In addition, our model can be easily extended to more periods. This would allow us to consider policies like spreading work schedules that decrease the penalty for commuting outside peak hours and a more uniform distribution of congestion across time.

Parking cost and availability Recent literature shows the importance of parking prices and availability on traffic levels (Ostermeijer et al., 2022). The model can easily evaluate such policy through targeted increases in the costs of car trips.